

Nonlinear Controller Design for a Buck Converter

By: Yonggang Yin

Supervised by: Dr. Xiaoping Liu

A Thesis Submitted to Faculty of Engineering
in partial fulfillment of requirements for the
Degree of Master of Science in Control Engineering
Lakehead University

Sept. 06, 2006



Library and
Archives Canada

Bibliothèque et
Archives Canada

Published Heritage
Branch

Direction du
Patrimoine de l'édition

395 Wellington Street
Ottawa ON K1A 0N4
Canada

395, rue Wellington
Ottawa ON K1A 0N4
Canada

Your file *Votre référence*
ISBN: 978-0-494-21524-1
Our file *Notre référence*
ISBN: 978-0-494-21524-1

NOTICE:

The author has granted a non-exclusive license allowing Library and Archives Canada to reproduce, publish, archive, preserve, conserve, communicate to the public by telecommunication or on the Internet, loan, distribute and sell theses worldwide, for commercial or non-commercial purposes, in microform, paper, electronic and/or any other formats.

The author retains copyright ownership and moral rights in this thesis. Neither the thesis nor substantial extracts from it may be printed or otherwise reproduced without the author's permission.

AVIS:

L'auteur a accordé une licence non exclusive permettant à la Bibliothèque et Archives Canada de reproduire, publier, archiver, sauvegarder, conserver, transmettre au public par télécommunication ou par l'Internet, prêter, distribuer et vendre des thèses partout dans le monde, à des fins commerciales ou autres, sur support microforme, papier, électronique et/ou autres formats.

L'auteur conserve la propriété du droit d'auteur et des droits moraux qui protègent cette thèse. Ni la thèse ni des extraits substantiels de celle-ci ne doivent être imprimés ou autrement reproduits sans son autorisation.

In compliance with the Canadian Privacy Act some supporting forms may have been removed from this thesis.

Conformément à la loi canadienne sur la protection de la vie privée, quelques formulaires secondaires ont été enlevés de cette thèse.

While these forms may be included in the document page count, their removal does not represent any loss of content from the thesis.

Bien que ces formulaires aient inclus dans la pagination, il n'y aura aucun contenu manquant.


Canada

Abstract

This thesis presents five different nonlinear control techniques for voltage regulation of a DC-DC buck converter operating in continuous conduction mode. A state space averaging model is derived from a non-ideal buck converter circuit with the consideration of resistances of each component.

Based on this model, different nonlinear control techniques have been developed to control the DC-DC buck converter. These include backstepping control, sliding mode control, backstepping sliding mode control, adaptive backstepping control, and adaptive backstepping sliding mode control. All these proposed controllers have been evaluated by computer simulation and implemented on the DC-DC buck converter which is built for this thesis.

Simulation and experimental results show that all the proposed controllers are able to stabilize the closed loop system and to achieve satisfactory voltage regulation performances under source voltage variations and load changes.

Key words: Backstepping, adaptive control, sliding model control, pulse width modulation, DC-DC buck converter.

Acknowledgements

During the last two years, many people have helped me in realization of this research.

Hereby, I would like to take this opportunity to express my gratitude for all of them.

First of all, I would like to express my deepest gratitude to my supervisor Dr. Xiaoping Liu for his fabulous suggestions and wise guidance and also for broadening my knowledge about nonlinear control, all of which are very helpful in my research.

I also express my sincere thanks to my co-supervisor Dr. M. Nasir Uddin for his suggestions and help. I am very grateful to Dr. Abdelhamid Tayebi and Dr. Krishnamoorthy Natarajan for their great lectures on modern control concepts and adaptive control in my academic studies.

I am grateful to my colleague and graduate students for technical discussions and valuable advices that improved the experiments of my research work. Many thanks to Warren Paju and Manfred Klein, the technologists of the Electrical Engineering Department, who have helped me in many ways.

Finally, I would like to thank my family for supporting and encouraging me during the research.

Content

Abstract

Acknowledgements

1. INTRODUCTION	1
1.1 Background.....	1
1.2 Literature Review	3
2. MODELING OF DC-DC BUCK CONVERTER	7
2.1 Introduction	7
2.2 State Space Averaging	7
3. NONLINEAR CONTROL THEORY	13
3.1 Introduction	13
3.2 Lyapunov Theory	14
3.3 Nonlinear Backstepping Control	16
3.4 Sling Mode Control	18
3.4.1 Reaching Condition	19
3.4.2 Existence Condition	19
3.4.3 Equivalent Control	20
3.4.4 Chattering	21
3.5 Adaptive Backstepping Control	23
3.6 Reduced Order Observer	27
4. NONLINEAR CONTROL DESIGN MEHTODS FOR BUCK CONVERTER...	31
4.1 Introduction	31
4.2 Backstepping Control	33
4.3 Sliding Mode Control	35
4.3.1 Design of Sliding Surface	35
4.3.2 Equivalent Control	36
4.3.3 Existence of Sliding Mode Control	37

4.3.4 Chattering	38
4.4 Backstepping Sliding Mode Control	39
4.5 Adaptive Backstepping Control	41
4.6 Adaptive Backstepping Sliding Mode Control	45
4.7 Estimation of the Inductor Current	48
5. SIMULATION ANALYSIS OF THE CONTROL STRATEGIES	50
5.1 Response to Setpoint Change	52
5.2 Response to Load Change	58
5.3 Response to Source Voltage Change	64
5.4 Simulation Results Comparison	70
6. EXPERIMENTAL SETUP AND RESULTS	71
6.1 Introduction	71
6.2 Experimental Setup	73
6.2.1 Buck Converter Circuit Card Description	74
6.2.2 DAQ Board	74
6.3 Experimental Results	76
6.3.1 Current Estimated Using Reduced Order Observer	77
6.3.1.1 Response to Output Voltage Reference	77
6.3.1.2 Response to Load Change	83
6.3.1.3 Response to Source Voltage Change	89
6.3.2 Current Measured Using Current Transducer	95
6.3.2.1 Response to Output Voltage Reference	95
6.3.2.2 Response to Load Change	101
6.3.2.3 Response to Source Voltage Change	107
6.3.3 PI Control Results	113
6.3.4 Experimental Results Comparison	115

7. CONCLUSIONS AND FUTURE WORK	117
7.1 Conclusions	117
7.2 Suggestions for Future Research	118
BIBLIOGRAPHY	119

List of Figures

2-1	The circuit of buck converter	8
2-2	Equivalent circuit for switch closed	8
2-3	Equivalent circuit for switch open	10
3-1	Chattering phenomenon in sliding mode control	22
3-2	Block diagram of reduced order observer	30
5-1	Backstepping – setpoint (simulation)	53
5-2	Sliding mode – setpoint (simulation)	53
5-3	Backstepping sliding mode – setpoint (simulation)	54
5-4	Adaptive backstepping – setpoint (simulation)	54
5-5	Adaptive backstepping sliding mode – setpoint (simulation)	55
5-6	$\hat{\theta}_2$ -Adaptive backstepping – setpoint (simulation)	55
5-7	$\hat{\theta}_5$ -Adaptive backstepping – setpoint (simulation)	56
5-8	$\hat{\theta}_2$ -Adaptive backstepping sliding mode – setpoint (simulation)	56
5-9	$\hat{\theta}_5$ -Adaptive backstepping sliding mode – setpoint (simulation)	57
5-10	Backstepping – load (simulation)	59
5-11	Sliding mode – load (simulation)	59
5-12	Backstepping sliding mode – load (simulation)	60
5-13	Adaptive backstepping – load (simulation)	60
5-14	Adaptive backstepping sliding mode – load (simulation)	61

5-15	$\hat{\theta}_2$ -Adaptive backstepping – load (simulation)	61
5-16	$\hat{\theta}_3$ -Adaptive backstepping – load (simulation)	62
5-17	$\hat{\theta}_2$ -Adaptive backstepping sliding mode – load (simulation)	62
5-18	$\hat{\theta}_3$ -Adaptive backstepping sliding mode – load (simulation).....	63
5-19	Backstepping – disturbance (simulation)	65
5-20	Sliding mode – disturbance (simulation)	65
5-21	Backstepping sliding mode – disturbance (simulation)	66
5-22	Adaptive backstepping – disturbance (simulation).....	66
5-23	Adaptive backstepping sliding mode – disturbance (simulation).....	67
5-24	$\hat{\theta}_2$ -Adaptive backstepping – disturbance (simulation).....	67
5-25	$\hat{\theta}_3$ -Adaptive backstepping – disturbance (simulation).....	68
5-26	$\hat{\theta}_2$ -Adaptive backstepping sliding mode – disturbance (simulation).....	68
5-27	$\hat{\theta}_3$ -Adaptive backstepping sliding mode – disturbance (simulation).....	69
6-1	Buck converter experimental system	72
6-2	Diagram of the experimental setup	73
6-3	Buck converter circuit card	75
6-4	Backstepping – setpoint (estimated current)	78
6-5	Sliding mode – setpoint (estimated current)	79
6-6	Backstepping sliding mode – setpoint (estimated current)	79
6-7	Adaptive backstepping – setpoint (estimated current)	80
6-8	Adaptive backstepping sliding mode – setpoint (estimated current)	80

6-9	$\hat{\theta}_2$ -Adaptive backstepping – setpoint (estimated current)	81
6-10	$\hat{\theta}_5$ -Adaptive backstepping – setpoint (estimated current)	81
6-11	$\hat{\theta}_2$ -Adaptive backstepping sliding mode – setpoint (estimated current)	82
6-12	$\hat{\theta}_5$ -Adaptive backstepping sliding mode – setpoint (estimated current)	82
6-13	Backstepping – load (estimated current).....	84
6-14	Sliding mode – load (estimated current)	84
6-15	Backstepping sliding mode – load (estimated current)	85
6-16	Adaptive backstepping– load (estimated current)	85
6-17	Adaptive backstepping sliding mode – load (estimated current)	86
6-18	$\hat{\theta}_2$ -Adaptive backstepping – load (estimated current)	86
6-19	$\hat{\theta}_5$ -Adaptive backstepping – load (estimated current)	87
6-20	$\hat{\theta}_2$ -Adaptive backstepping sliding mode – load (estimated current)	87
6-21	$\hat{\theta}_5$ -Adaptive backstepping sliding mode – load (estimated current)	88
6-22	Backstepping – disturbance (estimated current)	90
6-23	Sliding mode – disturbance (estimated current)	90
6-24	Backstepping sliding mode – disturbance (estimated current)	91
6-25	Adaptive backstepping – disturbance (estimated current)	91
6-26	Adaptive backstepping sliding mode – disturbance (estimated current)	92
6-27	$\hat{\theta}_2$ -Adaptive backstepping – disturbance (estimated current)	92
6-28	$\hat{\theta}_5$ -Adaptive backstepping – disturbance (estimated current)	93

6-29	$\hat{\theta}_2$ -Adaptive backstepping sliding mode – disturbance (estimated current)	93
6-30	$\hat{\theta}_5$ -Adaptive backstepping sliding mode – disturbance (estimated current)	94
6-31	Backstepping – setpoint (current sensor)	96
6-32	Sliding mode – setpoint (current sensor)	96
6-33	Backstepping sliding mode – setpoint (current sensor)	97
6-34	Adaptive backstepping – setpoint (current sensor)	97
6-35	Adaptive backstepping sliding mode – setpoint (current sensor)	98
6-36	$\hat{\theta}_2$ -Adaptive backstepping – setpoint (current sensor)	98
6-37	$\hat{\theta}_5$ -Adaptive backstepping – setpoint (current sensor)	99
6-38	$\hat{\theta}_2$ -Adaptive backstepping sliding mode – setpoint (current sensor)	99
6-39	$\hat{\theta}_5$ -Adaptive backstepping sliding mode – setpoint (current sensor)	100
6-40	Backstepping – load (current sensor)	102
6-41	Sliding mode – load (current sensor)	102
6-42	Backstepping sliding mode – load (current sensor)	103
6-43	Adaptive backstepping– load (current sensor)	103
6-44	Adaptive backstepping sliding mode – load (current sensor)	104
6-45	$\hat{\theta}_2$ -Adaptive backstepping – load (current sensor)	104
6-46	$\hat{\theta}_5$ -Adaptive backstepping – load (current sensor)	105
6-47	$\hat{\theta}_2$ -Adaptive backstepping sliding mode – load (current sensor)	105
6-48	$\hat{\theta}_5$ -Adaptive backstepping sliding mode – load (current sensor)	106
6-49	Backstepping – disturbance (current sensor)	108

6-50	Sliding mode – disturbance (current sensor)	108
6-51	Backstepping sliding mode – disturbance (current sensor)	109
6-52	Adaptive backstepping – disturbance (current sensor)	109
6-53	Adaptive backstepping sliding mode – disturbance (current sensor)	110
6-54	$\hat{\theta}_2$ -Adaptive backstepping – disturbance (current sensor)	110
6-55	$\hat{\theta}_3$ -Adaptive backstepping – disturbance (current sensor)	111
6-56	$\hat{\theta}_2$ -Adaptive backstepping sliding mode – disturbance (current sensor)	111
6-57	$\hat{\theta}_3$ -Adaptive backstepping sliding mode – disturbance (current sensor)	112
6-58	PI controller – setpoint	113
6-59	PI controller – load	114
6-60	PI controller – disturbance	114

List of Tables

Table.5-1	Specification of buck converter (simulation)	51
Table.5-2	Specification of design parameters (simulation)	51
Table.5-3	Simulation results comparison	70
Table.6-1	Specification of buck converter (experiment)	76
Table.6-2	Specification of design parameters (estimated current)	77
Table.6-3	Specification of design parameters (current sensor)	95
Table.6-4	Experimental results comparison (estimated current)	115
Table.6-5	Experimental results comparison (current transducer)	116

Chapter 1

Introduction

1.1 Background

DC-DC converters are used to convert unregulated dc voltages to regulated or variable dc voltages at the output [1]. They are widely used in the power supply equipment for most electronic systems. In recent years, pulse width modulation (PWM) DC-DC converters have become a popular topic for many researchers as the demands for highly efficient and small size power sources increase. Various analysis methods on general properties and robust stabilities for PWM converters have been reported in [6] [8].

Generally speaking, the DC-DC converter has nonlinear components. The value of inductor change nonlinearly if the converter is disturbed [12]. When the linear control theory is applied to a converter, it could be effective around a fixed operating point and with small disturbances. However, when the DC-DC converter has significant disturbances, the operating point will not be fixed at one nominal position and the controller must be robust against these uncertainties. It is therefore important to develop nonlinear control techniques for DC-DC converters with nonlinearities [11].

In order to make these controller design techniques relevant and applicable to DC-DC converters, an average model [2] is needed to describe the dynamics of DC-DC converters. The conventional averaging technique, which is easy to understand and straightforward to apply, particularly for DC-DC converters [7], gives a useful representation of the converter and allows simple design procedures for operation in certain regimes.

In this thesis, a state space averaging model is developed for a buck converter with the concern of resistances of each component in the converter circuit. Based on this model, different nonlinear control techniques have been developed. These include backstepping control, sliding mode control, backstepping sliding mode control, adaptive backstepping control, and adaptive backstepping sliding mode control. Our objective is concentrated on finding a proper controller for the switching DC-DC buck converter to minimize the steady state error in the presence of the output voltage variations and load changes. All these five nonlinear controllers are simulated using MATLAB and implemented on the prototype PWM DC-DC buck converter, which is constructed in laboratory with a fixed switching frequency. Moreover, the experimental result of the PI controller is also evaluated. Their behaviors are compared with the following basic conditions: steady state responses to setpoint changes, sensitivities to load changes, and disturbances in the power supply.

This thesis is organized as follows:

In Chapter 2, the state space averaging model of the DC-DC buck converter is derived in detail using the fundamental Kirchhoff's current and voltage laws.

In Chapter 3, Lyapunov theory, backstepping control, sliding mode control and adaptive backstepping control theory are reviewed, which will provide fundamental theories for the nonlinear controller design. And the reduced order observer is also introduced, which will be used to estimate the inductor current based on the output voltage measurements in Chapter 6.

Chapter 4 describes the design procedures of five different nonlinear controllers for the DC-DC buck converter. These include backstepping, sliding mode, backstepping sliding mode, adaptive backstepping, and adaptive backstepping sliding mode control. Simulations are performed to evaluate the proposed controllers using MATLAB software in Chapter 5.

In Chapter 6, a buck converter experimental system is constructed to implement the

nonlinear controllers designed in Chapter 4. The experimental results are shown and compared in terms of steady state errors, transient responses, and sensitivities to load changes and disturbances in the power supply.

In Chapter 7, the main contributions of this thesis are summarized and suggestions for future research work are given.

1.2 Literature Review

Backstepping is a systematic and recursive design methodology for nonlinear feedback control. This type of control has been well studied in [5]. The main advantage of backstepping is the construction of a Lyapunov function whose derivative can be made negative definite by a variety of control laws. The systematic construction of a Lyapunov function for the closed loop system makes the stabilization problem much easier for nonlinear systems. With backstepping, system nonlinearities do not have to be cancelled by the control law. Some useful uncertain nonlinearities can be retained, which can reduce control efforts and increase robustness to model errors [10].

Backstepping can be perfectly applied to a nonlinear system with a lower triangular form. For an ideal DC-DC buck converter circuit, the state space averaging model of the converter is shown to be in the lower triangular form [9]. However, for a non-ideal DC-DC buck converter circuit, with the consideration of the equivalent series resistance of the capacitor, the output voltage is not equal to the capacitor voltage and the averaging model does not possess a lower triangular form. To solve this problem, in [11] and [12], a reduced order model is derived in order to show that the equivalent series resistance of the capacitor can be ignored for the DC-DC buck converter. An averaging reduced slow model is derived with the two state variables formed by inductor current and output voltage, which is a suitable model for the backstepping approach.

Adaptive nonlinear controllers, which are designed for nonlinear systems with unknown parameters, have been developed in literature [5] [10]. Among many adaptive nonlinear

control techniques, backstepping control is regarded as a new breakthrough. This type of approach offers a systematic design procedure where unwanted cancellation of favorable nonlinearities can be avoided [5]. In contrast with the conventional approaches based on the certainty equivalence scheme, adaptive backstepping employs a tuning function as a parameter update law in the recursive design procedure. With this control technique, the global asymptotic stability of nonlinear systems with unknown parameters can be guaranteed.

In this thesis, the backstepping control technique is developed for a non-ideal DC-DC buck converter. With the selected two state variables, inductor current and output voltage, a state space averaging model is derived under some assumptions. Moreover, in the case of unknown parameters, adaptive backstepping is also developed to ensure the control objective. The parameter estimate update laws are designed such that the stability of the closed loop system is guaranteed when the parameter estimators are used by the controller.

Switch mode power supplies can be considered as a particular class of the variable structure systems (VSS), since their structure is periodically changed by the action of controlled switches and diodes [17]. From this point of view, sliding mode control, which is initially derived from the VSS theory, can be appropriately applied to DC-DC converters, especially to buck converters operating in the continuous conduction mode. This control technique offers several advantages: stability even for large source disturbances and load variations, robustness, good dynamic response and simple implementation. Its capabilities emerge especially in applications to high-order converters, yielding improved performances as compared to classical control techniques [31].

The feasible application of sliding mode control to switching mode power supplies has been widely investigated in literature [15]-[18]. However, it has been shown that sliding mode controlled converters generally suffer from significant switching frequency

variation when the input voltage and output load are varied [25]. Hence, it is more desirable to operate the converters at a constant switching frequency that does not deviate too far from its nominal value. One solution to this is to employ the PWM technique in the sliding mode control [14]. The idea is based on the assumption that the control action of a sliding mode controller is equivalent to the duty cycle control action of a PWM controller at a high switching frequency.

In order to obtain good performance under source disturbances and load variations, sliding mode control for power converters has been investigated in several different models, such as small signal model [19] and state space averaging model [20] [32]. In [27] and [28], a mathematical model is derived with the output voltage error and the rate of change in the voltage error as two state variables for the DC-DC buck converter. Moreover, various complex hybrid sliding mode control structures have been developed. By combining sliding mode control with other techniques, such as adaptive control techniques [23] [28], these hybrid controllers ensure the control objectives even though there exist unknown parameters in systems. Most of these hybrid controllers require complex implementation algorithms.

Chattering describes the phenomenon of finite frequency, finite amplitude oscillations appearing in many sliding mode control implementations. These oscillations appear because the high frequency switching excites unmodeled dynamics in the closed loop system [33]. Without a proper treatment in the control design, it has been a major obstacle for implementation of sliding mode control to a wide range of applications.

Many different schemes have been proposed in literature [19] [33] to eliminate the chattering. In [34], the chattering problem is studied and four solutions are presented. However, all four methods possess advantages and disadvantages which depend on the system specifications. When designing a sliding mode controller for a given system, all details of the controlled system should be carefully considered to choose a proper method to prevent chattering. Unfortunately, there is no unified method suitable for solving the

chattering problems for all systems.

In this thesis, the sliding mode control theory is reviewed and its application to PWM DC-DC buck converters is investigated. Two hybrid controllers, backstepping sliding mode control and adaptive backstepping sliding mode control, are also proposed. The simulation and experimental results on these controllers demonstrate their performances under setpoint variation, source deviations and load changes.

Chapter 2

Modeling of DC-DC Buck Converter

2.1 Introduction

Mathematical models for DC-DC buck converters can be found in many books [1] [2]. With the fundamental Kirchoff's current and voltage laws, the dynamic models of DC-DC buck converters can be derived. The methodology for the derivation of the model is quite straightforward. First, we fix the position of the switch and derive the differential equations of the circuit model. Second, we combine the derived models into a single one by using the switch position function whose values are in the binary set $\{0, 1\}$. Finally, by letting the switch position function take values in the closed interval of the real line $[0,1]$, we can obtain an average model from the switched model.

In this chapter, a state space averaging model is derived for a non-ideal DC-DC buck converter under some necessary assumptions so that it is suitable for nonlinear controller design in Chapter 4.

2.2 State Space Averaging

A buck converter is used to convert a high dc input voltage to a lower desired dc output voltage, and it is also called a step-down converter. The circuit of a buck converter is illustrated in Fig.2-1. In this diagram, the components of the buck converter are not ideal, and R_C , R_L , R_D and R_S denote the equivalent series resistance of the capacitor, inductor resistance, diode resistance and the resistance of the switch, respectively. The

switch is an electronic device that operates in either on or off mode. The switch is controlled by a switching signal with a period T in such a way that it is closed for $t_{on} = DT$ and open for $t_{off} = (1-D)T$, where D is the duty cycle of the switching signal.

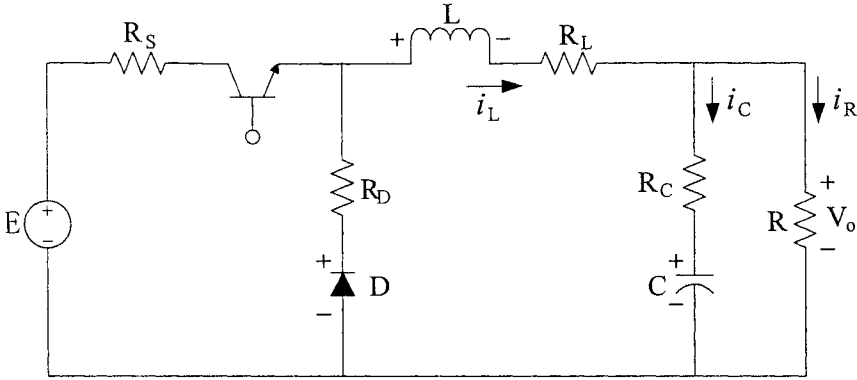


Fig.2-1: The circuit of buck converter

State space averaging method requires two set of state equations, which describe circuit dynamics when the switch is open and the switch is closed. Then the state equations are averaged over the switching period.

Switch Closed

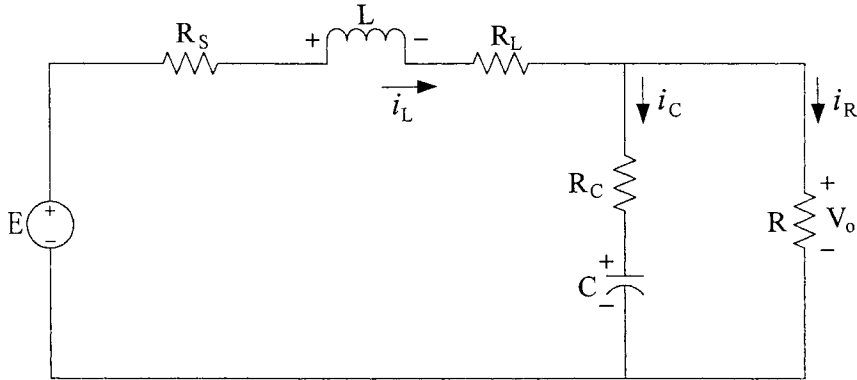


Fig.2-2: Equivalent circuit for switch closed

When the switch is closed, the diode is reverse biased and an equivalent circuit of the buck converter is shown in Fig.2-2. Using the Kirchhoff's voltage law in the outermost loop of the circuit, we get

$$L \frac{di_L}{dt} + (R_L + R_S)i_L + Ri_R = E \quad (2.1)$$

Kirchhoff's current law gives

$$i_R = i_L - i_C = i_L - C \frac{dv_C}{dt} \quad (2.2)$$

For the left inner loop, we use Kirchhoff's voltage law to get

$$L \frac{di_L}{dt} + (R_L + R_S)i_L + i_C R_C + v_C = E \quad (2.3)$$

Rearranging the equation (2.3) yields

$$i_C = C \frac{dv_C}{dt} = \frac{1}{RC} \left(E - L \frac{di_L}{dt} - (R_L + R_S)i_L - v_C \right) \quad (2.4)$$

Combining equations (2.1) to (2.4) gives the state equation

$$\frac{di_L}{dt} = -\frac{R}{(R + R_C)L} v_C - \left(\frac{RR_C}{(R + R_C)L} + \frac{R_L}{L} + \frac{R_S}{L} \right) i_L + \frac{E}{L} \quad (2.5)$$

Kirchhoff's voltage law around the right inner loop gives

$$v_C + i_C R_C = i_R R \quad (2.6)$$

Combining equation (2.6) with (2.1) gives the state equation

$$\frac{dv_C}{dt} = -\frac{1}{(R + R_C)C} v_C + \frac{R}{(R + R_C)C} i_L \quad (2.7)$$

Switch Open

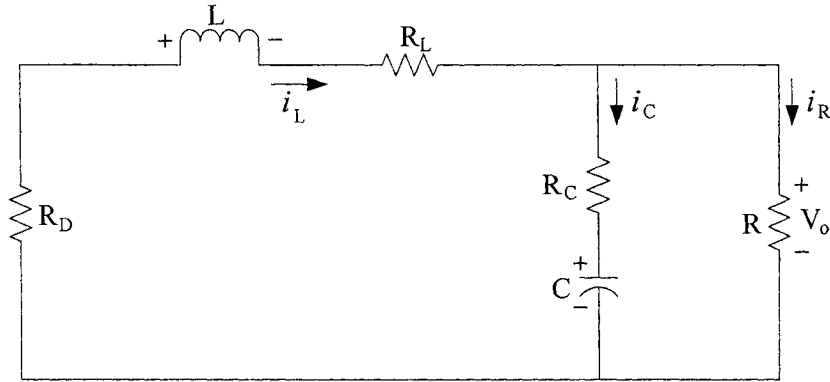


Fig.2-3: Equivalent circuit for switch open

While the switch is open, the diode becomes forward biased to carry the inductor current. Fig.2-3 shows the equivalent circuit of the buck converter during the time when the switch is open.

Using the same strategy, the following differential equations can be easily obtained:

$$\frac{dv_C}{dt} = -\frac{1}{(R+R_C)C}v_C + \frac{R}{(R+R_C)C}i_L \quad (2.8)$$

$$\frac{di_L}{dt} = -\frac{R}{(R+R_C)L}v_C - \left(\frac{RR_C}{(R+R_C)L} + \frac{R_L}{L} + \frac{R_D}{L} \right) i_L \quad (2.9)$$

Note that both diode and switch resistances are quite small and there is no much difference. Therefore, it is assumed that $R_S = R_D$ for simplifying the analysis. With this assumption, the following equations can be derived from (2.5), (2.7), (2.8), and (2.9):

$$\frac{dv_C}{dt} = -\frac{1}{(R+R_C)C}v_C + \frac{R}{(R+R_C)C}i_L$$

$$\frac{di_L}{dt} = -\frac{R}{(R+R_C)L}v_C - \left(\frac{RR_C}{(R+R_C)L} + \frac{R_L}{L} + \frac{R_S}{L} \right) i_L + \frac{E}{L}u \quad (2.10)$$

This model is usually referred to as the switched model because the switch position function u takes values in the discrete set $\{0,1\}$.

The averaged model would be represented exactly by the same model by redefining the control input u as a function taking values in the closed interval $[0,1]$. Now a pulse width modulation (PWM) circuit is used to determine the switch position. The PWM policy is specified as follows,

$$\mu(t) = \begin{cases} 1 & \text{for } t_k \leq t < t_k + \mu(t_k)T \\ 0 & \text{for } t_k + \mu(t_k)T \leq t < t_k + T \end{cases} \quad (2.11)$$

where t_k represents a sampling instant defined by $t_k = t_k + T$, $k = 0, 1, \dots$, T is the fixed switching period, the duty ratio function $\mu(t)$, taking values from the closed interval $[0,1]$, is a control input to the system.

The averaged model of the buck converter is then described as follows:

$$\begin{aligned} \frac{dv_C}{dt} &= -\frac{1}{(R+R_C)C}v_C + \frac{R}{(R+R_C)C}i_L \\ \frac{di_L}{dt} &= -\frac{R}{(R+R_C)L}v_C - \left(\frac{RR_C}{(R+R_C)L} + \frac{R_L}{L} + \frac{R_S}{L} \right) i_L + \frac{E}{L}\mu \end{aligned} \quad (2.12)$$

For the buck converter, the output voltage v_o can be determined from the following equation

$$v_o = Ri_R = R(i_L - i_C) = R \left(i_L - \frac{v_o - v_C}{R_C} \right) \quad (2.13)$$

Solving (2.13) for v_o produces

$$v_o = \left(\frac{RR_C}{R+R_C} \right) i_L + \left(\frac{R}{R+R_C} \right) v_C \quad (2.14)$$

Note that the capacitor resistance R_C is very small compared with the load resistance R .

Hence, for simplicity, it is reasonable to neglect R_C . As a result, it follows from (2.14)

that

$$v_o = v_C \quad (2.15)$$

Another reason for neglecting R_C is to make the mathematical model suitable for the backstepping controller design.

Simplifying the averaged model, equations (2.10) can be written as follows

$$\begin{aligned} \dot{x}_1 &= \theta_1 x_1 + \theta_2 x_2 \\ \dot{x}_2 &= \theta_3 x_1 + \theta_4 x_2 + \theta_5 \mu \end{aligned} \quad (2.16)$$

where x_1 and x_2 represent, respectively, the capacitor voltage and inductor current.

The parameters $\theta_1, \theta_2, \theta_3, \theta_4$ and θ_5 are defined by the following equations:

$$\theta_1 = -\frac{1}{(R+R_C)C}$$

$$\theta_2 = \frac{R}{(R+R_C)C}$$

$$\theta_3 = -\frac{R}{(R+R_C)L}$$

$$\theta_4 = -\frac{RR_C}{(R+R_C)L} - \frac{R_L}{L} - \frac{R_S}{L}$$

$$\theta_5 = \frac{E}{L}$$

Chapter 3

Nonlinear Control Theory

3.1 Introduction

Lyapunov theory has been an important tool in the study of nonlinear theory. Although there might be some difficulties to find a Lyapunov function for a given system, if one is found, the system is known to be stable. Backstepping is a systematic and recursive design method for nonlinear feedback control based on Lyapunov theory. The main advantage of backstepping is the systematic construction of a Lyapunov function for the closed loop system. The backstepping design procedure consists of several steps. A virtual control law is constructed for each subsystem until a control law for the whole system has been constructed. Backstepping method is applicable to systems in the lower triangular form [5].

Sliding mode control is well known for its robustness and stability. Using the high speed switching operation makes the system phase trajectory approach a surface $S = 0$, which is called sliding mode surface or switching surface. And the surface can be reached as long as the existence condition $S\dot{S} < 0$ is satisfied. When system state vectors enter the sliding surface, they are limited in the surface $S = 0$ [3].

Adaptive control [4] is always applied to a system which has parameter uncertainties. If such parameter uncertainties are not reduced properly, it may cause inaccuracy or instability for the control system. The task of adaptive control is to maintain the consistent performance of a system in the presence of uncertainties or unknown variations in plant parameters.

In this chapter, we present Lyapunov theory, backstepping control, sliding mode control and adaptive backstepping control theory, which will provide fundamental theories for the nonlinear controller design in Chapter 4. A reduced order observer design is also introduced, which will be used to estimate the inductor current in Chapter 6.

3.2 Lyapunov Theory

In this section we define the notion of stability in the Lyapunov sense, and review the main tools for proving stability of an equilibrium point.

Consider the system

$$\dot{x} = f(x) \quad (3.1)$$

where x is the system state vector.

Let $x = x_e$ be an equilibrium point of the system, that is, $f(x_e) = 0$. The stability properties of this equilibrium point are characterized by the following definition.

Definition 3.1 (Lyapunov stability) The equilibrium point $x = x_e$ of (3.1) is

- stable if for each $\varepsilon > 0$ there exists $\delta(\varepsilon) > 0$ such that

$$\|x(0) - x_e\| < \delta \Rightarrow \|x(t) - x_e\| < \varepsilon, \quad \forall t \geq 0$$

- unstable if it is not stable
- asymptotically stable if it is stable and in addition there exists $r > 0$ such that

$$\|x(0) - x_e\| < r \Rightarrow \lim_{t \rightarrow \infty} x(t) = x_e$$

- globally asymptotically stable (GAS) if it is asymptotically stable for all initial conditions, that is, if

$$\lim_{t \rightarrow \infty} x(t) = x_e, \quad \forall x(0)$$

Let us first introduce some useful concepts, which are often used in discussing Lyapunov's direct method (or second method).

Definition 3.2 A function $V(x)$ is said to be

- positive definite if $V(0) = 0$ and $V(x) > 0, \quad x \neq 0$
- positive semi-definite if $V(0) = 0$ and $V(x) \geq 0, \quad x \neq 0$
- negative (semi-)definite if $-V(x)$ is positive (semi-)definite
- radially unbounded if $V(x) \rightarrow \infty$ as $\|x\| \rightarrow \infty$

We now state the main theorem to be used for proving global asymptotic stability

Theorem 3.1 Consider the system (3.1) and let $f(0) = 0$. Let $V(x)$ be a positive definite, radially unbounded, continuously differentiable scalar function. If

$$\dot{V}(x) < 0, \quad x \neq 0$$

then $x = 0$ is a globally asymptotically stable (GAS) equilibrium point.

In some cases, global asymptotic stability can be shown when $\dot{V}(x)$ is only negative semi-definite.

Theorem 3.2 Consider the system (3.1) and let $f(0) = 0$. Let $V(x)$ be a positive definite, radially unbounded, continuously differentiable scalar function, such that

$$\dot{V}(x) \leq 0, \quad \forall x$$

let $S = \{x : \dot{V}(x) = 0\}$ and suppose that no other solution than $x(t) = 0$ can stay forever in S . Then $x = 0$ is a globally asymptotically stable equilibrium point.

Note that both theorems give no clue about how to find the function V satisfying the conditions necessary to show GAS. In some cases, there are natural Lyapunov function candidates like energy functions in electrical or mechanical systems. In other cases, it is basically a matter of trial and error.

3.3 Nonlinear Backstepping Control

Let us assume that the plant parameters are known. The application of backstepping approach to nonlinear system with the lower triangular structure is illustrated as follows.

Consider an SISO nonlinear system of the following form

$$\begin{aligned}\dot{x}_1 &= f_1(x_1) + g_1(x_1)x_2 \\ \dot{x}_2 &= f_2(x_1, x_2) + g_2(x_1, x_2)x_3 \\ \dot{x}_3 &= f_3(x_1, x_2, x_3) + g_3(x_1, x_2, x_3)u\end{aligned}\quad (3.2)$$

where f_i and g_i are smooth functions and $g_i(0) \neq 0$, x_1, x_2 and x_3 are the state variables, u is the control input.

First, choose the Lyapunov function V_1 , that is,

$$V_1(x_1) = \frac{1}{2}x_1^2 \quad (3.3)$$

the derivative of the Lyapunov function V_1 is given by

$$\dot{V}_1 = x_1\dot{x}_1 \quad (3.4)$$

If x_2 is considered to be the virtual control for the first equation of (3.2), it would be designed as the following equation

$$x_2 = \alpha_1(x_1) = \frac{1}{g_1(x_1)}(-c_1x_1 - f_1(x_1)) \quad (3.5)$$

which will make the derivative of V_1

$$\dot{V}_1 = -c_1x_1^2 \quad (3.6)$$

negative definite, where $c_1 > 0$ is a design parameter.

Second, x_3 is viewed as the virtual control in the second equation of (3.2), introducing the new error variable $x_2 - \alpha_1(x_1)$.

Choose the Lyapunov function V_2

$$V_2(x_1, x_2) = V_1 + \frac{1}{2}(x_2 - \alpha_1)^2 \quad (3.7)$$

Then, the derivative of the Lyapunov function V_2 is

$$\dot{V}_2 = \dot{V}_1 + (x_2 - \alpha_1)(f_2(x_1, x_2) + g_2(x_1, x_2)x_3 - \frac{\partial \alpha_1}{\partial x_1}(f_1(x_1) + g_1(x_1)x_2)) \quad (3.8)$$

The virtual input x_3 is given by

$$x_3 = \alpha_2(x_1, x_2) = \frac{1}{g_2(x_1, x_2)}(-c_2(x_2 - \alpha_1) - f_2(x_1, x_2) + \frac{\partial \alpha_1}{\partial x_1}(f_1(x_1) + g_1(x_1)x_2)) \quad (3.9)$$

which results that the derivative of V_2

$$\dot{V}_2 = -c_1x_1^2 - c_2(x_2 - \alpha_1)^2 \quad (3.10)$$

is negative definite, where $c_2 > 0$ is a design parameter.

Finally, introduce the new error variable $x_3 - \alpha_2(x_1, x_2)$ and design our actual feedback control u to stabilize the system by using the Lyapunov function V_3

$$V_3(x_1, x_2, x_3) = V_2 + \frac{1}{2}(x_3 - \alpha_2)^2 \quad (3.11)$$

The derivative of the Lyapunov function is

$$\begin{aligned} \dot{V}_3 = \dot{V}_2 + (x_3 - \alpha_2)(f_3(x_1, x_2, x_3) + g_3(x_1, x_2, x_3)u \\ - \frac{\partial \alpha_2}{\partial x_1}(f_1(x_1) + g_1(x_1)x_2) - \frac{\partial \alpha_2}{\partial x_2}(f_2(x_1, x_2) + g_2(x_1, x_2)x_3)) \end{aligned} \quad (3.12)$$

The control u can be chosen as follows:

$$\begin{aligned} u = \frac{1}{g_3(x_1, x_2, x_3)}[-c_3(x_3 - \alpha_2) - f_3(x_1, x_2, x_3) \\ + \frac{\partial \alpha_2}{\partial x_1}(f_1(x_1) + g_1(x_1)x_2) + \frac{\partial \alpha_2}{\partial x_2}(f_2(x_1, x_2) + g_2(x_1, x_2)x_3)] \end{aligned} \quad (3.13)$$

to make \dot{V}_3 negative definite, that is

$$\dot{V}_3 = -c_1 x_1^2 - c_2 (x_2 - \alpha_1)^2 - c_3 (x_3 - \alpha_2)^2 < 0 \quad (3.14)$$

Where $c_3 > 0$ is a design parameter.

In summary, for system (3.2), the backstepping controller can be implemented as follows:

$$u = \frac{1}{g_3(x_1, x_2, x_3)} [-c_3 (x_3 - \alpha_2) - f_3(x_1, x_2, x_3) + \frac{\partial \alpha_2}{\partial x_1} (f_1(x_1) + g_1(x_1)x_2) + \frac{\partial \alpha_2}{\partial x_2} (f_1(x_1, x_2) + g_1(x_1, x_2)x_3)]$$

where $\alpha_1(x_1) = \frac{1}{g_1(x_1)} (-c_1 x_1 - f_1(x_1))$

$$\alpha_2(x_1, x_2) = \frac{1}{g_2(x_1, x_2)} (-c_2 (x_2 - \alpha_1) - f_2(x_1, x_2) + \frac{\partial \alpha_1}{\partial x_1} (f_1(x_1) + g_1(x_1)x_2))$$

3.4 Sliding Mode Control

The sliding mode control scheme consists of two steps. The first involves the design of a sliding surface so that the sliding motion satisfies the design specifications. The second is concerned with the selection of a control law, which will make the sliding surface attractive to the system state. It is worth noting that this control law is not necessarily to be discontinuous.

Let's consider the following general system with a scalar control input

$$\dot{x} = f(x, t, u) \quad (3.15)$$

where x is the column vector, f is a function vector with dimension n , and u represents the control input.

The function vector f is discontinuous on the surface $S(x, t) = 0$, that is,

$$f(x, t, u) = \begin{cases} f^+(x, t, u^+) & \text{for } S > 0 \\ f^-(x, t, u^+) & \text{for } S < 0 \end{cases} \quad (3.16)$$

The system is in sliding mode if its representative point moves on the sliding surface $S(x, t) = 0$.

3.4.1 Reaching Condition

Consider the system $\dot{x} = f(x, t, u)$ with the scalar discontinuous input u which is given by

$$u = \begin{cases} u^+ & \text{for } S(x) > 0 \\ u^- & \text{for } S(x) < 0 \end{cases} \quad (3.17)$$

Let $[x^+]$ and $[x^-]$ be the steady state representative point corresponding to the input u^+ and u^- , where x is a column vector. Then a sufficient condition for the system to reach the sliding surface is given by

$$\begin{aligned} [x^+] &\in S(x) < 0 \\ [x^-] &\in S(x) > 0 \end{aligned} \quad (3.18)$$

This means, if the steady state point for one substructure belongs to the region of the phase space reserved to the other substructure, sooner or later the system representative point will hit the sliding surface.

3.4.2 Existence Condition

The sliding mode existence condition requires that when the system phase trajectories are near the sliding surface $S(x, t) = 0$ in both regions, they must be directed toward the sliding surface. In other words, for the points which satisfy $S > 0$, the corresponding state velocity vector f^+ must be directed toward the sliding surface when it approaches

the sliding surface, and the corresponding state velocity vector f^- will do the same movement for the points satisfying $S < 0$.

Indicating with subscript N the components of the state velocity vectors f^+ and f^- orthogonal to the sliding surface, the following equations can be obtained

$$\begin{aligned}\lim_{S \rightarrow 0^+} f_N^+ < 0 &\Rightarrow \lim_{S \rightarrow 0^+} \nabla S f^+ < 0 \\ \lim_{S \rightarrow 0^-} f_N^- > 0 &\Rightarrow \lim_{S \rightarrow 0^-} \nabla S f^- > 0\end{aligned}\quad (3.19)$$

Since

$$\frac{dS}{dt} = \sum_{i=1}^n \frac{\partial S}{\partial x_i} \frac{dx_i}{dt} = \nabla S f \quad (3.20)$$

The existence condition of the sliding mode becomes

$$\lim_{S \rightarrow 0^+} \frac{dS}{dt} < 0, \quad \lim_{S \rightarrow 0^-} \frac{dS}{dt} > 0 \quad \Rightarrow \lim_{S \rightarrow 0} \frac{dS}{dt} < 0 \quad (3.21)$$

When the inequality equation (3.21) holds in the entire state space and not only in the region around the sliding surface, then this condition is also sufficient condition for the system to reach the sliding surface.

3.4.3 Equivalent Control

In this section, we focus on the behavior of the system operated in a sliding regime.

Equation (3.22) defines a system that is linear with the control input,

$$\dot{x} = f(x, t) + g(x, t)u \quad (3.22)$$

The scalar control input u is discontinuous on the sliding surface $S(x, t) = 0$, while f and g are discontinuous function vectors. Under sliding mode control, the system trajectories should stay on the sliding surface $S(x, t) = 0$, that is,

$$S(x,t) = 0 \Rightarrow \dot{S}(x,t) = 0 \quad (3.23)$$

$$\dot{S}(x,t) = \frac{dS}{dt} = \sum_{i=1}^n \frac{\partial S}{\partial x_i} \frac{dx_i}{dt} = \nabla S \dot{x} = J \dot{x} \quad (3.24)$$

where J is a $1 \times n$ matrix, the elements of which are the derivatives of the sliding surface with respect to the state variables. Using equations (3.22) and (3.24), we obtain

$$J \dot{x} = J f(x,t) + J g(x,t)u_{eq} = 0 \quad (3.25)$$

where the control input u was substituted by a equivalent control u_{eq} that represents an equivalent continuous control input, which maintains the system on the sliding surface.

Rearranging the equation (3.25), we get

$$u_{eq} = -(J g)^{-1} J f(x,t) \quad (3.26)$$

Substituting equation (3.26) into equation (3.22) leads to

$$\dot{x} = [I - g(J g)^{-1} J] f(x,t) \quad (3.27)$$

Equation (3.27) describes the system motion under sliding mode control. It is important to note that the matrix $I - g(J g)^{-1} J$ is not of full rank. This is because, under sliding regime, the system motion is constrained to be on the sliding surface. As a consequence, the equivalent system described by equation (3.27) is of the order $n-1$.

This equivalent control u_{eq} is also valid for multiple control inputs. In this case, the system motion is constrained on the hyper surface obtained by the intersection of the individual switching surface $S_i(x,t) = 0$.

3.4.4 Chattering

The chattering phenomenon is described as finite frequency, finite amplitude oscillations in the neighborhood of the sliding manifold. These oscillations are caused by the high

frequency switching of a sliding mode controller exciting unmodeled dynamics in the closed loop system. The chattering phenomenon shown in Fig.3-1 appears in many sliding mode implementations.

The chattering should be definitely eliminated. Otherwise it would result in loud noise, high wear of moving mechanical parts. Many different schemes have been proposed in research literature to eliminate the chattering [12] [13].

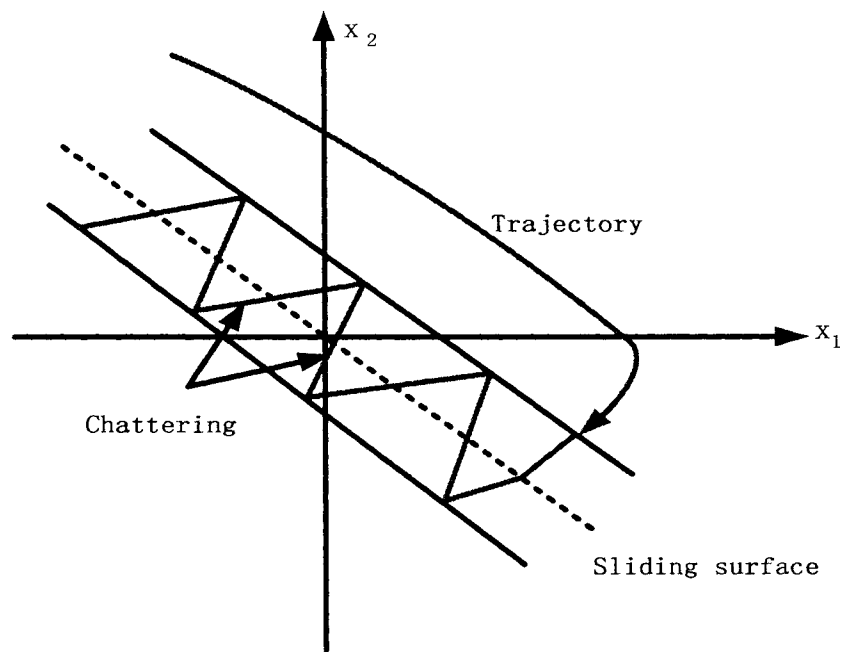


Fig.3-1: Chattering phenomenon in sliding mode control

In summary, the sliding mode controller can be expressed as

$$u = \begin{cases} u^+ & \text{for } S(x) > 0 \\ u_{eq} & \text{for } S(x) = 0 \\ u^- & \text{for } S(x) < 0 \end{cases}$$

3.5 Adaptive Backstepping Control

For systems with parametric uncertainties, there exists adaptive backstepping [5]. Here, a tuning function is designed as a parameter update law such that closed loop system stability is guaranteed. In what follows, the application of adaptive backstepping procedure for a third order nonlinear system in the lower triangular structure is developed.

Consider the following system

$$\begin{aligned}\dot{x}_1 &= x_2 + \phi_1(x_1)\theta \\ \dot{x}_2 &= x_3 + \phi_2(x_1, x_2)\theta \\ \dot{x}_3 &= u + \phi_3(x_1, x_2, x_3)\theta\end{aligned}\tag{3.28}$$

where θ is the unknown constant parameter. x_1, x_2 and x_3 are the state variables and u is the control input. $\phi_1(0) = 0, \phi_2(0) = 0$ and $\phi_3(0) = 0$.

First, if x_2 is considered to be a virtual input for the first equation of (3.28), an adaptive controller can be designed as

$$x_2 = \alpha_1(x_1, \hat{\theta}) = -c_1 z_1 - \phi_1(x_1)\hat{\theta}\tag{3.29}$$

where $z_1 = x_1$ and $\hat{\theta}$ is the estimation of the unknown parameter. Introducing the new error variable $z_2 = x_2 - \alpha_1$, the \dot{z}_1 equation becomes

$$\dot{z}_1 = \alpha_1 + z_2 + \phi_1(x_1)\theta\tag{3.30}$$

Select the Lyapunov function V_1

$$V_1 = \frac{1}{2}z_1^2 + \frac{1}{2\gamma}\tilde{\theta}^2\tag{3.31}$$

where $\tilde{\theta} = \theta - \hat{\theta}$ is the parameter estimation error.

The derivative of the Lyapunov function is

$$\begin{aligned}\dot{V}_1 &= z_1(\alpha_1 + z_2 + \phi_1\theta) - \frac{1}{\gamma}\tilde{\theta}\dot{\hat{\theta}} \\ &= z_1(\alpha_1 + z_2 + \phi_1\hat{\theta}) - \frac{1}{\gamma}\tilde{\theta}(\dot{\hat{\theta}} - \gamma\phi_1z_1)\end{aligned}\quad (3.32)$$

We can eliminate $\tilde{\theta}$ from \dot{V}_1 with the update law $\dot{\hat{\theta}} = \gamma\sigma_1$, where

$$\sigma_1(x_1) = \phi_1(x_1)z_1 \quad (3.33)$$

Since x_2 is a virtual control input, here, we retain the $\tilde{\theta}$ term in \dot{V}_1

$$\dot{V}_1 = -c_1z_1^2 + z_1z_2 + \tilde{\theta}\left(-\frac{1}{\gamma}\dot{\hat{\theta}} + \sigma_1\right) \quad (3.34)$$

Second, x_3 is viewed as the virtual control for the second equation of (3.28).

Introducing the new error variable $z_3 = x_3 - \alpha_2$, the \dot{z}_2 equation becomes

$$\begin{aligned}\dot{z}_2 &= \dot{x}_2 - \frac{\partial\alpha_1}{\partial x_1}\dot{x}_1 - \frac{\partial\alpha_1}{\partial\hat{\theta}}\dot{\hat{\theta}} \\ &= x_3 + \phi_2\theta - \frac{\partial\alpha_1}{\partial x_1}\dot{x}_1 - \frac{\partial\alpha_1}{\partial\hat{\theta}}\dot{\hat{\theta}} \\ &= z_3 + \alpha_2 - \frac{\partial\alpha_1}{\partial x_1}x_2 - \frac{\partial\alpha_1}{\partial\hat{\theta}}\dot{\hat{\theta}} - \frac{\partial\alpha_1}{\partial x_1}\phi_1\theta + \phi_2\theta\end{aligned}\quad (3.35)$$

Choose a Lyapunov function V_2

$$V_2 = V_1 + \frac{1}{2}z_2^2 \quad (3.36)$$

The derivative of the Lyapunov function is

$$\begin{aligned}\dot{V}_2 &= -c_1z_1^2 + z_2(z_1 + z_3 + \alpha_2 - \frac{\partial\alpha_1}{\partial x_1}x_2 - \frac{\partial\alpha_1}{\partial\hat{\theta}}\dot{\hat{\theta}} - \frac{\partial\alpha_1}{\partial x_1}\phi_1\theta + \phi_2\theta) + \tilde{\theta}\left(-\frac{1}{\gamma}\dot{\hat{\theta}} + \sigma_1\right) \\ &= -c_1z_1^2 + z_2(z_1 + z_3 + \alpha_2 - \frac{\partial\alpha_1}{\partial x_1}x_2 - \frac{\partial\alpha_1}{\partial\hat{\theta}}\dot{\hat{\theta}} - \frac{\partial\alpha_1}{\partial x_1}\phi_1\hat{\theta} + \phi_2\hat{\theta}) + \tilde{\theta}\left(-\frac{1}{\gamma}\dot{\hat{\theta}} + \sigma_1 + z_2\left(-\frac{\partial\alpha_1}{\partial x_1}\phi_1 + \phi_2\right)\right)\end{aligned}\quad (3.37)$$

From the equation (3.37), the term $\hat{\theta}$ can be eliminated with the update law $\dot{\hat{\theta}} = \gamma\sigma_2$, where

$$\sigma_2(x_1, x_2, \hat{\theta}) = \sigma_1 + z_2 \left(-\frac{\partial \alpha_1}{\partial x_1} \phi_1 + \phi_2 \right) \quad (3.38)$$

If x_3 is actual control for the given system, we could let $z_3 \equiv 0$, that is, $x_3 \equiv \alpha_2$. α_2 can be designed as follows

$$\alpha_2(x_1, x_2, \hat{\theta}) = -z_1 - c_2 z_2 + \frac{\partial \alpha_1}{\partial x_1} x_2 + \frac{\partial \alpha_1}{\partial \hat{\theta}} \gamma \sigma_2 + \frac{\partial \alpha_1}{\partial x_1} \phi_1 \hat{\theta} - \phi_2 \hat{\theta} \quad (3.39)$$

to make $\dot{V}_2 = -c_1 z_1^2 - c_2 z_2^2$

Since x_3 is virtual control, we retain the tuning function σ_2 in \dot{V}_2 , that is,

$$\dot{V}_2 = -c_1 z_1^2 - c_2 z_2^2 + z_2 z_3 + z_2 \frac{\partial \alpha_1}{\partial \hat{\theta}} (\gamma \sigma_2 - \dot{\hat{\theta}}) + \tilde{\theta} \left(\sigma_2 - \frac{1}{\gamma} \dot{\hat{\theta}} \right) \quad (3.40)$$

Finally, the derivative of z_3 can be expressed as

$$\begin{aligned} \dot{z}_3 &= \dot{x}_3 - \dot{\alpha}_2 = u + \phi_3 \theta - \frac{\partial \alpha_2}{\partial x_1} \dot{x}_1 - \frac{\partial \alpha_2}{\partial x_2} \dot{x}_2 - \frac{\partial \alpha_2}{\partial \hat{\theta}} \dot{\hat{\theta}} \\ &= u + \phi_3 \theta - \frac{\partial \alpha_2}{\partial x_1} x_2 - \frac{\partial \alpha_2}{\partial x_1} \phi_1 \theta - \frac{\partial \alpha_2}{\partial x_2} x_3 - \frac{\partial \alpha_2}{\partial x_2} \phi_2 \theta - \frac{\partial \alpha_2}{\partial \hat{\theta}} \dot{\hat{\theta}} \end{aligned} \quad (3.41)$$

Now, choose the Lyapunov function V_3

$$V_3 = V_2 + \frac{1}{2} z_3^2 \quad (3.42)$$

The derivative of V_3 is given by

$$\begin{aligned} \dot{V}_3 &= -c_1 z_1^2 - c_2 z_2^2 + z_2 \frac{\partial \alpha_1}{\partial \hat{\theta}} (\gamma \sigma_2 - \dot{\hat{\theta}}) \\ &\quad + z_3 \left(z_2 + u + \phi_3 \theta - \frac{\partial \alpha_2}{\partial x_1} x_2 - \frac{\partial \alpha_2}{\partial x_1} \phi_1 \theta - \frac{\partial \alpha_2}{\partial x_2} x_3 - \frac{\partial \alpha_2}{\partial x_2} \phi_2 \theta - \frac{\partial \alpha_2}{\partial \hat{\theta}} \dot{\hat{\theta}} \right) + \tilde{\theta} \left(\sigma_2 - \frac{1}{\gamma} \dot{\hat{\theta}} \right) \end{aligned}$$

$$\begin{aligned}
&= -c_1 z_1^2 - c_2 z_2^2 + z_2 \frac{\partial \alpha_1}{\partial \hat{\theta}} (\gamma \sigma_2 - \dot{\hat{\theta}}) \\
&\quad + z_3 (z_2 + u + \phi_3 \hat{\theta} - \frac{\partial \alpha_2}{\partial x_1} x_2 - \frac{\partial \alpha_2}{\partial x_1} \phi_1 \hat{\theta} - \frac{\partial \alpha_2}{\partial x_2} x_3 - \frac{\partial \alpha_2}{\partial x_2} \phi_2 \hat{\theta} - \frac{\partial \alpha_2}{\partial \hat{\theta}} \dot{\hat{\theta}}) \\
&\quad + \tilde{\theta} (\sigma_2 - \frac{1}{\gamma} \dot{\hat{\theta}} + z_3 (\phi_3 - \frac{\partial \alpha_2}{\partial x_1} \phi_1 - \frac{\partial \alpha_2}{\partial x_2} \phi_2))
\end{aligned} \tag{3.43}$$

In equation (3.43), the term $\dot{\hat{\theta}}$ can be eliminated with the update law $\dot{\hat{\theta}} = \gamma \sigma_3$, where σ_3 is tuning function

$$\sigma_3(x_1, x_2, x_3, \hat{\theta}) = \sigma_2 + z_3 (\phi_3 - \frac{\partial \alpha_2}{\partial x_1} \phi_1 - \frac{\partial \alpha_2}{\partial x_2} \phi_2) \tag{3.44}$$

The control input can be designed as follows

$$u = -z_2 - c_3 z_3 - \phi_3 \hat{\theta} + \frac{\partial \alpha_2}{\partial x_1} x_2 + \frac{\partial \alpha_2}{\partial x_1} \phi_1 \hat{\theta} + \frac{\partial \alpha_2}{\partial x_2} x_3 + \frac{\partial \alpha_2}{\partial x_2} \phi_2 \hat{\theta} + \frac{\partial \alpha_2}{\partial \hat{\theta}} \gamma \sigma_3 + v_3 \tag{3.45}$$

where v_3 is a correction term to be determined later. \dot{V}_3 becomes

$$\dot{V}_3 = -c_1 z_1^2 - c_2 z_2^2 - c_3 z_3^2 + z_2 \frac{\partial \alpha_1}{\partial \hat{\theta}} (\gamma \sigma_2 - \dot{\hat{\theta}}) + z_3 v_3 \tag{3.46}$$

Note that

$$\dot{\hat{\theta}} - \gamma \sigma_2 = \gamma \sigma_3 - \gamma \sigma_2 = \gamma \sigma_3 (\phi_3 - \frac{\partial \alpha_2}{\partial x_1} \phi_1 - \frac{\partial \alpha_2}{\partial x_2} \phi_2) \tag{3.47}$$

and equation (3.46) can be rewritten as

$$\dot{V}_3 = -c_1 z_1^2 - c_2 z_2^2 - c_3 z_3^2 + z_3 (v_3 - z_2 \frac{\partial \alpha_1}{\partial \hat{\theta}} \gamma (\phi_3 - \frac{\partial \alpha_2}{\partial x_1} \phi_1 - \frac{\partial \alpha_2}{\partial x_2} \phi_2)) \tag{3.48}$$

Now the correction term v_3 is chosen as

$$v_3 = z_2 \frac{\partial \alpha_1}{\partial \hat{\theta}} \gamma (\phi_3 - \frac{\partial \alpha_2}{\partial x_1} \phi_1 - \frac{\partial \alpha_2}{\partial x_2} \phi_2) \tag{3.49}$$

Finally, the derivative of V_3 can be obtained

$$\dot{V}_3 = -c_1 z_1^2 - c_2 z_2^2 - c_3 z_3^2 < 0 \quad (3.50)$$

In summary, the adaptive backstepping controller for a given system (3.28) can be designed as follows

$$u = -z_2 - c_3 z_3 - \phi_3 \hat{\theta} + \frac{\partial \alpha_2}{\partial x_1} x_2 + \frac{\partial \alpha_2}{\partial x_1} \phi_1 \hat{\theta} + \frac{\partial \alpha_2}{\partial x_2} x_3 + \frac{\partial \alpha_2}{\partial x_2} \phi_2 \hat{\theta} + \frac{\partial \alpha_2}{\partial \hat{\theta}} \gamma \sigma_3 + v_3$$

with the update law $\dot{\hat{\theta}} = \gamma \sigma_3$

where $\alpha_1(x_1, \hat{\theta}) = -c_1 z_1 - \phi_1(x_1) \hat{\theta}$

$$\alpha_2(x_1, x_2, \hat{\theta}) = -z_1 - c_2 z_2 + \frac{\partial \alpha_1}{\partial x_1} x_2 + \frac{\partial \alpha_1}{\partial \hat{\theta}} \gamma \sigma_2 + \frac{\partial \alpha_1}{\partial x_1} \phi_1 \hat{\theta} - \phi_2 \hat{\theta}$$

$$v_3 = z_2 \frac{\partial \alpha_1}{\partial \hat{\theta}} \gamma (\phi_3 - \frac{\partial \alpha_2}{\partial x_1} \phi_1 - \frac{\partial \alpha_2}{\partial x_2} \phi_2)$$

3.6 Reduced Order Observer

Suppose not all state variables can be measured. Then the state vector x can be partitioned into two sets,

x_1 : Variables that can be measured directly

x_2 : Variables that cannot be measured

The state equations are written as follows

$$\dot{x}_1 = A_{11} x_1 + A_{12} x_2 + B_1 \mu$$

$$\dot{x}_2 = A_{21} x_1 + A_{22} x_2 + B_2 \mu$$

(3.51)

and the observation equation is

$$y = C_1 x_1 \quad (3.52)$$

where C_1 is square and nonsingular matrix.

For the full order observer, we could get the observer equations

$$\begin{aligned}\dot{\hat{x}}_1 &= A_{11}\hat{x}_1 + A_{12}\hat{x}_2 + B_1\mu + L_1(y - C_1\hat{x}_1) \\ \dot{\hat{x}}_2 &= A_{21}\hat{x}_1 + A_{22}\hat{x}_2 + B_2\mu + L_2(y - C_1\hat{x}_1)\end{aligned}\tag{3.53}$$

Because we can measure the state variables x_1 directly, there is no need to implement the first observer equation for \hat{x}_1 .

$$\hat{x}_1 = x_1 = C_1^{-1}y\tag{3.54}$$

In this case the observer for those state variables that cannot be measured becomes

$$\dot{\hat{x}}_2 = A_{21}C_1^{-1}y + A_{22}\hat{x}_2 + B_2\mu\tag{3.55}$$

which is a dynamic system of the same order as the number of state variables that cannot be measured. The dynamic behavior of this reduced order observer is governed by the eigenvalues of A_{22} , a matrix over which the designer has no control. Since there is no assurance that the eigenvalues of A_{22} are stable, we need a more general system for the reconstruction of \hat{x}_2 . We take

$$\hat{x}_2 = Ly + z\tag{3.56}$$

where $\dot{z} = Fz + Gy + H\mu$

Define the estimation error

$$e = x - \hat{x} = \begin{bmatrix} x_1 - \hat{x}_1 \\ x_2 - \hat{x}_2 \end{bmatrix} = \begin{bmatrix} e_1 \\ e_2 \end{bmatrix} = \begin{bmatrix} 0 \\ e_2 \end{bmatrix}\tag{3.57}$$

then we get

$$\begin{aligned}\dot{e}_2 &= \dot{x}_2 - \dot{\hat{x}}_2 \\ &= A_{21}x_1 + A_{22}x_2 + B_2\mu - [L\dot{y} + \dot{z}]\end{aligned}$$

$$\begin{aligned}
&= A_{21}x_1 + A_{22}x_2 + B_2\mu - LC_1\dot{x}_1 - Fz - Gy - H\mu \\
&= A_{21}x_1 + A_{22}x_2 + B_2\mu - LC_1(A_{11}x_1 + A_{12}x_2 + B_1\mu) - F(\hat{x}_2 - Ly) - Gy - H\mu
\end{aligned} \tag{3.58}$$

Since

$$\hat{x}_2 - Ly = x_2 - e_2 - Ly = x_2 - e_2 - LC_1x_1 \tag{3.59}$$

we get

$$\dot{e}_2 = Fe_2 + (A_{21} - LC_1A_{11} - GC_1 + FLC_1)x_1 + (A_{22} - LC_1A_{12} - F)x_2 + (B_2 - LC_1B_1 - H)\mu \tag{3.60}$$

The matrices multiplying x_1 , x_2 and μ must be zero so that the error could be independent of x_1 , x_2 and μ

$$\begin{aligned}
F &= A_{22} - LC_1A_{12} \\
H &= B_2 - LC_1B_1 \\
G &= (A_{21} - LC_1A_{11})C_1^{-1} + FL
\end{aligned} \tag{3.61}$$

Then

$$\dot{e}_2 = Fe_2 \tag{3.62}$$

and for stability the eigenvalues of F must lie in the left half s -plane. Therefore, we see that the problem of reduced order observer is similar to the full order observer with $(A_{22} - LC_1A_{12})$ playing the role of $(A - LC)$. The block diagram schematic is shown in Fig.3-2.

In summary, the reduced order observer can be implemented by introducing new state variables z . The state variables x_2 , which can not be measured, can be estimated with the equation

$$\begin{aligned}
\hat{x}_2 &= Ly + z \\
\dot{z} &= (A_{22} - LC_1A_{12})z + [(A_{21} - LC_1A_{11})C_1^{-1} + FL]y + (B_2 - LC_1B_1)\mu
\end{aligned}$$

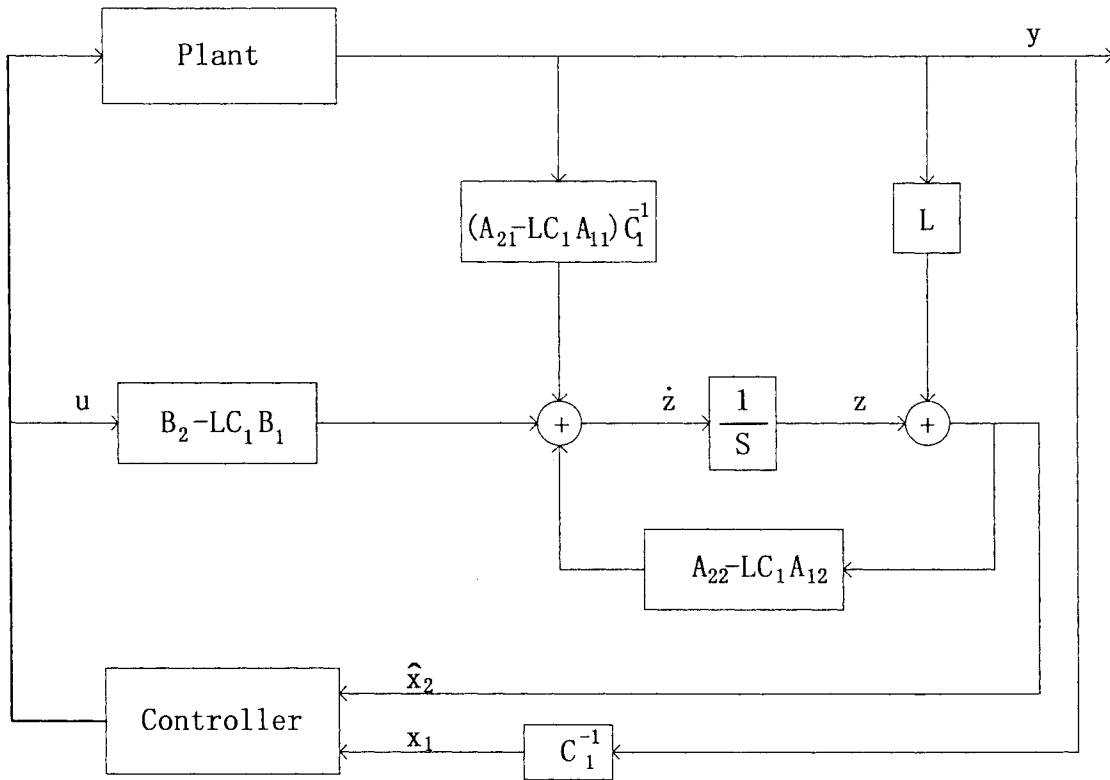


Fig.3-2: Block diagram of reduced order observer

Chapter 4

Nonlinear Control Design Methods for Buck Converter

4.1 Introduction

DC-DC power converters, as one type of the simplest power electronic circuits, have been widely used in power supply equipment for most electronic systems. In recent years, several different nonlinear control techniques have been developed for DC-DC power converters. These include feedback linearization technique [26], self-tuned dither control [13], sliding mode control [22]-[24], backstepping control strategy [11] [21], and so on. In this chapter, the following five nonlinear controllers are designed for a DC-DC buck converter based on three nonlinear control methods discussed in the previous chapter.

- Backstepping control
- Sliding mode control
- Backstepping sliding mode control
- Adaptive backstepping control
- Adaptive backstepping sliding mode control

Our objective is to develop feedback controllers for the DC-DC buck converter to minimize the steady state error in the presence of load changes and input voltage variations.

Before we start to design the nonlinear controllers, let's recall the state space averaging model of the DC-DC buck converter introduced in Chapter 2,

$$\dot{x}_1 = \theta_1 x_1 + \theta_2 x_2 \quad (4.1)$$

$$\dot{x}_2 = \theta_3 x_1 + \theta_4 x_2 + \theta_5 \mu \quad (4.2)$$

where $\theta_1, \theta_2, \theta_3, \theta_4$ and θ_5 are the parameters of the buck converter defined by the following equations,

$$\theta_1 = -\frac{1}{(R + R_C)C}$$

$$\theta_2 = \frac{R}{(R + R_C)C}$$

$$\theta_3 = -\frac{R}{(R + R_C)L}$$

$$\theta_4 = -\frac{RR_C}{(R + R_C)L} - \frac{R_L}{L} - \frac{R_S}{L}$$

$$\theta_5 = \frac{E}{L}$$

x_1 and x_2 represent, respectively, the output capacitor voltage v_C and inductor current i_L , R_C , R_L and R_S denote the resistance of the capacitor, inductor and switch/diode, respectively, E stands for the value of the external source voltage, R is the load resistance.

Note that θ_5 is always greater than the zero if $E \neq 0$ and θ_2 is always greater than zero if the load resistance R is not zero. Throughout the thesis, we assume that $E \neq 0$ and $R \neq 0$.

In order to achieve a good control performance, an integral term is introduced to eliminate the steady state error. The state equation is given by:

$$\dot{\xi} = x_1 - V_d \quad (4.3)$$

where V_d is the desired output voltage.

4.2 Backstepping Control

According to the backstepping design theory, a controller is designed in the following steps:

Step1. In equation (4.3), x_1 is viewed as a virtual input. Select the Lyapunov function:

$$V_1 = \frac{1}{2} \xi^2 \quad (4.4)$$

Then the virtual control

$$x_1 = \alpha_0 = -c_0 \xi + V_d \quad (4.5)$$

makes the derivative of V_1 , that is,

$$\dot{V}_1 = \xi \dot{\xi} = -c_0 \xi^2 + \xi(x_1 - \alpha_0) \quad (4.6)$$

negative definite, where $c_0 > 0$ is a design parameter.

Differentiating α_0 to get $\dot{\alpha}_0$ and $\ddot{\alpha}_0$ as follows:

$$\dot{\alpha}_0 = -c_0 \dot{\xi} + \dot{V}_d = -c_0(x_1 - V_d) + \dot{V}_d \quad (4.7)$$

$$\ddot{\alpha}_0 = -c_0(\dot{x}_1 - \dot{V}_d) + \ddot{V}_d = -c_0(\theta_1 x_1 + \theta_2 x_2) + c_0 \dot{V}_d + \ddot{V}_d \quad (4.8)$$

Step2. The derivative of the new error $x_1 - \alpha_0$ is expressed as

$$\dot{x}_1 - \dot{\alpha}_0 = \theta_1 x_1 + \theta_2 x_2 - \dot{\alpha}_0 \quad (4.9)$$

The augmented Lyapunov function is chosen as

$$V_2 = V_1 + \frac{1}{2}(x_1 - \alpha_0)^2 \quad (4.10)$$

The derivative of V_2 , using (4.6) and (4.9), is

$$\begin{aligned} \dot{V}_2 &= \dot{V}_1 + (x_1 - \alpha_0)(\dot{x}_1 - \dot{\alpha}_0) \\ &= -c_0 \xi^2 + \xi(x_1 - \alpha_0) + (x_1 - \alpha_0)(\dot{x}_1 - \dot{\alpha}_0) \\ &= -c_0 \xi^2 + (x_1 - \alpha_0)(\xi + \theta_1 x_1 + \theta_2 x_2 - \dot{\alpha}_0) \end{aligned} \quad (4.11)$$

The virtual control can be designed for x_2 , that is,

$$x_2 = \alpha_1 = \frac{1}{\theta_2} [-c_1(x_1 - \alpha_0) - \xi - \theta_1 x_1 + \dot{\alpha}_0] \quad (4.12)$$

to make \dot{V}_2 negative definite, i.e.

$$\begin{aligned} \dot{V}_2 &= -c_0 \xi^2 + (x_1 - \alpha_0)(\xi + \theta_1 x_1 + \theta_2 x_2 - \dot{\alpha}_0 + \theta_2 \alpha_1 - \theta_2 \dot{\alpha}_1) \\ &= -c_0 \xi^2 + (x_1 - \alpha_0)[\xi + \theta_1 x_1 + \theta_2 x_2 - \dot{\alpha}_0 + (-c_1(x_1 - \alpha_0) - \xi - \theta_1 x_1 + \dot{\alpha}_0) - \theta_2 \dot{\alpha}_1] \\ &= -c_0 \xi^2 + (x_1 - \alpha_0)[-c_1(x_1 - \alpha_0) + \theta_2(x_2 - \alpha_1)] \\ &= -c_0 \xi^2 - c_1(x_1 - \alpha_0)^2 + \theta_2(x_1 - \alpha_0)(x_2 - \alpha_1) \end{aligned} \quad (4.13)$$

where $c_1 > 0$ is a design parameter.

Step3. It follows from (4.12) that the time derivative of α_1 is given by

$$\begin{aligned} \dot{\alpha}_1 &= \frac{1}{\theta_2} [-c_1(\dot{x}_1 - \dot{\alpha}_0) - \dot{\xi} - \theta_1 \dot{x}_1 + \ddot{\alpha}_0] \\ &= \frac{1}{\theta_2} [(c_1 \dot{\alpha}_0 - (x_1 - \alpha_0) + \ddot{\alpha}_0) + (-c_1 - \theta_1)(\theta_1 x_1 + \theta_2 x_2)] \end{aligned} \quad (4.14)$$

The derivative of $x_2 - \alpha_1$ can be expressed as

$$\dot{x}_2 - \dot{\alpha}_1 = \theta_3 x_1 + \theta_4 x_2 + \theta_5 \mu - \dot{\alpha}_1 \quad (4.15)$$

At this point, select a Lyapunov function and design control input μ to make its derivative negative definite. To this end, choose

$$V_3 = V_2 + \frac{1}{2}(x_2 - \alpha_1)^2 \quad (4.16)$$

then its derivative, using equations (4.13) and (4.15), is

$$\begin{aligned} \dot{V}_3 &= \dot{V}_2 + (x_2 - \alpha_1)(\dot{x}_2 - \dot{\alpha}_1) \\ &= -c_0 \xi^2 - c_1(x_2 - \alpha_1)^2 + \theta_2(x_1 - \alpha_0)(x_2 - \alpha_1) + (x_2 - \alpha_1)(\dot{x}_2 - \dot{\alpha}_1) \end{aligned}$$

$$= -c_0 \xi^2 - c_1 (x_2 - \alpha_1)^2 + (x_2 - \alpha_1) [\theta_2 (x_1 - \alpha_0) + \theta_3 x_1 + \theta_4 x_2 + \theta_5 \mu - \dot{\alpha}_1] \quad (4.17)$$

The control input μ , which cancels the indefinite term in \dot{V}_3 , is given by.

$$\mu = \frac{1}{\theta_5} [-c_2 (x_2 - \alpha_1) - \theta_2 (x_1 - \alpha_0) - \theta_3 x_1 - \theta_4 x_2 + \dot{\alpha}_1] \quad (4.18)$$

where $c_2 > 0$ is a design parameter.

With the designed control input μ , the derivative of the Lyapunov function V_3 is

$$\dot{V}_3 = -c_0 \xi^2 - c_1 (x_1 - \alpha_0)^2 - c_2 (x_2 - \alpha_1)^2 \quad (4.19)$$

which is negative definite.

4.3 Sliding Mode Control

4.3.1 Design of Sliding Surface

In sliding mode control, the input switching states μ , which corresponds to the turning on and off of the power converter's switch, is determined by a sliding surface S .

The basic idea of sliding mode control is to design a certain sliding surface in its control law that will direct the trajectory of the state variables towards a desired origin. For our system's model, assume the output voltage error is $e_1 = v_o - V_d$, where V_d is output reference voltage. The following sliding surface is chosen

$$S = \dot{e}_1 + K e_1 = 0 \quad (4.20)$$

where K is a sliding coefficient. Then the dynamic performance of the error e_1 is

$$e_1(t) = e_1(\tau) e^{-K(t-\tau)} \quad (4.21)$$

Where τ is any point in time and $e_1(\tau)$ is the voltage error at τ .

According to Routh criteria, when the sliding coefficient $K > 0$ is met, the error e_1

converges to zero. Note that $x_1 = v_o$ and

$$\dot{e}_1 = \dot{v}_o = \theta_1 x_1 + \theta_2 x_2 \quad (4.22)$$

From (4.20) and (4.22), it follows that

$$\begin{aligned} S &= \dot{e}_1 + Ke_1 = \theta_1 x_1 + \theta_2 x_2 + K(x_1 - V_d) \\ &= (\theta_1 + K)x_1 + \theta_2 x_2 + KV_d. \end{aligned} \quad (4.23)$$

The purpose of the sliding surface is to serve as a boundary to split the phase plane into two regions. Each of these regions is specified with a switching state to direct the phase trajectory toward the sliding surface. It is only when the phase trajectory reaches and tracks the sliding line toward the origin that the system is considered to be stable.

4.3.2 Equivalent Control

The equivalent control input μ_{eq} can be formulated by setting $\dot{S} = 0$

$$\begin{aligned} \dot{S} &= (\theta_1 + K)\dot{x}_1 + \theta_2 \dot{x}_2 \\ &= (\theta_1 + K)(\theta_3 x_1 + \theta_4 x_2 + \theta_5 \mu) + \theta_2(\theta_3 x_1 + \theta_4 x_2 + \theta_5 \mu) \\ &= ((\theta_1 + K)\theta_3 + \theta_2 \theta_3)x_1 + ((\theta_1 + K)\theta_4 + \theta_2 \theta_4)x_2 + (\theta_1 + K)\theta_5 \mu + \theta_2 \theta_5 \mu \end{aligned} \quad (4.24)$$

General speaking, the control input has two forms: $\mu = 0.5(1 + \text{sign}(S))$ or $\mu = 0.5(1 - \text{sign}(S))$ in DC-DC converters. How to select a control input value is depend on the sliding surface $S = 0$ and approaching condition $S\dot{S} < 0$. Assume the control input is $\mu = 0.5(1 - \text{sign}(S))$. Then,

$$\mu = \begin{cases} 0 & \text{for } S > 0 \\ 1 & \text{for } S < 0 \end{cases} \quad (4.25)$$

To get equivalent control, let $\dot{S} = 0$. Using equation (4.24), we have

$$\mu_{eq} = -\frac{(\theta_1 + K)\theta_1 + \theta_2\theta_3}{\theta_2\theta_5}x_1 - \frac{(\theta_1 + K)\theta_2 + \theta_2\theta_4}{\theta_2\theta_5}x_2 \quad (4.26)$$

where μ_{eq} is continuous and $0 < \mu_{eq} < 1$.

4.3.3 Existence of Sliding Mode Control

Although abiding the hitting condition, which states that the system trajectory must eventually reach the sliding surface, the control law in (4.25) only provides the general requirement that the trajectories will be driven toward the sliding surface. However there is no assurance that the trajectory can be maintained on this surface. To ensure that the trajectory is maintained on the sliding surface, the existence condition, which is derived from Lyapunov's second method to determine asymptotic stability, must be obeyed

$$\lim_{S \rightarrow 0} S\dot{S} < 0 \quad (4.27)$$

Thus, by substituting the time derivative of S , the condition for the existence of a sliding mode is

$$S\dot{S} = S[(\theta_1 + K)\theta_1 + \theta_2\theta_3]x_1 + [(\theta_1 + K)\theta_2 + \theta_2\theta_4]x_2 + \theta_2\theta_5\mu < 0 \quad (4.28)$$

The control input μ includes two parts

$$\mu = \mu_{eq} + \mu_n \quad (4.29)$$

where μ_{eq} is equivalent control and μ_n is nonlinear switching control.

Substituting equation (4.29) into (4.28) produces

$$S\dot{S} = S(\theta_2\theta_5\mu_n) < 0 \Rightarrow S\mu_n < 0 \quad (4.30)$$

When $S > 0$, $\mu = 0$ and $0 < \mu_{eq} < 1$, $\mu_n = \mu - \mu_{eq} < 0$. At this time, the condition

$S\dot{S} = S\mu_n < 0$ is met. On the other hand, when $S < 0$, $\mu = 1$ and $0 < \mu_{eq} < 1$,

$\mu_n = \mu - \mu_{eq} > 0$. At this time, the condition $S\dot{S} = S\mu_n < 0$ is also met. Therefore, the condition $S\dot{S} < 0$ is always met, then the sliding mode exists and sliding mode control is effective.

4.3.4 Chattering

Ideally, a converter will switch at infinite frequency with its phase trajectory moving on the sliding surface when it enters sliding mode operation. However, in the presence of switching imperfections, such as switching time constant and time delay, this is not possible. The discontinuity will produce a particular dynamic behavior around the sliding surface known as chattering. If the chattering is left uncontrolled, the converter system will become self-oscillation at a very high switching frequency corresponding to the chattering dynamics. This is undesirable because high switching frequency will result in excessive switching losses, inductor losses, and electromagnetic interference noise.

To solve this problem, the control law in (4.25) is redefined as

$$\mu = \begin{cases} 0 & \text{for } S > k \\ \mu_{eq} & \text{for } -k \leq S \leq k \\ 1 & \text{for } S < -k \end{cases} \quad (4.31)$$

where k is an arbitrarily small value. The reason for introducing a hysteresis band with the boundary condition $S > k$ and $S < -k$ is to provide a form of control to the switching frequency of the converter [25]. This is a method commonly employed to alleviate the chattering effect of sliding mode control.

4.4 Backstepping Sliding Mode Control

The design procedures are shown as follows.

Step1. In equation (4.3), x_1 is viewed as a virtual input. Select the Lyapunov function:

$$V_1 = \frac{1}{2} \xi^2 \quad (4.32)$$

Then the virtual control

$$x_1 = \alpha_0 = -c_0 \xi + \dot{V}_d \quad (4.33)$$

makes the derivative of V_1 , that is,

$$\dot{V}_1 = \xi \dot{\xi} = -c_0 \xi^2 + \xi(x_1 - \alpha_0) \quad (4.34)$$

negative definite, where $c_0 > 0$ is a design parameter.

Differentiating α_0 yields

$$\dot{\alpha}_0 = -c_0 \dot{\xi} + \dot{V}_d = -c_0(x_1 - \dot{V}_d) + \dot{V}_d \quad (4.35)$$

$$\ddot{\alpha}_0 = -c_0(\dot{x}_1 - \dot{V}_d) + \ddot{V}_d = -c_0(\theta_1 x_1 + \theta_2 x_2) + c_0 \dot{V}_d + \ddot{V}_d \quad (4.36)$$

Step2. The derivative of the error $x_1 - \alpha_0$ is expressed as

$$\dot{x}_1 - \dot{\alpha}_0 = \theta_1 x_1 + \theta_2 x_2 - \dot{\alpha}_0 \quad (4.37)$$

The augmented Lyapunov function is chosen as

$$V_2 = V_1 + \frac{1}{2}(x_1 - \alpha_0)^2 \quad (4.38)$$

The derivative of V_2 , using (4.34) and (4.37), is

$$\begin{aligned} \dot{V}_2 &= \dot{V}_1 + (x_1 - \alpha_0)(\dot{x}_1 - \dot{\alpha}_0) \\ &= -c_0 \xi^2 + \xi(x_1 - \alpha_0) + (x_1 - \alpha_0)(\dot{x}_1 - \dot{\alpha}_0) \\ &= -c_0 \xi^2 + (x_1 - \alpha_0)(\xi + \theta_1 x_1 + \theta_2 x_2 - \dot{\alpha}_0) \end{aligned} \quad (4.39)$$

The virtual control can be designed for x_2 as

$$x_2 = \alpha_1 = \frac{1}{\theta_2} [-c_1(x_1 - \alpha_0) - \xi - \theta_1 x_1 + \dot{\alpha}_0] \quad (4.40)$$

to make \dot{V}_2 negative definite, i.e.

$$\begin{aligned} \dot{V}_2 &= -c_0 \xi^2 + (x_1 - \alpha_0)(\xi + \theta_1 x_1 + \theta_2 x_2 - \dot{\alpha}_0 + \theta_2 \alpha_1 - \theta_2 \dot{\alpha}_1) \\ &= -c_0 \xi^2 + (x_1 - \alpha_0)[\xi + \theta_1 x_1 + \theta_2 x_2 - \dot{\alpha}_0 + (-c_1(x_1 - \alpha_0) - \xi - \theta_1 x_1 + \dot{\alpha}_0) - \theta_2 \dot{\alpha}_1] \\ &= -c_0 \xi^2 + (x_1 - \alpha_0)[-c_1(x_1 - \alpha_0) + \theta_2(x_2 - \alpha_1)] \\ &= -c_0 \xi^2 - c_1(x_1 - \alpha_0)^2 + \theta_2(x_1 - \alpha_0)(x_2 - \alpha_1) \end{aligned} \quad (4.41)$$

where $c_1 > 0$ is a design parameter.

Step3. It follows from (4.40) that the time derivative of α_1 is given by

$$\begin{aligned} \dot{\alpha}_1 &= \frac{1}{\theta_2} [-c_1(\dot{x}_1 - \dot{\alpha}_0) - \dot{\xi} - \theta_1 \dot{x}_1 + \ddot{\alpha}_0] \\ &= \frac{1}{\theta_2} [(c_1 \dot{\alpha}_0 - (x_1 - V_d) + \ddot{\alpha}_0) + (-c_1 - \theta_1)(\theta_1 x_1 + \theta_2 x_2)] \end{aligned} \quad (4.42)$$

The derivative of $x_2 - \alpha_1$ can be expressed as

$$\dot{x}_2 - \dot{\alpha}_1 = \theta_3 x_1 + \theta_4 x_2 + \theta_5 \mu - \dot{\alpha}_1 \quad (4.43)$$

At this point we will define a sliding surface S , select a Lyapunov function V_3 and design a feedback law μ to make \dot{V}_3 negative definite.

$$\begin{aligned} S &= x_2 - \alpha_1 \\ V_3 &= V_2 + \frac{1}{2} S^2 \end{aligned} \quad (4.44)$$

The derivative of Lyapunov function V_3 , using equations (4.41), (4.42) and (4.43), is:

$$\begin{aligned}
\dot{V}_3 &= \dot{V}_2 + S\dot{S} \\
&= -c_0\xi^2 - c_1(x_2 - \alpha_1)^2 + \theta_2(x_1 - \alpha_0)(x_2 - \alpha_1) + S(\dot{x}_2 - \dot{\alpha}_1) \\
&= -c_0\xi^2 - c_1(x_1 - \alpha_0)^2 + S[\theta_2(x_1 - \alpha_0) + \theta_3x_1 + \theta_4x_2 + \theta_5\mu - \dot{\alpha}_1]
\end{aligned} \tag{4.45}$$

The feedback law μ , which cancels the indefinite term in \dot{V}_3 , is given by.

$$\mu = \frac{1}{\theta_5}[-\theta_2(x_1 - \alpha_0) - \theta_3x_1 - \theta_4x_2 + \dot{\alpha}_1 - k_1S - k_2\text{sign}(S)] \tag{4.46}$$

where $k_1 \geq 0$ and $k_2 > 0$ are design parameters and $\text{sign}(\cdot)$ is a sign function.

Notice that the control law (4.46) reduces to a type of sliding mode control if the parameter k_1 is zero and to a type of backstepping control when $k_2 = 0$.

With the designed control input μ , the derivative of the Lyapunov function V_3 is

$$\begin{aligned}
\dot{V}_3 &= -c_0\xi^2 - c_1(x_1 - \alpha_0)^2 - k_1S^2 - k_2S \cdot \text{sign}(S) \\
&= -c_0\xi^2 - c_1(x_1 - \alpha_0)^2 - k_1S^2 - k_2|S|
\end{aligned} \tag{4.47}$$

which is negative definite.

4.5 Adaptive Backstepping Control

The performance of a backstepping controller is good under the condition that parameters of the buck converter model are well known. In real situation, it is hard to know the exact values of parameters. For instance, the load resistance is unknown and time-varying. Therefore, an adaptive backstepping controller is introduced to the buck converter to deal with the unknown parameters. Since the parameters $\theta_1, \theta_2, \theta_3, \theta_4$ and θ_5 are unknown, the parameter estimators will be introduced in the following design procedures.

Step1. In equation (4.3), x_1 is viewed as a virtual input. Select the Lyapunov function:

$$V_1 = \frac{1}{2} \xi^2 \quad (4.48)$$

Then the virtual control

$$x_1 = \alpha_0 = -c_0 \xi + V_d \quad (4.49)$$

makes the derivative of V_1 , that is,

$$\dot{V}_1 = \xi \dot{\xi} = -c_0 \xi^2 + \xi(x_1 - \alpha_0) \quad (4.50)$$

negative definite, where $c_0 > 0$ is a design parameter.

Differentiating α_0 , we have

$$\dot{\alpha}_0 = -c_0 \dot{\xi} + \dot{V}_d = -c_0(x_1 - V_d) + \dot{V}_d \quad (4.51)$$

$$\ddot{\alpha}_0 = -c_0(\dot{x}_1 - \dot{V}_d) + \ddot{V}_d = -c_0(\theta_1 x_1 + \theta_2 x_2) + c_0 \dot{V}_d + \ddot{V}_d \quad (4.52)$$

Step2. The derivative of the error $x_1 - \alpha_0$ is expressed as

$$\dot{x}_1 - \dot{\alpha}_0 = \theta_1 x_1 + \theta_2 x_2 - \dot{\alpha}_0 \quad (4.53)$$

The augmented Lyapunov function is chosen as

$$V_2 = V_1 + \frac{1}{2} (x_1 - \alpha_0)^2 \quad (4.54)$$

The derivative of V_2 , using (4.50) and (4.53), is

$$\begin{aligned} \dot{V}_2 &= \dot{V}_1 + (x_1 - \alpha_0)(\dot{x}_1 - \dot{\alpha}_0) \\ &= -c_0 \xi^2 + \xi(x_1 - \alpha_0) + (x_1 - \alpha_0)(\dot{x}_1 - \dot{\alpha}_0) \\ &= -c_0 \xi^2 + (x_1 - \alpha_0)(\xi + \theta_1 x_1 + \theta_2 x_2 - \dot{\alpha}_0) \end{aligned} \quad (4.55)$$

The virtual control can be designed for x_2 to make \dot{V}_2 negative definite, that is,

$$x_2 = \alpha_1 = \frac{1}{\hat{\theta}_2} \left[-c_1 (x_1 - \alpha_0) - \xi - \hat{\theta}_1 x_1 + \dot{\alpha}_0 \right] \quad (4.56)$$

where $\hat{\theta}_1$ and $\hat{\theta}_2$ denote the estimates of the parameters θ_1 and θ_2 , $c_1 > 0$ is a design parameter.

From (4.55), together with (4.56), the resulting derivative becomes:

$$\begin{aligned}
\dot{V}_2 &= -c_0 \xi^2 + (x_1 - \alpha_0)(\xi + \theta_1 x_1 + \theta_2 x_2 - \dot{\alpha}_0 + \hat{\theta}_2 \alpha_1 - \hat{\theta}_2 \alpha_1) \\
&= -c_0 \xi^2 + (x_1 - \alpha_0) \left[-c_1 (x_1 - \alpha_0) + (\theta_1 - \hat{\theta}_1) x_1 + \theta_2 x_2 - \hat{\theta}_2 \alpha_1 \right] \\
&= -c_0 \xi^2 - c_1 (x_1 - \alpha_0)^2 + (x_1 - \alpha_0) \left[(\theta_1 - \hat{\theta}_1) x_1 + (\theta_2 - \hat{\theta}_2) x_2 \right] + \hat{\theta}_2 (x_1 - \alpha_0) (x_2 - \alpha_1) \quad (4.57)
\end{aligned}$$

Step3. From (4.56), taking the derivative of α_1 gives:

$$\begin{aligned}
\dot{\alpha}_1 &= -\frac{1}{\hat{\theta}_2^2} \left[-c_1 (x_1 - \alpha_0) - \xi - \hat{\theta}_1 x_1 + \dot{\alpha}_0 \right] \dot{\hat{\theta}}_2 \\
&\quad + \frac{1}{\hat{\theta}_2} \left(c_1 \dot{\alpha}_0 - \dot{\xi} - \dot{\hat{\theta}}_1 x_1 + c_0 \dot{V}_d + \ddot{V}_d \right) + \frac{1}{\hat{\theta}_2} \left(-c_1 - \hat{\theta}_1 - c_0 \right) \dot{x}_1 \\
&= A + B(\theta_1 x_1 + \theta_2 x_2) \quad (4.58)
\end{aligned}$$

where $A = -\frac{1}{\hat{\theta}_2^2} \left[-c_1 (x_1 - \alpha_0) - \xi - \hat{\theta}_1 x_1 + \dot{\alpha}_0 \right] \dot{\hat{\theta}}_2 + \frac{1}{\hat{\theta}_2} \left(c_1 \dot{\alpha}_0 - \dot{\xi} - \dot{\hat{\theta}}_1 x_1 + c_0 \dot{V}_d + \ddot{V}_d \right)$

$$B = \frac{1}{\hat{\theta}_2} \left(-c_1 - \hat{\theta}_1 - c_0 \right)$$

The derivative of $x_2 - \alpha_1$ can be expressed as

$$\dot{x}_2 - \dot{\alpha}_1 = \theta_3 x_1 + \theta_4 x_2 + \theta_5 \mu - \dot{\alpha}_1 \quad (4.59)$$

From the equation (4.57) to (4.59), the presence of parameter estimates suggests the following Lyapunov function:

$$V_3 = V_2 + \frac{1}{2} (x_2 - \alpha_1)^2 + \frac{1}{2\gamma_i} \sum_{i=1}^5 (\theta_i - \hat{\theta}_i)^2 \quad (4.60)$$

where $\gamma_i (i = 1, \dots, 5)$ are constant positive adaptive gains.

The derivative of this function, using equations (4.57), (4.58) and (4.59), is:

$$\begin{aligned}
\dot{V}_3 &= \dot{V}_2 + (x_2 - \alpha_1)(\dot{x}_2 - \dot{\alpha}_1) + \frac{1}{\gamma_i} \sum_{i=1}^5 (\theta_i - \hat{\theta}_i) (-\dot{\hat{\theta}}_i) \\
&= -c_0 \xi^2 - c_1 (x_1 - \alpha_0)^2 + (x_1 - \alpha_0) \left[(\theta_1 - \hat{\theta}_1) x_1 + (\theta_2 - \hat{\theta}_2) x_2 \right] + \frac{1}{\gamma_i} \sum_{i=1}^5 (\theta_i - \hat{\theta}_i) (-\dot{\hat{\theta}}_i) \\
&\quad + (x_2 - \alpha_1) \left[\hat{\theta}_2 (x_1 - \alpha_0) + \theta_3 x_1 + \theta_4 x_2 + \theta_5 \mu - A - B (\theta_1 x_1 + \theta_2 x_2) \right] \tag{4.61}
\end{aligned}$$

The control μ can be obtained by canceling the indefinite terms in the last bracket in (4.61) and the estimates $\hat{\theta}_i$ are used to deal with the unknown parameters $\theta_i (i = 1, \dots, 5)$.

$$\mu = \frac{1}{\hat{\theta}_5} \left[-c_2 (x_2 - \alpha_1) - \hat{\theta}_2 (x_1 - \alpha_0) - \hat{\theta}_3 x_1 - \hat{\theta}_4 x_2 + A + B (\hat{\theta}_1 x_1 + \hat{\theta}_2 x_2) \right] \tag{4.62}$$

Substituting the control μ in (4.61), the derivation of V_3 becomes:

$$\begin{aligned}
\dot{V}_3 &= -c_0 \xi^2 - c_1 (x_1 - \alpha_0)^2 - c_2 (x_2 - \alpha_1)^2 + (\theta_1 - \hat{\theta}_1) \left[(x_1 - \alpha_0) x_1 - B (x_2 - \alpha_1) x_1 - \frac{1}{\gamma_1} \dot{\hat{\theta}}_1 \right] \\
&\quad + (\theta_2 - \hat{\theta}_2) \left[(x_1 - \alpha_0) x_2 - B (x_2 - \alpha_1) x_2 - \frac{1}{\gamma_2} \dot{\hat{\theta}}_2 \right] + (\theta_3 - \hat{\theta}_3) \left[(x_2 - \alpha_1) x_1 - \frac{1}{\gamma_3} \dot{\hat{\theta}}_3 \right] \\
&\quad + (\theta_4 - \hat{\theta}_4) \left[(x_2 - \alpha_1) x_2 - \frac{1}{\gamma_4} \dot{\hat{\theta}}_4 \right] + (\theta_5 - \hat{\theta}_5) \left[(x_2 - \alpha_1) \mu - \frac{1}{\gamma_5} \dot{\hat{\theta}}_5 \right] \tag{4.63}
\end{aligned}$$

Now the $(\theta_i - \hat{\theta}_i)$ term can be eliminated with the update laws:

$$\begin{aligned}
\dot{\hat{\theta}}_1 &= \gamma_1 x_1 [(x_1 - \alpha_0) - B(x_2 - \alpha_1)] \\
\dot{\hat{\theta}}_2 &= \gamma_2 x_2 [(x_1 - \alpha_0) - B(x_2 - \alpha_1)] \\
\dot{\hat{\theta}}_3 &= \gamma_3 x_1 (x_2 - \alpha_1) \\
\dot{\hat{\theta}}_4 &= \gamma_4 x_2 (x_2 - \alpha_1) \\
\dot{\hat{\theta}}_5 &= \gamma_5 (x_2 - \alpha_1) \mu \tag{4.64}
\end{aligned}$$

which makes the derivation of V_3

$$\dot{V}_3 = -c_0 \xi^2 - c_1 (x_1 - \alpha_0)^2 - c_2 (x_2 - \alpha_1)^2 \quad (4.65)$$

negative semi-definite.

4.6 Adaptive Backstepping Sliding Mode Control

The design procedure of an adaptive backstepping sliding mode controller is shown below.

Step1. In equation (4.3), x_1 is viewed as a virtual input. Select the Lyapunov function:

$$V_1 = \frac{1}{2} \xi^2 \quad (4.66)$$

Then the virtual control

$$x_1 = \alpha_0 = -c_0 \xi + V_d \quad (4.67)$$

makes the derivative of V_1 , that is,

$$\dot{V}_1 = \xi \dot{\xi} = -c_0 \xi^2 + \xi (x_1 - \alpha_0) \quad (4.68)$$

negative definite, where $c_0 > 0$ is a design parameter.

Differentiating α_0 yields

$$\dot{\alpha}_0 = -c_0 \dot{\xi} + \dot{V}_d = -c_0 (x_1 - V_d) + \dot{V}_d \quad (4.69)$$

$$\ddot{\alpha}_0 = -c_0 (\dot{x}_1 - \dot{V}_d) + \ddot{V}_d = -c_0 (\theta_1 x_1 + \theta_2 x_2) + c_0 \dot{V}_d + \ddot{V}_d \quad (4.70)$$

Step2. The derivative of the error $x_1 - \alpha_0$ is expressed as

$$\dot{x}_1 - \dot{\alpha}_0 = \theta_1 x_1 + \theta_2 x_2 - \dot{\alpha}_0 \quad (4.71)$$

The augmented Lyapunov function is chosen as

$$V_2 = V_1 + \frac{1}{2} (x_1 - \alpha_0)^2 \quad (4.72)$$

The derivative of V_2 , using (4.68) and (4.71), is

$$\begin{aligned}
\dot{V}_2 &= \dot{V}_1 + (x_1 - \alpha_0)(\dot{x}_1 - \dot{\alpha}_0) \\
&= -c_0 \xi^2 + \xi(x_1 - \alpha_0) + (x_1 - \alpha_0)(\dot{x}_1 - \dot{\alpha}_0) \\
&= -c_0 \xi^2 + (x_1 - \alpha_0)(\xi + \theta_1 x_1 + \theta_2 x_2 - \dot{\alpha}_0)
\end{aligned} \tag{4.73}$$

The virtual control can be designed for x_2 to make \dot{V}_2 negative definite, that is,

$$x_2 = \alpha_1 = \frac{1}{\hat{\theta}_2} \left[-c_1(x_1 - \alpha_0) - \xi - \hat{\theta}_1 x_1 + \dot{\alpha}_0 \right] \tag{4.74}$$

where $\hat{\theta}_1$ and $\hat{\theta}_2$ denote the estimates of the parameters θ_1 and θ_2 , $c_1 > 0$ is a design parameter.

From (4.73), together with (4.74), the resulting derivative becomes:

$$\begin{aligned}
\dot{V}_2 &= -c_0 \xi^2 + (x_1 - \alpha_0)(\xi + \theta_1 x_1 + \theta_2 x_2 - \dot{\alpha}_0 + \hat{\theta}_2 \alpha_1 - \hat{\theta}_2 \alpha_1) \\
&= -c_0 \xi^2 + (x_1 - \alpha_0) \left[-c_1(x_1 - \alpha_0) + (\theta_1 - \hat{\theta}_1)x_1 + \theta_2 x_2 - \hat{\theta}_2 \alpha_1 \right] \\
&= -c_0 \xi^2 - c_1(x_1 - \alpha_0)^2 + (x_1 - \alpha_0) \left[(\theta_1 - \hat{\theta}_1)x_1 + (\theta_2 - \hat{\theta}_2)x_2 \right] + \hat{\theta}_2(x_1 - \alpha_0)(x_2 - \alpha_1)
\end{aligned} \tag{4.75}$$

Step3. From (4.74), taking the derivative of α_1 gives:

$$\begin{aligned}
\dot{\alpha}_1 &= -\frac{1}{\hat{\theta}_2^2} \left[-c_1(x_1 - \alpha_0) - \xi - \hat{\theta}_1 x_1 + \dot{\alpha}_0 \right] \dot{\hat{\theta}}_2 \\
&\quad + \frac{1}{\hat{\theta}_2} \left(c_1 \dot{\alpha}_0 - \dot{\xi} - \dot{\hat{\theta}}_1 x_1 + c_0 \dot{V}_d + \ddot{V}_d \right) + \frac{1}{\hat{\theta}_2} \left(-c_1 - \hat{\theta}_1 - c_0 \right) \dot{x}_1 \\
&= A + B(\theta_1 x_1 + \theta_2 x_2)
\end{aligned} \tag{4.76}$$

where $A = -\frac{1}{\hat{\theta}_2^2} \left[-c_1(x_1 - \alpha_0) - \xi - \hat{\theta}_1 x_1 + \dot{\alpha}_0 \right] \dot{\hat{\theta}}_2 + \frac{1}{\hat{\theta}_2} \left(c_1 \dot{\alpha}_0 - \dot{\xi} - \dot{\hat{\theta}}_1 x_1 + c_0 \dot{V}_d + \ddot{V}_d \right)$

$$B = \frac{1}{\hat{\theta}_2} \left(-c_1 - \hat{\theta}_1 - c_0 \right)$$

The derivative of $x_2 - \alpha_1$ can be expressed as

$$\dot{x}_2 - \dot{\alpha}_1 = \theta_3 x_1 + \theta_4 x_2 + \theta_5 \mu - \dot{\alpha}_1 \quad (4.77)$$

Now we define a sliding surface S , select a Lyapunov function V_3 and design control input μ to make its derivative negative semi-definite

$$S = x_2 - \alpha_1$$

$$V_3 = V_2 + \frac{1}{2} S^2 + \frac{1}{2\gamma_i} \sum_{i=1}^5 (\theta_i - \hat{\theta}_i)^2 \quad (4.78)$$

where $\gamma_i (i=1, \dots, 5)$ are constant positive adaptive gains.

The derivative of Lyapunov function V_3 , using equations (4.75), (4.76) and (4.77), is

$$\begin{aligned} \dot{V}_3 &= \dot{V}_2 + S\dot{S} + \frac{1}{\gamma_i} \sum_{i=1}^5 (\theta_i - \hat{\theta}_i) (-\dot{\hat{\theta}}_i) \\ &= -c_0 \xi^2 - c_1 (x_1 - \alpha_0)^2 + (x_1 - \alpha_0) \left[(\theta_1 - \hat{\theta}_1) x_1 + (\theta_2 - \hat{\theta}_2) x_2 \right] + \frac{1}{\gamma_i} \sum_{i=1}^5 (\theta_i - \hat{\theta}_i) (-\dot{\hat{\theta}}_i) \\ &\quad + S \left[\hat{\theta}_2 (x_1 - \alpha_0) + \theta_3 x_1 + \theta_4 x_2 + \theta_5 \mu - A - B(\theta_1 x_1 + \theta_2 x_2) \right] \end{aligned} \quad (4.79)$$

The control μ can be obtained by canceling the indefinite terms in the last bracket in (4.79) and the estimates $\hat{\theta}_i$ are used to deal with the unknown parameters $\theta_i (i=1, \dots, 5)$.

$$\mu = \frac{1}{\hat{\theta}_5} \left[-\hat{\theta}_2 (x_1 - \alpha_0) - \hat{\theta}_3 x_1 - \hat{\theta}_4 x_2 + A + B(\hat{\theta}_1 x_1 + \hat{\theta}_2 x_2) - k_1 s - k_2 \text{sign}(s) \right] \quad (4.80)$$

where $k_1 \geq 0$ and $k_2 > 0$ are design parameters and $\text{sign}(\cdot)$ is a sign function.

Notice that the control law (4.80) becomes a sliding mode control law if the parameter k_1 is set to zero and it becomes an adaptive backstepping controller as $k_2 = 0$.

With the designed control input μ , the derivative of Lyapunov function V_3 becomes

$$\begin{aligned}
\dot{V}_3 = & -c_0\xi^2 - c_1(x_1 - \alpha_0)^2 + (\theta_1 - \hat{\theta}_1) \left[(x_1 - \alpha_0)x_1 - BSx_1 - \frac{1}{\gamma_1} \dot{\hat{\theta}}_1 \right] \\
& + (\theta_2 - \hat{\theta}_2) \left[(x_1 - \alpha_0)x_2 - BSx_2 - \frac{1}{\gamma_2} \dot{\hat{\theta}}_2 \right] + (\theta_3 - \hat{\theta}_3) \left[Sx_1 - \frac{1}{\gamma_3} \dot{\hat{\theta}}_3 \right] \\
& + (\theta_4 - \hat{\theta}_4) \left[Sx_2 - \frac{1}{\gamma_4} \dot{\hat{\theta}}_4 \right] + (\theta_5 - \hat{\theta}_5) \left[S\mu - \frac{1}{\gamma_5} \dot{\hat{\theta}}_5 \right] - k_1S^2 - k_2S \cdot \text{sign}(S)
\end{aligned} \tag{4.81}$$

Now the $(\theta_i - \hat{\theta}_i)$ term can be eliminated with the update laws:

$$\begin{aligned}
\dot{\hat{\theta}}_1 &= \gamma_1 x_1 [(x_1 - \alpha_0) - BS] \\
\dot{\hat{\theta}}_2 &= \gamma_2 x_2 [(x_1 - \alpha_0) - BS] \\
\dot{\hat{\theta}}_3 &= \gamma_3 x_1 S \\
\dot{\hat{\theta}}_4 &= \gamma_4 x_2 S \\
\dot{\hat{\theta}}_5 &= \gamma_5 S \mu
\end{aligned} \tag{4.82}$$

which makes the derivation of V_3

$$\begin{aligned}
\dot{V}_3 &= -c_0\xi^2 - c_1(x_1 - \alpha_0)^2 - k_1S^2 - k_2S \cdot \text{sign}(S) \\
&= -c_0\xi^2 - c_1(x_1 - \alpha_0)^2 - k_1S^2 - k_2|S|
\end{aligned} \tag{4.83}$$

negative semi-definite.

4.7 Estimation of the Inductor Current

In our experimental system, the output voltage x_1 can be accurately measured. For the other state variable, inductor current x_2 can be measured with a current sensor. Meanwhile, inductor current also can be estimated using a reduced order observer.

According to the reduced order observer design theory, the differential equation for the output voltage x_1

$$\dot{x}_1 = \theta_1 x_1 + \theta_2 x_2 \quad (4.84)$$

is first rearranged to serve as a measurement equation for x_2

$$\theta_2 x_2 = \dot{x}_1 - \theta_1 x_1 = z \quad (4.85)$$

where z can be considered as a new measurement.

Since the state equation for x_2 is

$$\dot{x}_2 = \theta_3 x_1 + \theta_4 x_2 + \theta_5 \mu \quad (4.86)$$

The reduced order estimator with z is given by

$$\dot{\hat{x}}_2 = \theta_3 x_1 + \theta_4 \hat{x}_2 + \theta_5 \mu + L_{est} (z - \theta_2 \hat{x}_2) \quad (4.87)$$

where L_{est} is an estimator gain which can be selected by using the pole placement method.

Now we introduce a new state variable x_3

$$x_3 = \hat{x}_2 - L_{est} x_1 \quad (4.88)$$

Then differentiating the new variable x_3 , we obtain

$$\begin{aligned} \dot{x}_3 &= \dot{\hat{x}}_2 - L_{est} \dot{x}_1 = \theta_3 x_1 + \theta_4 \hat{x}_2 + \theta_5 \mu + L_{est} (z - \theta_2 \hat{x}_2) - L_{est} \dot{x}_1 \\ &= \theta_3 x_1 + \theta_4 \hat{x}_2 + \theta_5 \mu + L_{est} (\dot{x}_1 - \theta_1 x_1) - L_{est} \theta_2 \hat{x}_2 - L_{est} \dot{x}_1 \\ &= (\theta_3 + L_{est} \theta_4 - L_{est} \theta_1 - L_{est}^2 \theta_2) x_1 + (\theta_4 - L_{est} \theta_2) x_3 + \theta_5 \mu \end{aligned} \quad (4.89)$$

Finally, the inductor current \hat{x}_2 can be computed from the following equation

$$\hat{x}_2 = x_3 + L_{est} x_1 \quad (4.90)$$

Chapter 5

Simulation Analysis of the Control Strategies

The five nonlinear controllers developed on the state space averaged model of the DC-DC buck converter in Chapter 4, namely backstepping, sliding mode, backstepping sliding mode, adaptive backstepping, and adaptive backstepping sliding mode controller, are simulated on a computer using MATLAB. The responses of the controllers have been compared with the following conditions:

- Setpoint changes from 8 volts to 10 volts
- Load resistance changes from 8 ohms to 4 ohms
- 2 volt step disturbance in the power supply.

The specifications of the converter are given in Table.5-1. In the simulation, the value of the desired output voltage is set to be $V_d = 8$ volts. The design parameters of the proposed controllers, which were chosen by trial and error, are shown in Table.5-2.

Note that the parameter estimators $\hat{\theta}_2$ and $\hat{\theta}_3$ appear in denominators in the proposed adaptive controllers, which implies that they must be non-zero. It is worth monitoring their values in the simulation.

Parameter name	Symbol	Value
Power supply	E	20 volts
Inductance	L	92 μH
Capacitance	C	220 μF
Load resistance	R	8 Ω
Inductor resistance	R_L	74 $m\Omega$
Capacitor ESR	R_C	70 $m\Omega$
Diode resistance	R_D	30 $m\Omega$
Switching resistance	R_S	44 $m\Omega$
Table.5-1: Specification of buck converter (simulation)		

Control strategy	Design parameters
Backstepping	$c_0 = 120, c_1 = 60000, c_2 = 50000$
Sliding mode	$K = 20000$
Backstepping sliding mode	$c_0 = 120, c_1 = 60000, k_1 = 50000, k_2 = 2000$
Adaptive backstepping	$c_0 = 120, c_1 = 60000, c_2 = 50000, \gamma_i = 10^{-2} (i=1, \dots, 5)$
Adaptive backstepping sliding mode	$c_0 = 120, c_1 = 60000, k_1 = 50000, k_2 = 2000$ $\gamma_i = 10^{-2} (i=1, \dots, 5)$
Table.5-2: Specification of design parameters (simulation)	

5.1 Response to Setpoint Change

In order to study the ability of the developed controllers to regulate the output voltage to the desired value, in this section, the output voltage reference is changed from 8 volts to 10 volts at the time 0.1s.

Fig.5-1 depicts the performance of the backstepping controller. It can be seen that when the setpoint changed, the output voltage exhibits a good performance in tracking the output reference voltage.

The behavior of the sliding mode controller is shown in Fig.5-2. It is obvious that sliding mode control has some overshoots.

The response of the backstepping sliding mode controller is shown in Fig.5-3. It has been found that this controller has a good performance in output voltage regulation.

In the case of the unknown parameters, the two adaptive controllers, adaptive backstepping controller and adaptive backstepping sliding mode controller, are simulated. Their performances to the setpoint changes are presented in Fig.5-4 and Fig.5-5, respectively. It can be observed that they all have good voltage regulation.

For the two adaptive controllers, it is necessary to check the behaviors of the parameter estimators $\hat{\theta}_2$ and $\hat{\theta}_3$, which are displayed in Fig.5-6, Fig.5-7, Fig.5-8 and Fig.5-9. It can be seen that the values of these parameter estimators are changing but never go to zero.

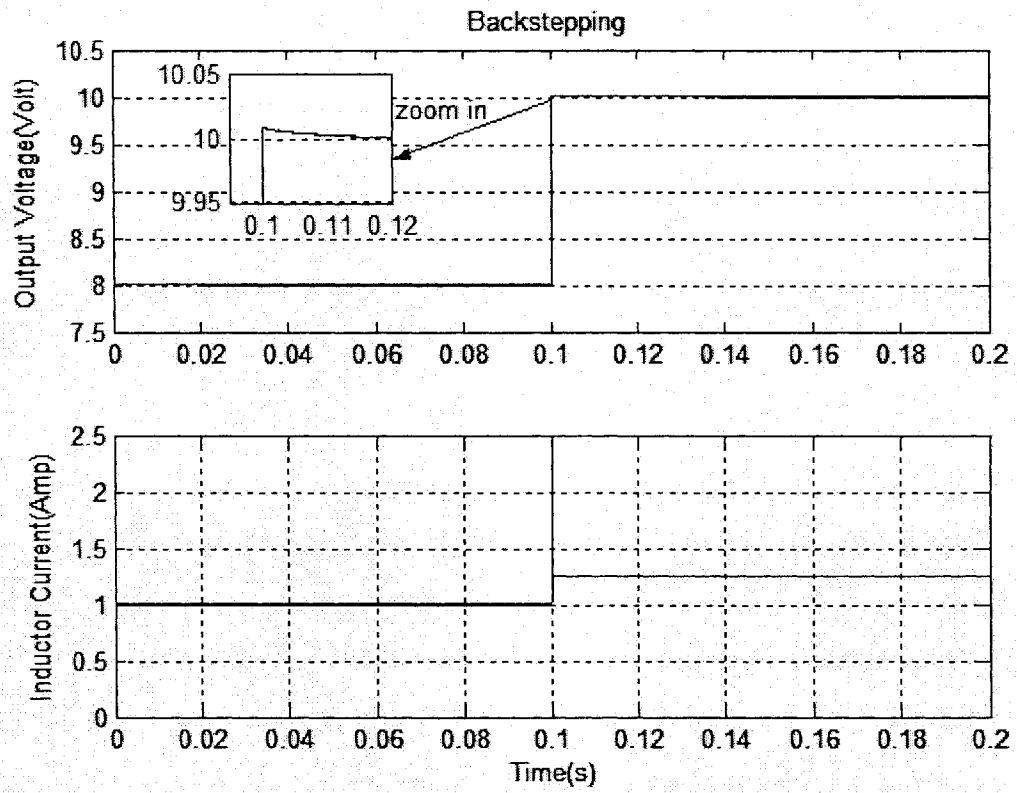


Fig.5-1: Backstepping

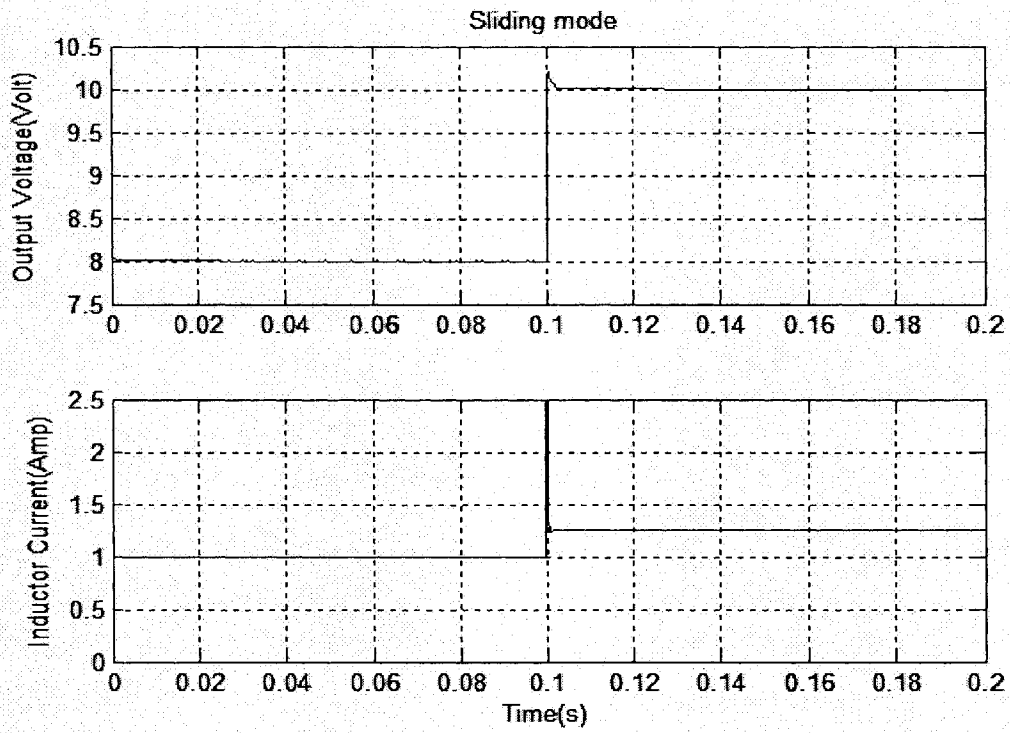


Fig.5-2: Sliding mode

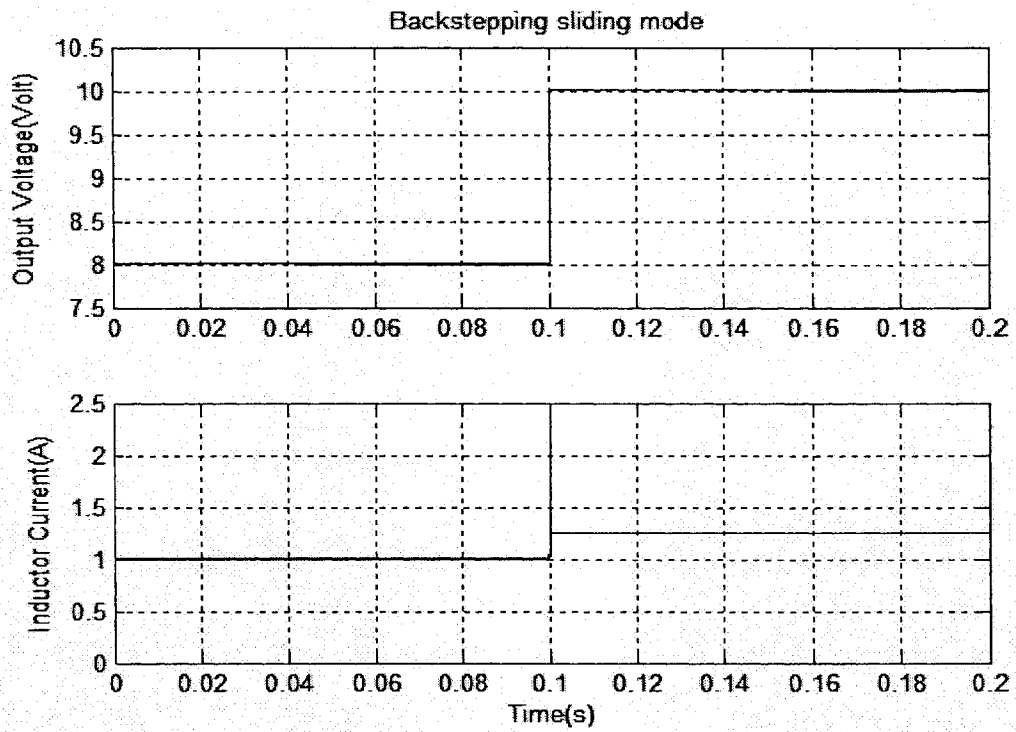


Fig.5-3: Backstepping sliding mode

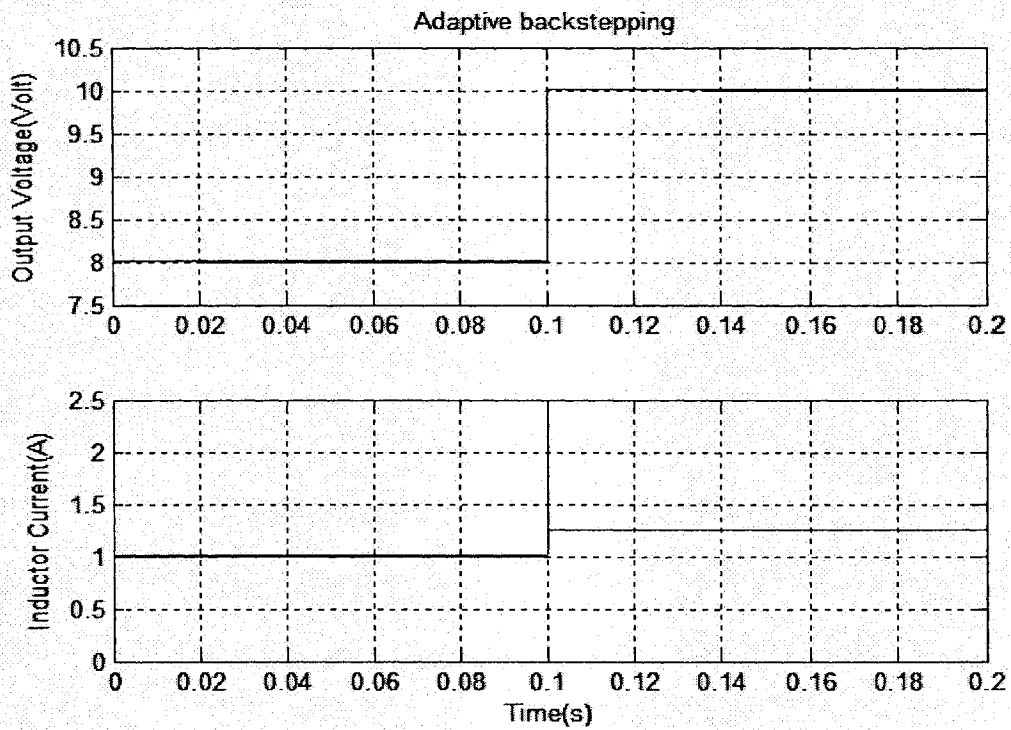


Fig.5-4: Adaptive backstepping

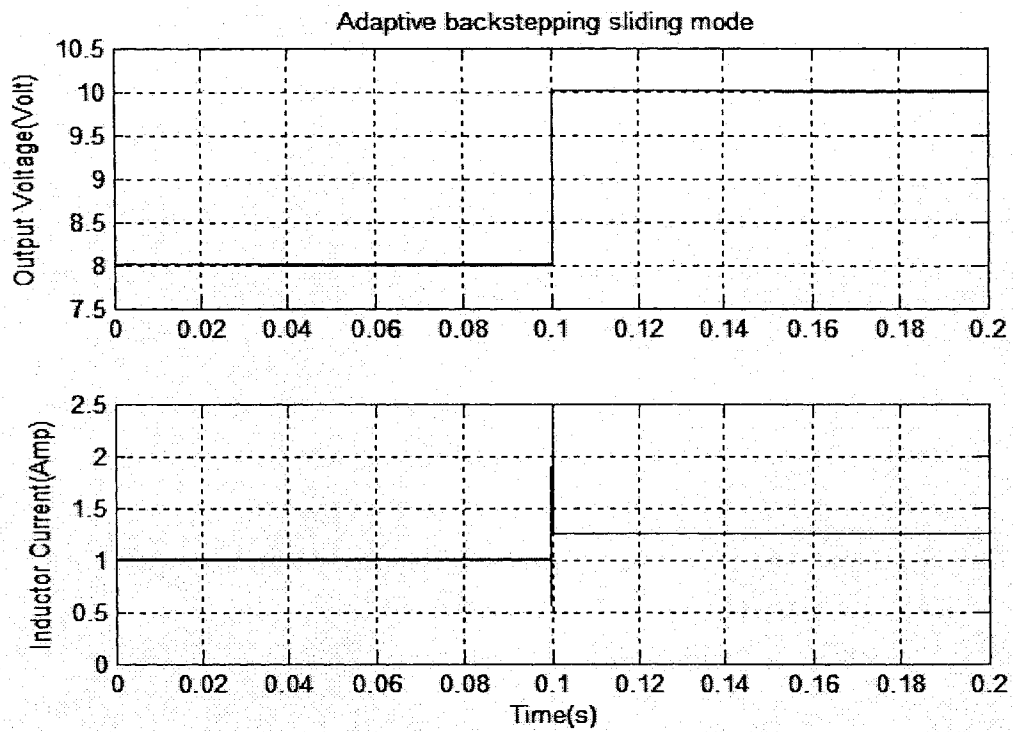


Fig.5-5: Adaptive backstepping sliding mode

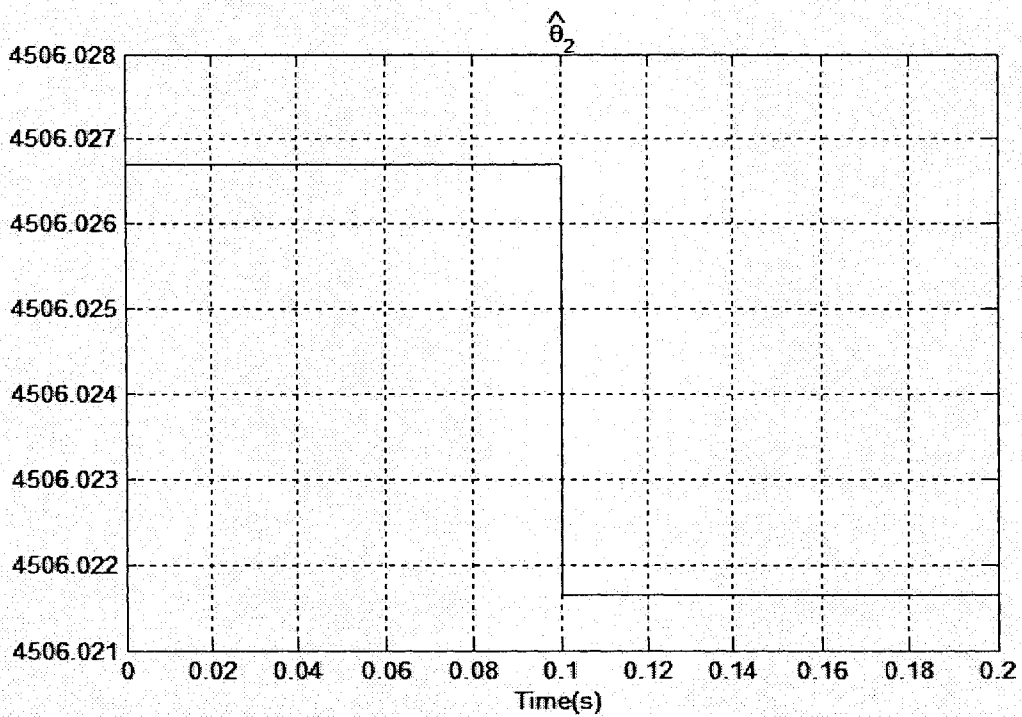


Fig.5-6: $\hat{\theta}_2$ - Adaptive backstepping

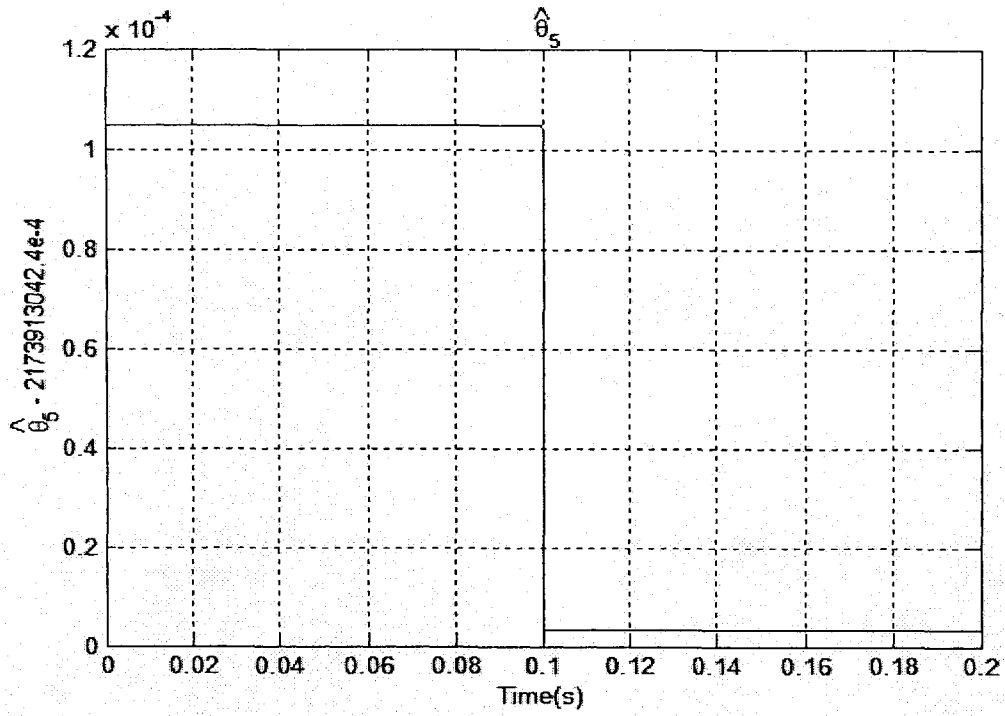


Fig.5-7: $\hat{\theta}_5$ - Adaptive backstepping

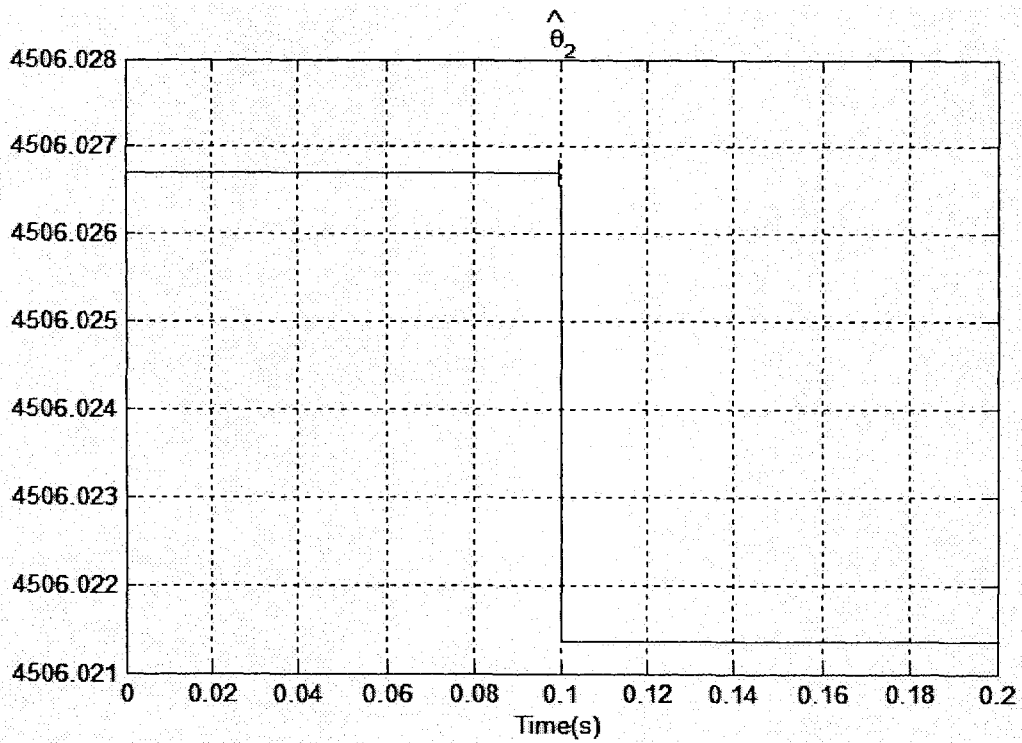


Fig.5-8: $\hat{\theta}_2$ - Adaptive backstepping sliding mode

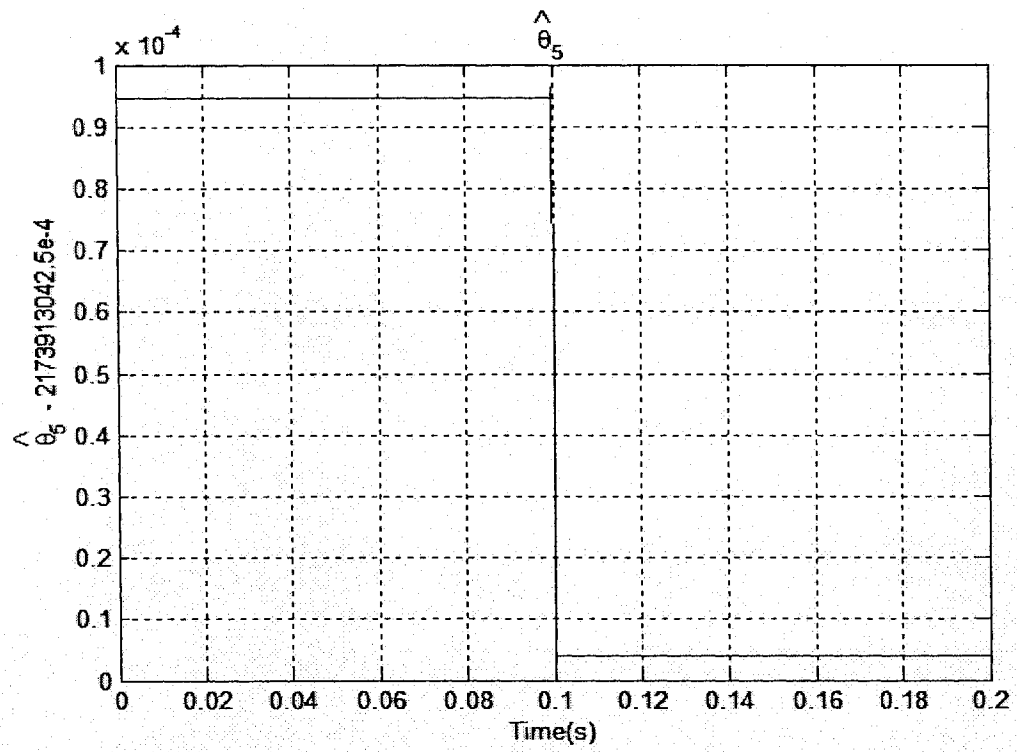


Fig.5-9: $\hat{\theta}_5$ - Adaptive backstepping sliding mode

5.2 Response to Load Change

In this section, the performances of the proposed controllers are analyzed in the presence of load variations. The load resistance is changed from its normal value $R = 8\Omega$ to $R = 4\Omega$ during the time interval $[0.1, 0.15]$ s.

The behaviors of the controllers are shown in Fig.5-10, Fig.5-11, Fig.5-12, Fig.5-13 and Fig.5-14. It can be seen that the backstepping, backstepping sliding mode, adaptive backstepping, and adaptive backstepping sliding mode controller have similar performances. Their output voltage exhibits about $160mV$ overshoots during the load variations. The performance of the sliding mode controller shows larger overshoots and faster response time to the load changes.

For the two adaptive controllers, the behaviors of the parameter estimators $\hat{\theta}_2$ and $\hat{\theta}_3$ are shown in Fig.5-15, Fig.5-16, Fig.5-17 and Fig.5-18. It can be seen that the values of these parameter estimators are not zero.

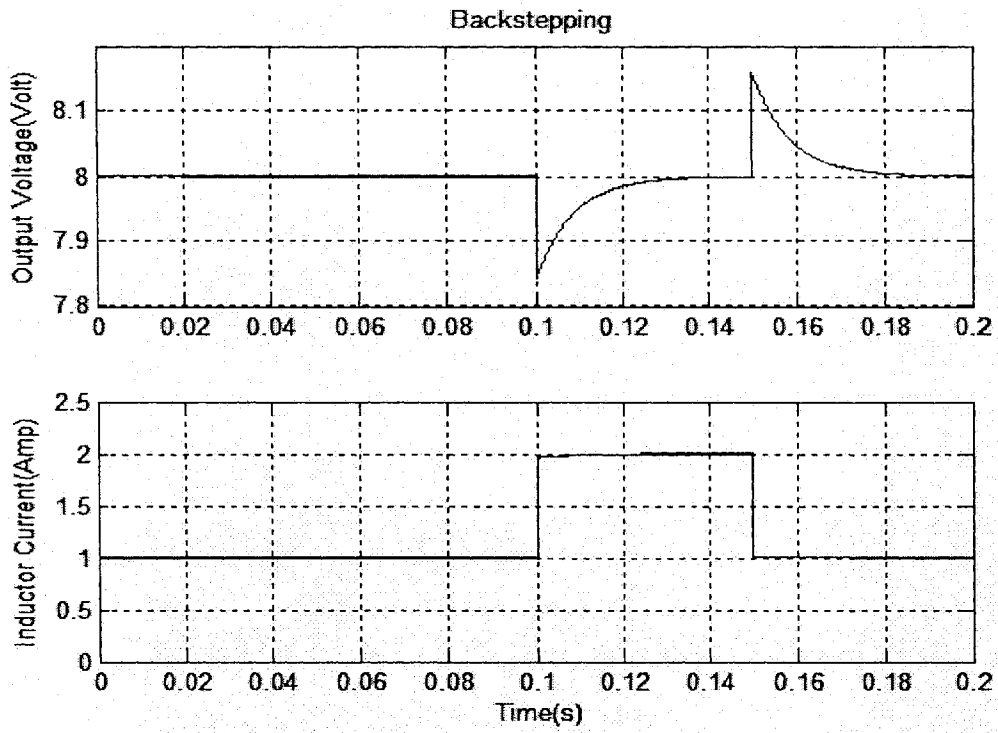


Fig.5-10: Backstepping

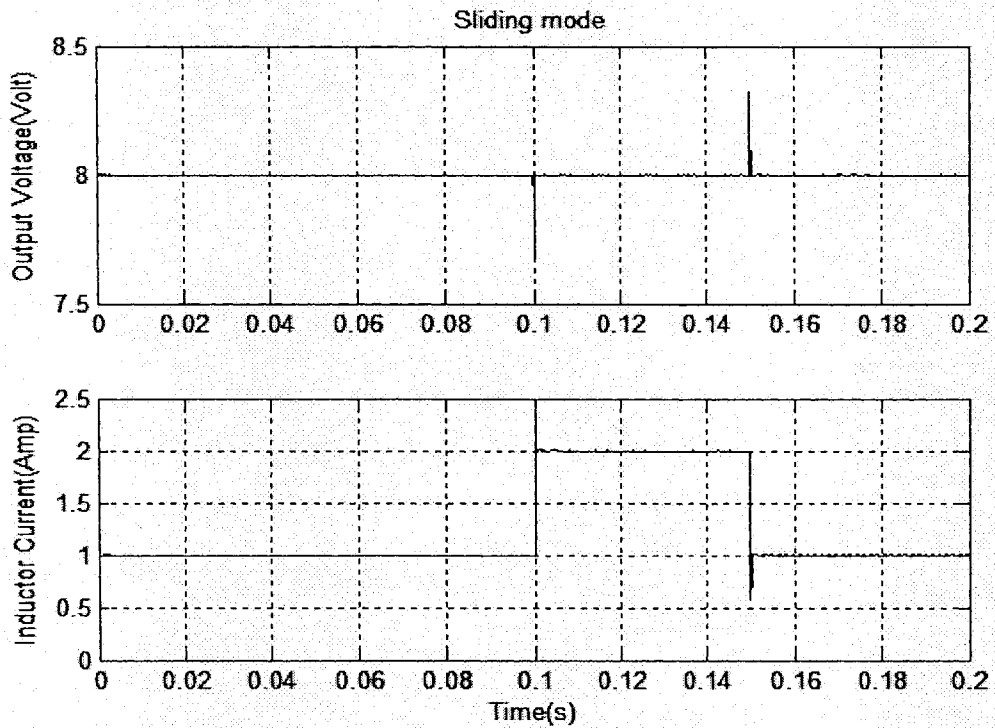


Fig.5-11: Sliding mode

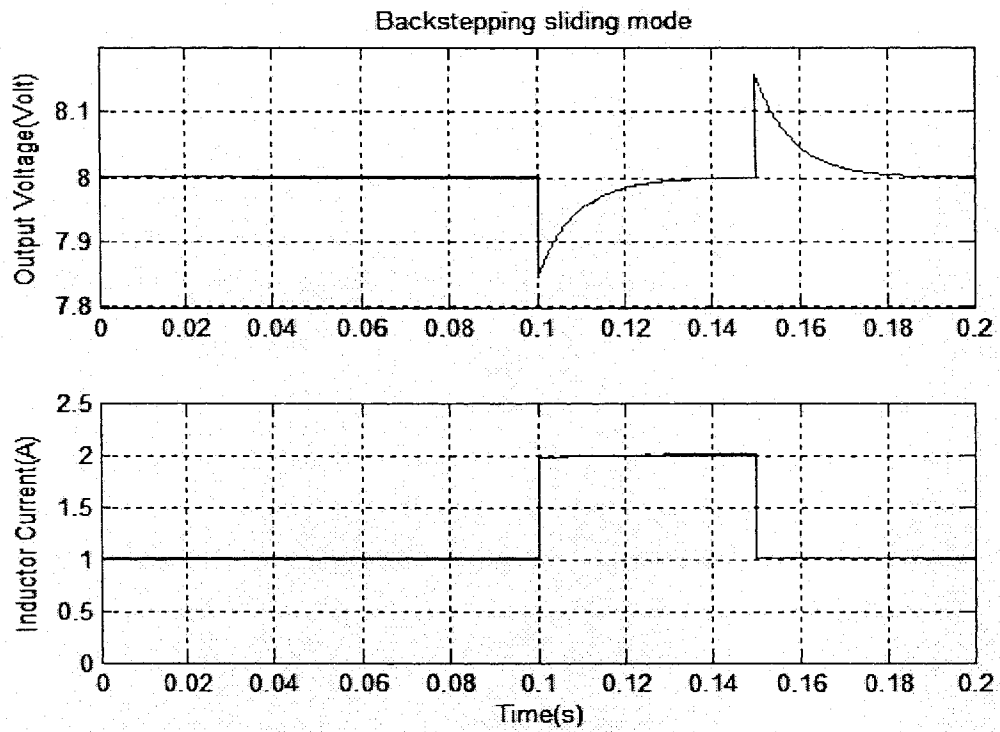


Fig.5-12: Backstepping sliding mode

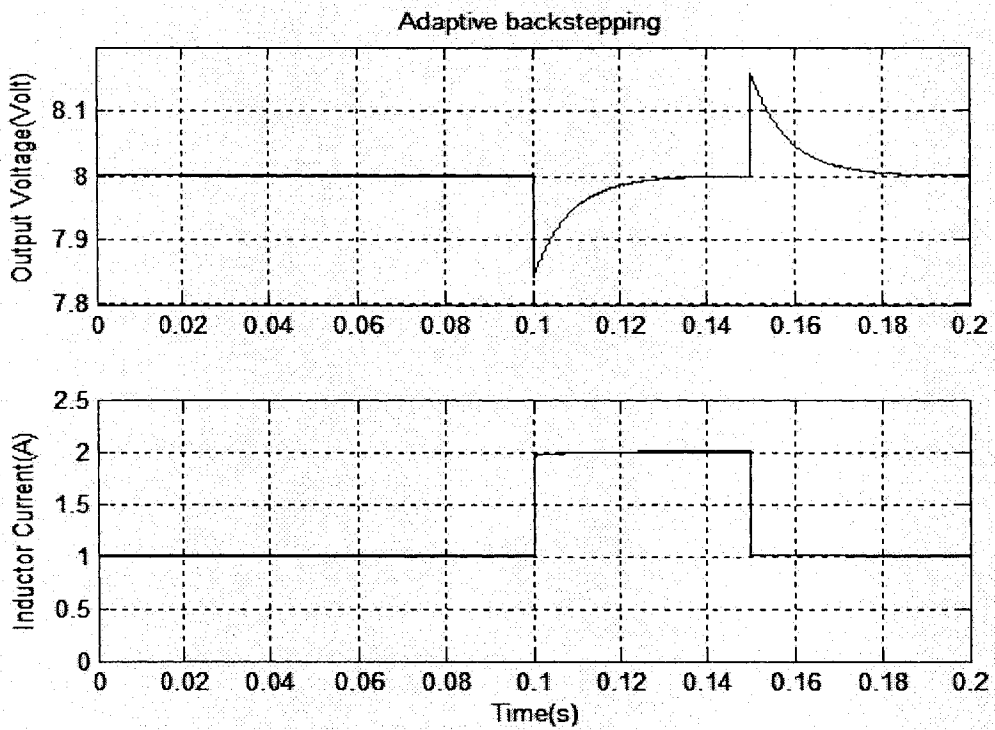


Fig.5-13: Adaptive backstepping

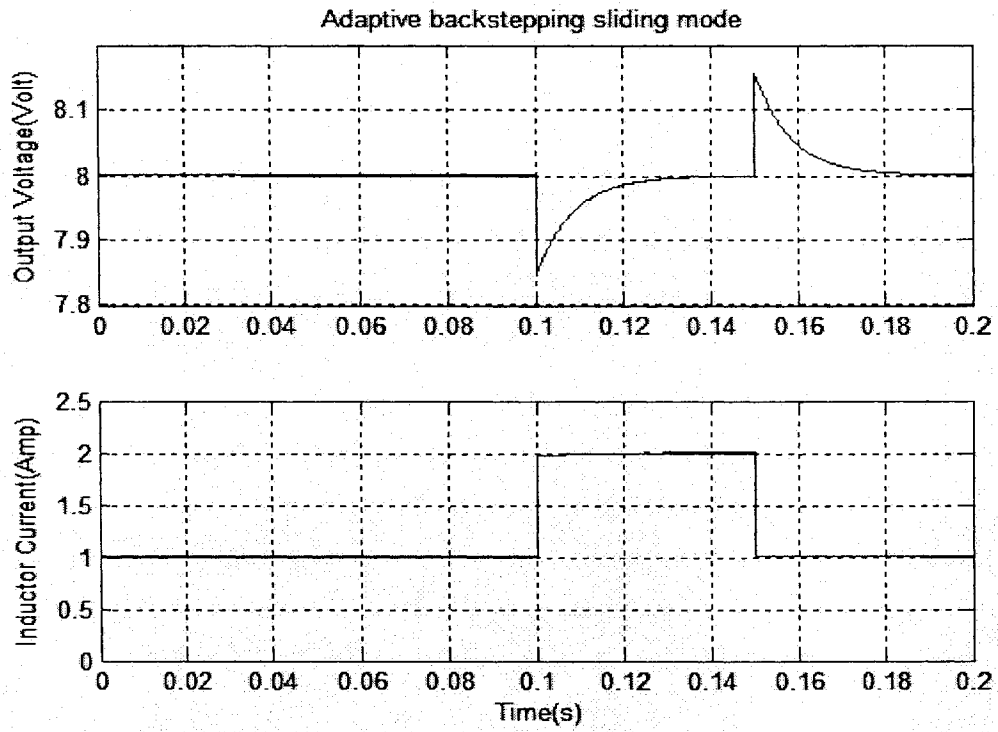


Fig.5-14: Adaptive backstepping sliding mode

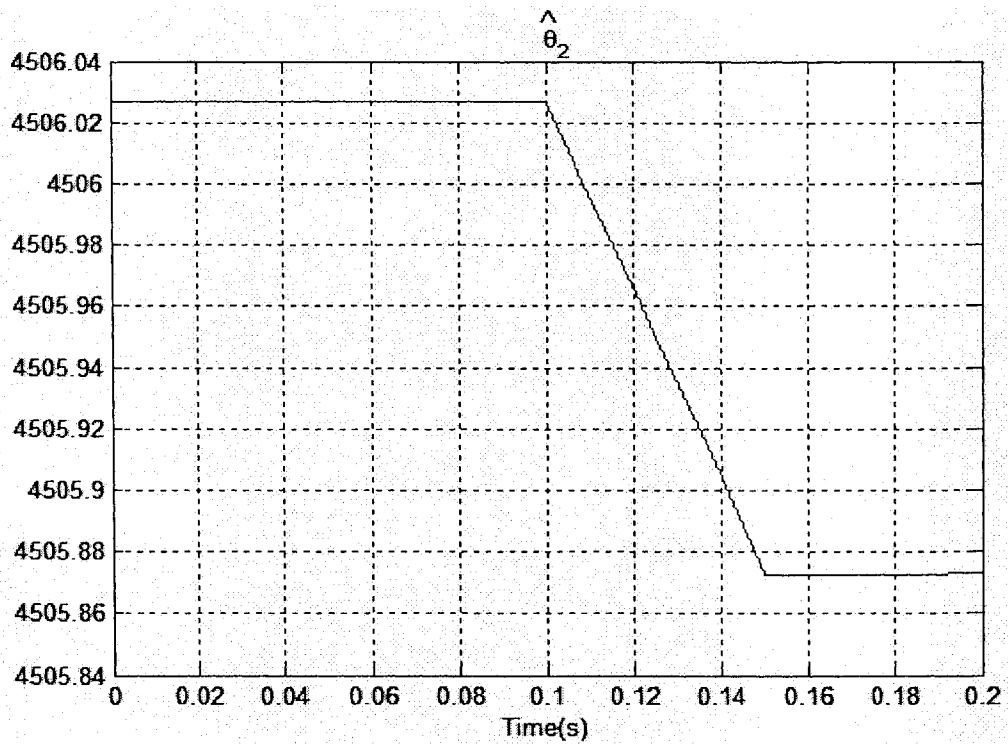


Fig.5-15: $\hat{\theta}_2$ -Adaptive backstepping

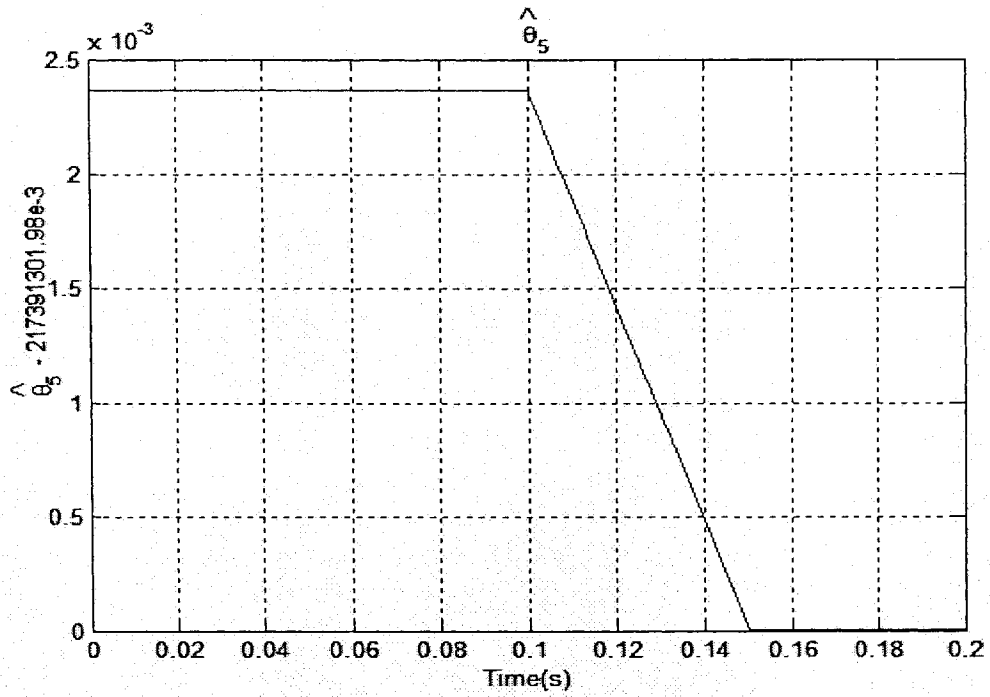


Fig.5-16: $\hat{\theta}_5$ -Adaptive backstepping

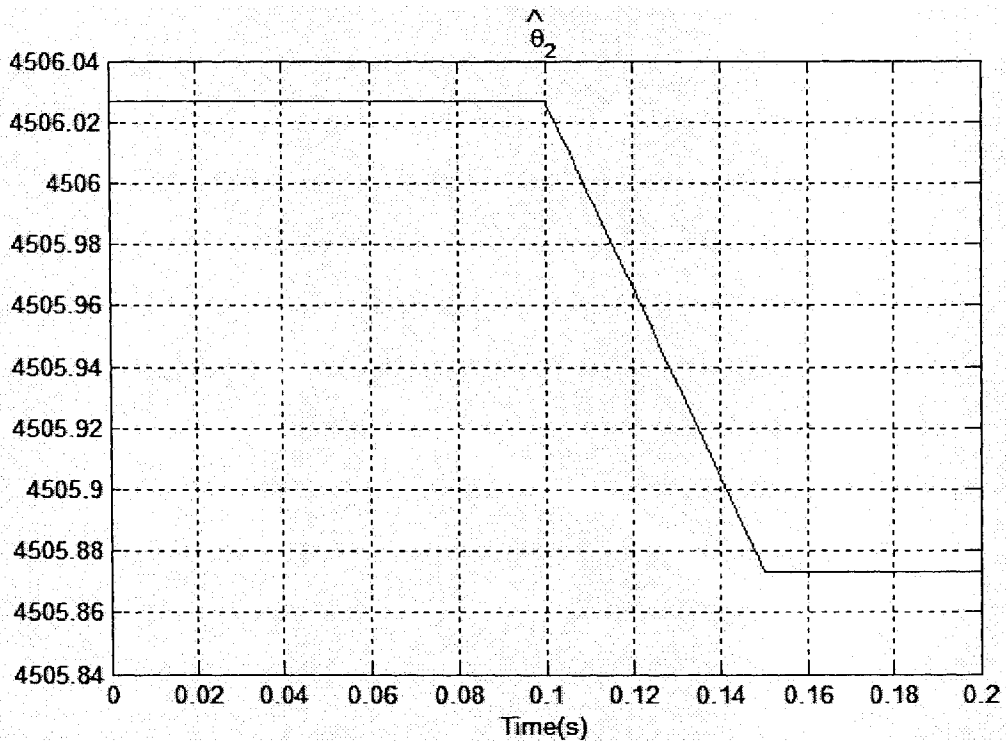


Fig.5-17: $\hat{\theta}_2$ -Adaptive backstepping sliding mode

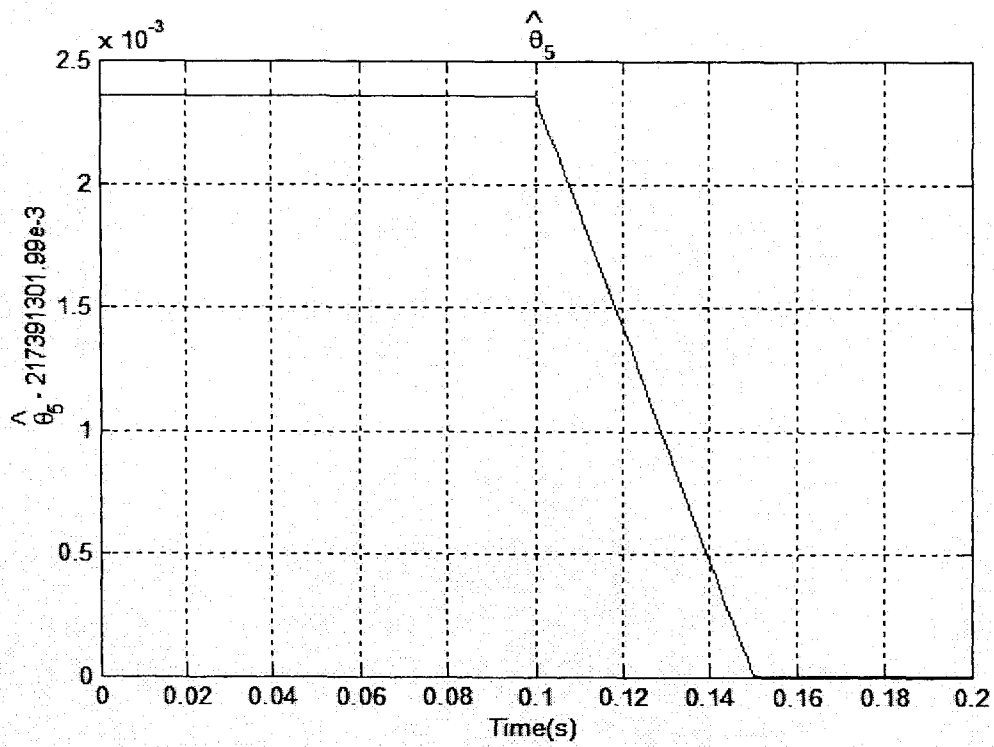


Fig.5-18: $\hat{\theta}_5$ -Adaptive backstepping sliding mode

5.3 Response to Source Voltage Change

The ability of the proposed controllers to attenuate pulse disturbances at the source voltage is studied because it might occur in practice. In this simulation, the disturbance is introduced by changing power supply from 20 volts to 18 volts during the time period [0.1, 0.15]s.

Fig.5-19, Fig.5-20, Fig.5-21, Fig.5-22 and Fig.5-23 display the performances of the controllers. It can be seen that the backstepping controller has about $15mV$ overshoots, its output voltage dropped and then recovered to the desired voltage during the disturbances. The performance of sliding mode controller to source voltage changes has larger overshoots but faster response time. The backstepping sliding mode has similar performance to the backstepping controller. Adaptive backstepping and adaptive backstepping sliding mode controller show better performances due to the smaller overshoots.

For the two adaptive controllers, the behaviors of the parameter estimators $\hat{\theta}_2$ and $\hat{\theta}_5$ shown in Fig.5-24, Fig.5-25, Fig.5-26 and Fig.5-27 indicate that the values of these parameter estimators converge to some non-zero values.

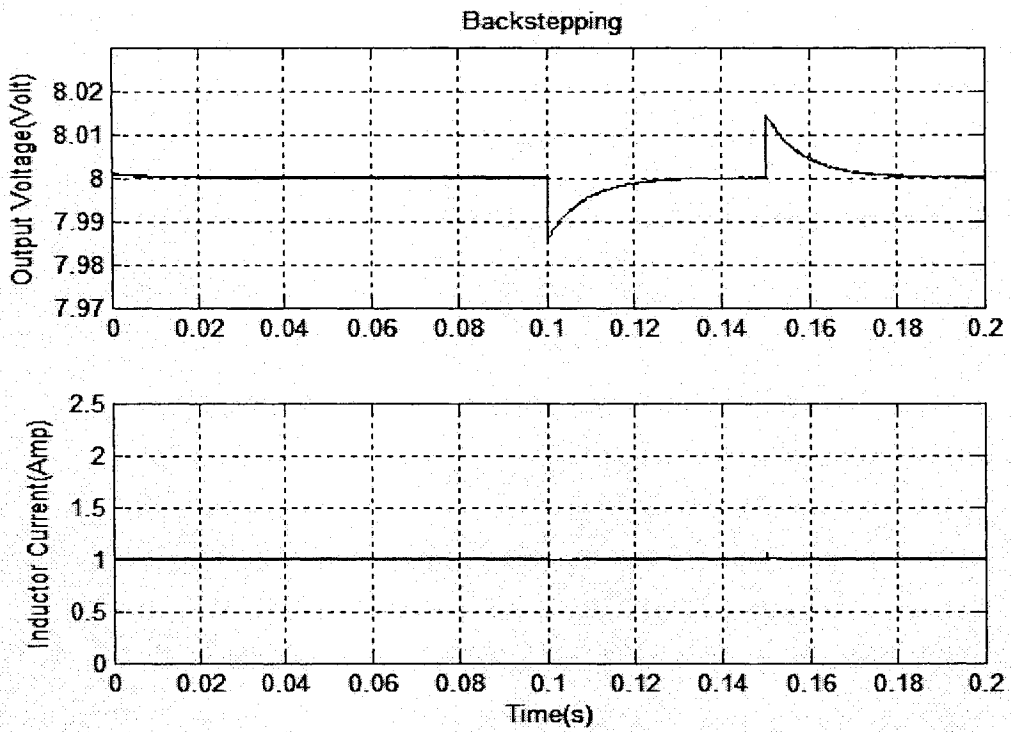


Fig.5-19: Backstepping

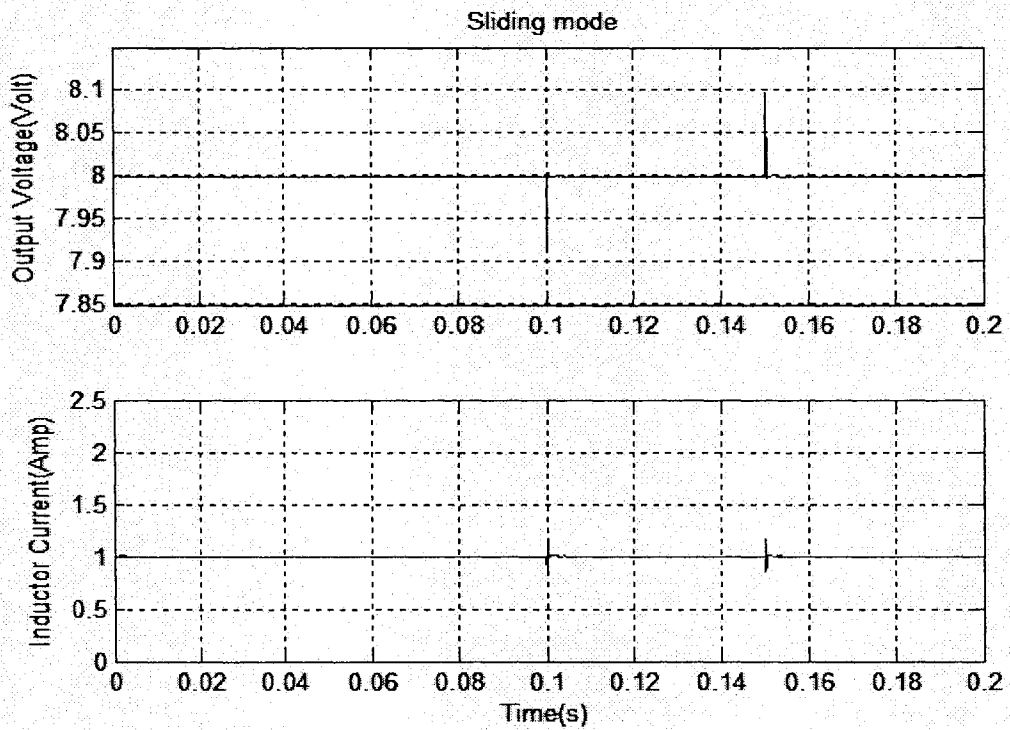


Fig.5-20: Sliding mode

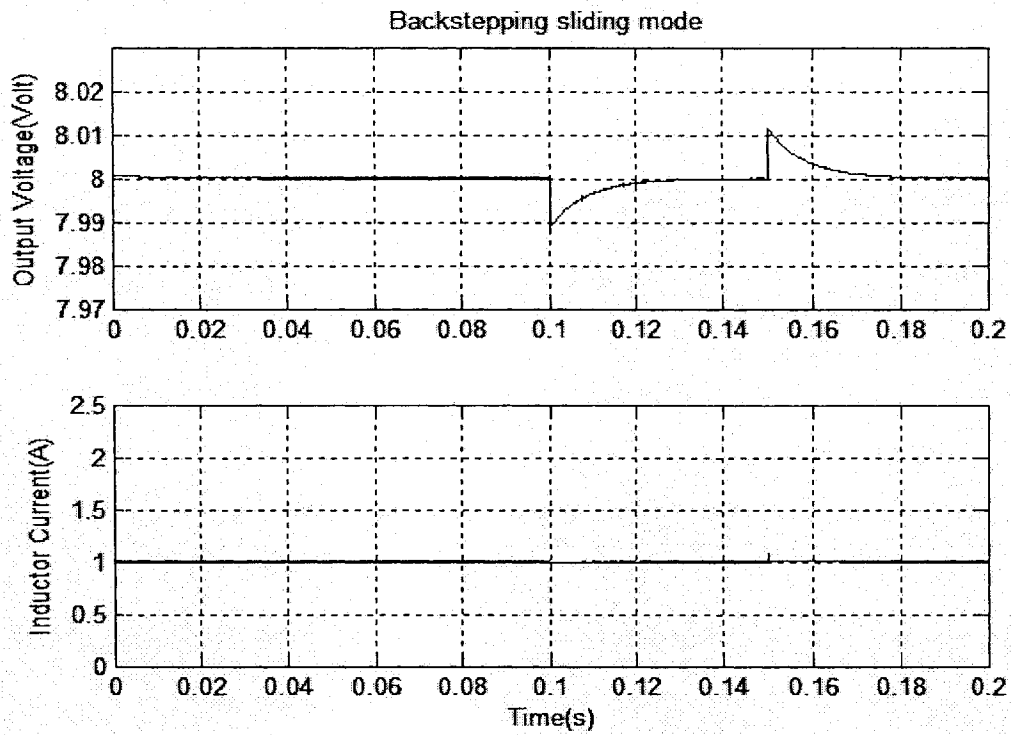


Fig.5-21: Backstepping sliding mode

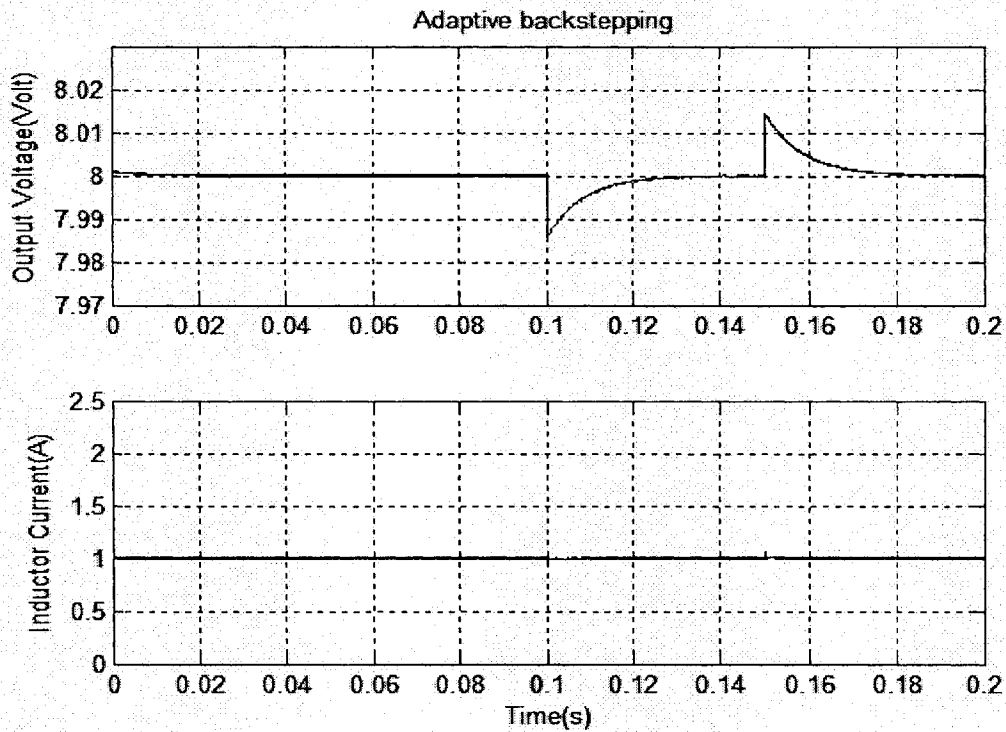


Fig.5-22: Adaptive backstepping

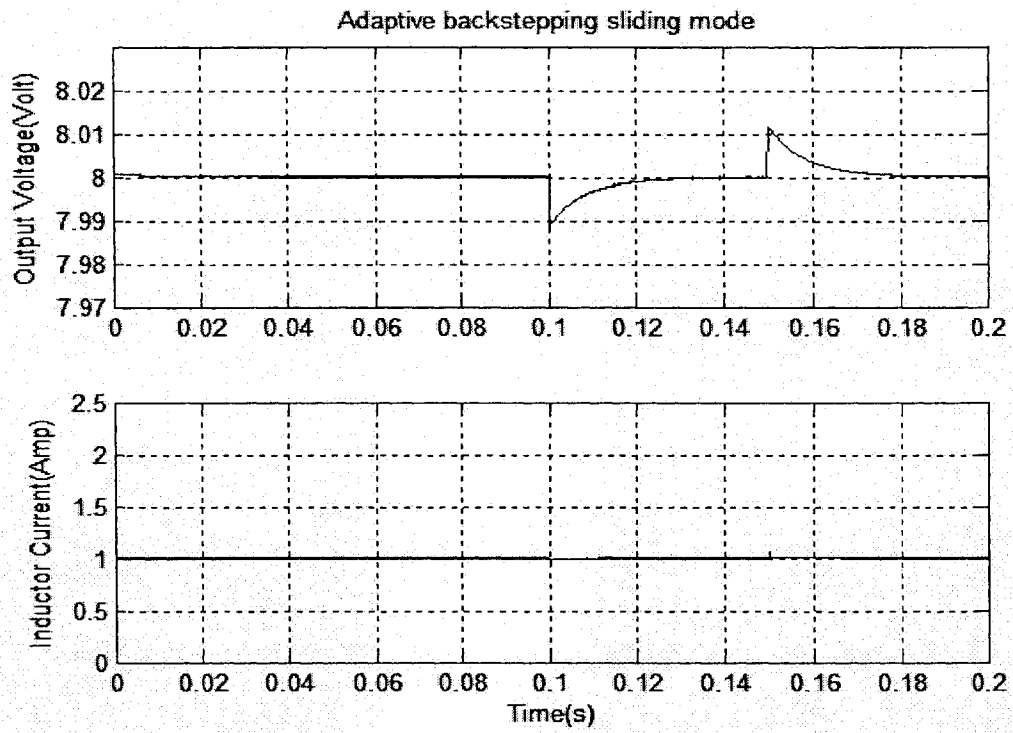


Fig.5-23: Adaptive backstepping sliding mode

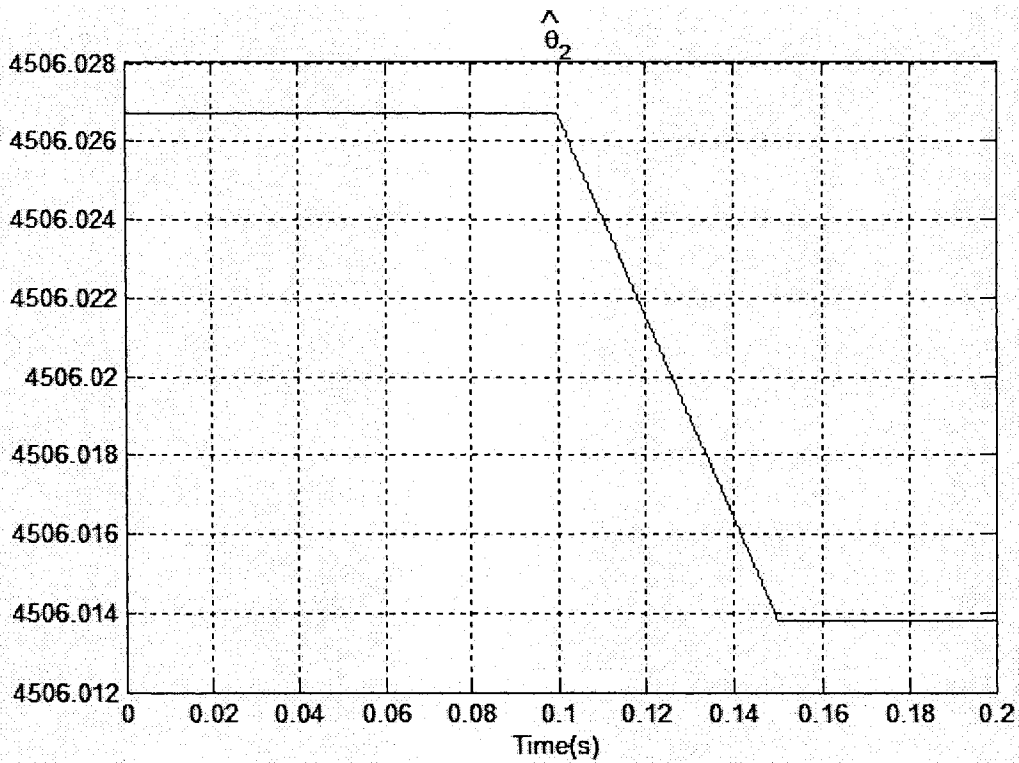


Fig.5-24: $\hat{\theta}_2$ -Adaptive backstepping

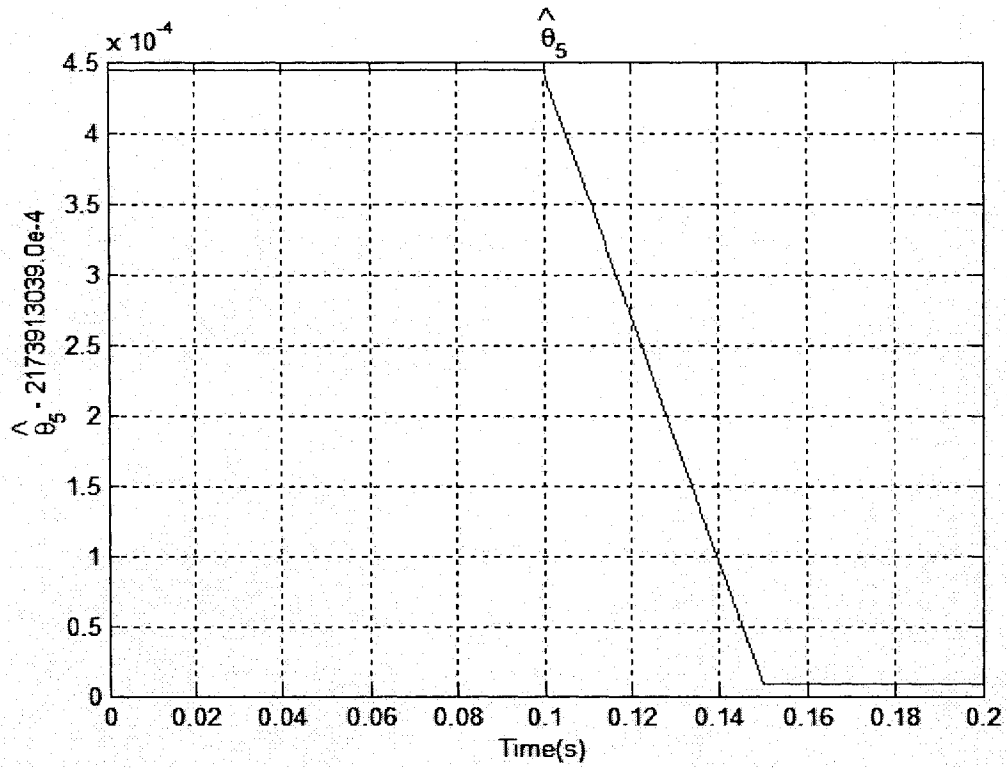


Fig.5-25: $\hat{\theta}_5$ - Adaptive backstepping

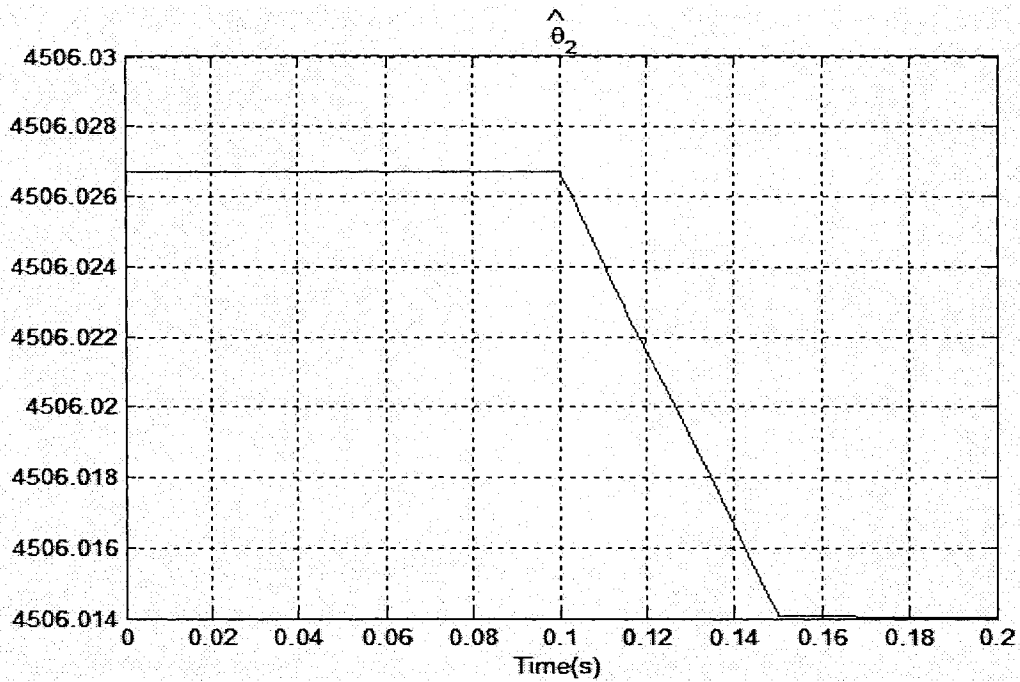


Fig.5-26: $\hat{\theta}_2$ - Adaptive backstepping sliding mode

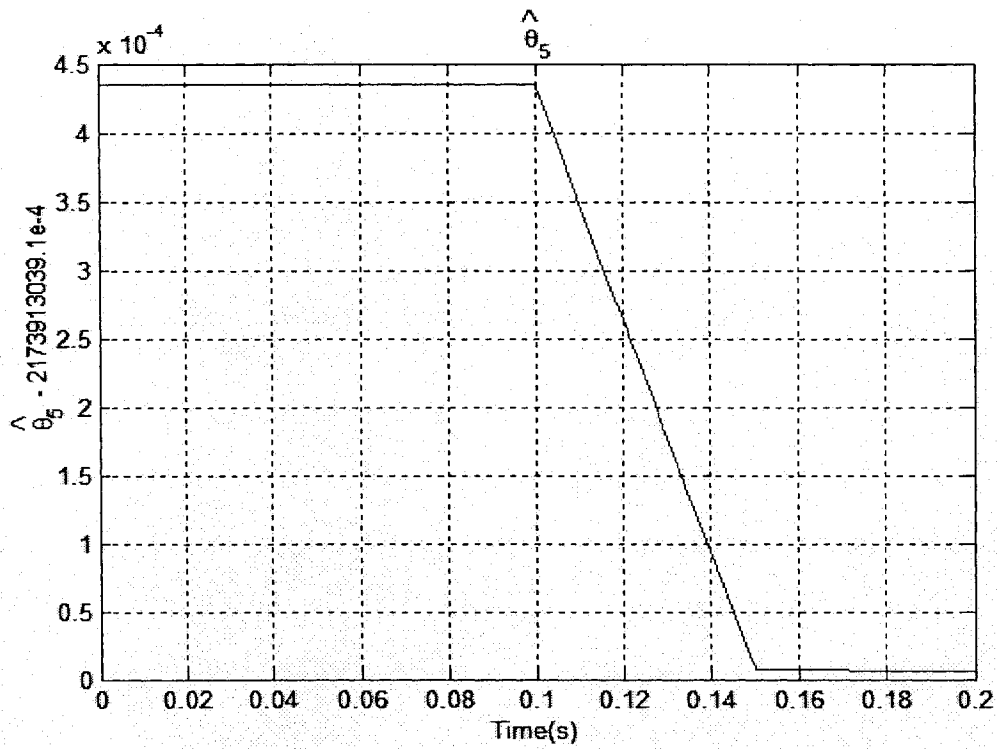


Fig.5-27: $\hat{\theta}_5$ -Adaptive backstepping sliding mode

5.4 Simulation Results Comparison

All the designed nonlinear controllers are simulated under three conditions using MATLAB. The performances, which are compared in terms of steady state error, transient response and settling time, are shown in Table 5-3.

Control strategy		Setpoint change	Load change	Source voltage change
Backstepping	Steady state error	0.1 <i>mV</i>	0.1 <i>mV</i>	0.1 <i>mV</i>
	Transient response (peak value)	8.5 <i>mV</i>	159.6 <i>mV</i>	14.4 <i>mV</i>
	Settling time	25 <i>ms</i>	45 <i>ms</i>	40 <i>ms</i>
Sliding mode	Steady state error	< 0.01 <i>mV</i>	< 0.01 <i>mV</i>	< 0.01 <i>mV</i>
	Transient response	192.5 <i>mV</i>	323 <i>mV</i>	97 <i>mV</i>
	Settling time	26 <i>ms</i>	1 <i>ms</i>	4 <i>ms</i>
Backstepping sliding mode	Steady state error	< 0.01 <i>mV</i>	< 0.01 <i>mV</i>	< 0.01 <i>mV</i>
	Transient response	8.5 <i>mV</i>	156.8 <i>mV</i>	11.6 <i>mV</i>
	Settling time	25 <i>ms</i>	45 <i>ms</i>	40 <i>ms</i>
Adaptive backstepping	Steady state error	0.1 <i>mV</i>	0.1 <i>mV</i>	0.1 <i>mV</i>
	Transient response	8.5 <i>mV</i>	159.5 <i>mV</i>	14.4 <i>mV</i>
	Settling time	25 <i>ms</i>	45 <i>ms</i>	40 <i>ms</i>
Adaptive backstepping sliding mode	Steady state error	< 0.01 <i>mV</i>	< 0.01 <i>mV</i>	< 0.01 <i>mV</i>
	Transient response	8.5 <i>mV</i>	156.8 <i>mV</i>	11.4 <i>mV</i>
	Settling time	25 <i>ms</i>	45 <i>ms</i>	40 <i>ms</i>
Table.5-3: Simulation results comparison				

Chapter 6

Experimental Setup and Results

6.1 Introduction

In this chapter, a buck converter experimental system is constructed in the laboratory to implement the nonlinear controllers designed in Chapter 4. The whole experimental system is shown in Fig.6-1. It consists of the buck converter circuit card, data acquisition (DAQ) board, and personal computer (PC). The buck converter circuit receives control signals from the DAQ board placed in the computer. The DAQ board acquires the output voltage signal from the buck converter circuit card by using an A/D converter. Two DC power supplies are needed to operate the whole system, one to provide energy to the buck converter system and the other to feed the electronic parts of the card.

The prototype buck converter circuit card is assembled using low cost commercial electronic components. The controllers are implemented on the PC through the DAQ board. This is clearly not a practical solution because the computer implementation is too expensive. We could have performed it with analog circuits, but this is not the essential point of our study. Our objective is to test the proposed controllers and compare the controller performances using a standard laboratory setup.

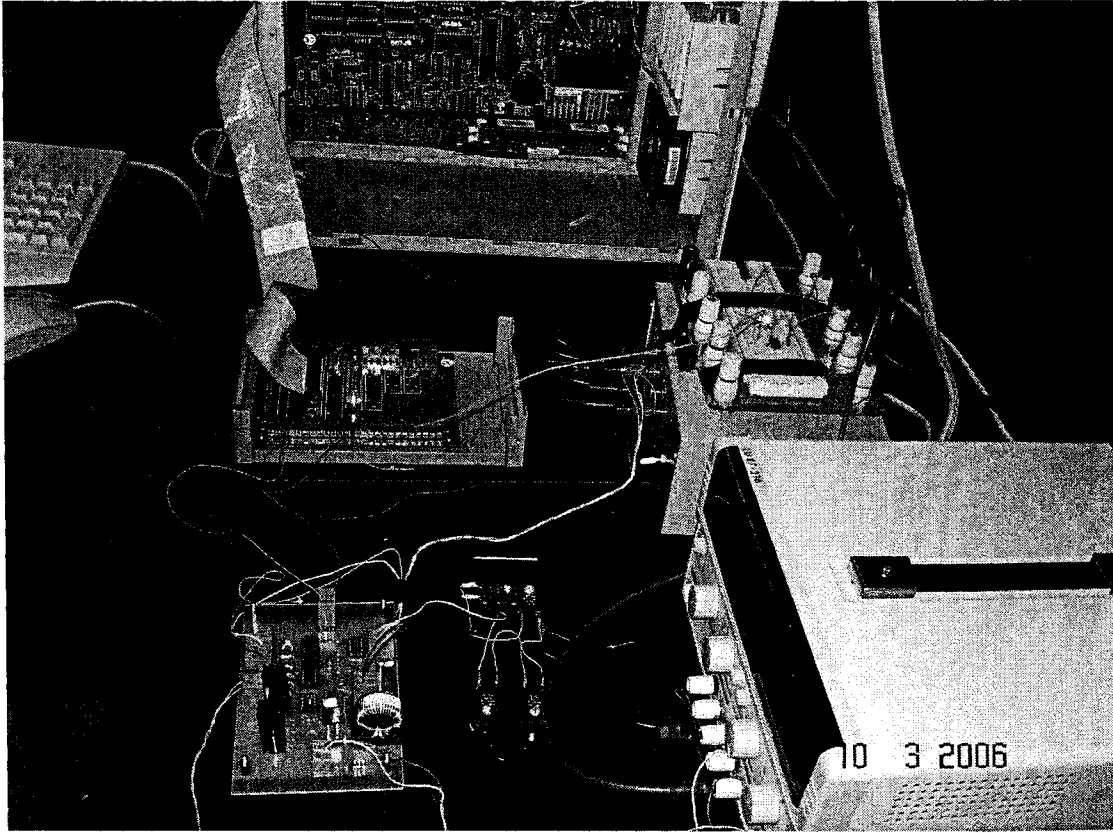


Fig.6-1: Buck converter experimental system

6.2 Experimental Setup

The diagram of the experimental setup is shown in Fig.6-2. The proposed controllers are implemented on PC using Visual C++ language, which contains the description of the controllers. In each sampling period, the computer obtains the output voltage from the buck converter circuit, calculates the control input in terms of duty cycle and translates the duty cycle to voltage signal which is sent to the PWM circuit to generate PWM signals to control the buck converter. Time derivatives in some of the control laws are accomplished with Runge-Kutta method.

In this experiment, the sampling period is set as 1 millisecond, which is fast enough for the computer to finish reading signals from the boards, calculating and sending signals back to the boards.

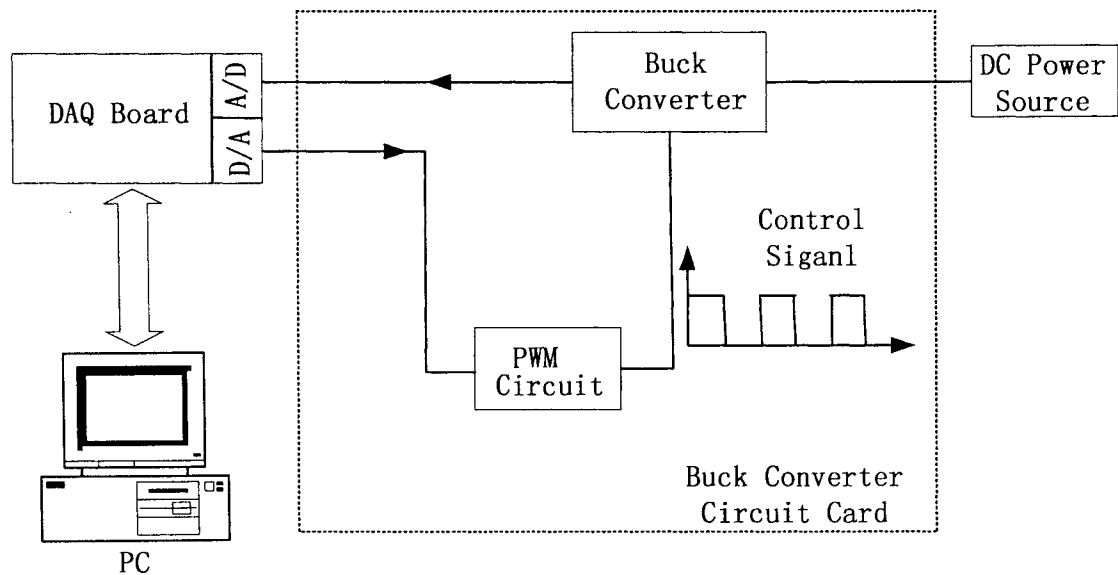


Fig.6-2: Diagram of the experimental setup

6.2.1 Buck Converter Circuit Card Description

Fig.6-3 shows the buck converter circuit card, which is built with a buck converter circuit, a pulse width modulation circuit, and a MOSFET driver circuit.

The buck converter circuit is basically composed of an inductor, a capacitor, a resistance load, a MOSFET (IRF540N) and a rapid diode (MUR1520) in a suitable manner. All these elements are fed by a DC power supply. The values of these components are shown in Table.6-1, which are taken from the datasheets.

The buck converter circuit can be controlled by means of a PWM control circuit or by directly introducing a switching signal coming from the DAQ board. In our experiment, the PWM control circuit is designed using a TL494 integrated circuit. The PWM control circuit, which is shown in Fig.6-3, converts a continuous voltage signal in the range [0, 5] to a PWM signal of the duty ratio from 0 to 100%. Output pulse width modulation is accomplished by comparison of the positive sawtooth waveform across the capacitor to the external control signals fed into deadtime control.

The MOSFET is a voltage controlled device and its on state is achieved when the gate-to-source voltage sufficiently exceeds the threshold voltage. The MOSFET driver circuit is performed by using chip IR4428. The PS8601 eight pin optocoupler, made by NEC, is used to create a floating ground between the MOSFET and the control circuit.

The output voltage of buck converter circuit will be fed into the DAQ board to be used in the control law. A voltage divider is used to reduce the level of the output voltage signal in such a way that its final value is always in the range [0, 10] volts.

6.2.2 DAQ Board

In the laboratory the data exchange between instruments and a computer can be realized by using a DAQ board. A typical commercial DAQ board contains analog to digital converters (ADC) and digital to analog converters (DAC) that allow input and output of

analog and digital signals in addition to digital input/output channels.

The DAQ board used for our experiment is ADIO1600 from ICS Advent. It is a multi-function high-speed analog/digital I/O card for use in computers. With this card installed, the computer can be used as a precision data acquisition and control system. The DAQ board is plugged in PCI slot inside the computer, and the connection to buck converter circuit is made via a 37-pin D type connector.

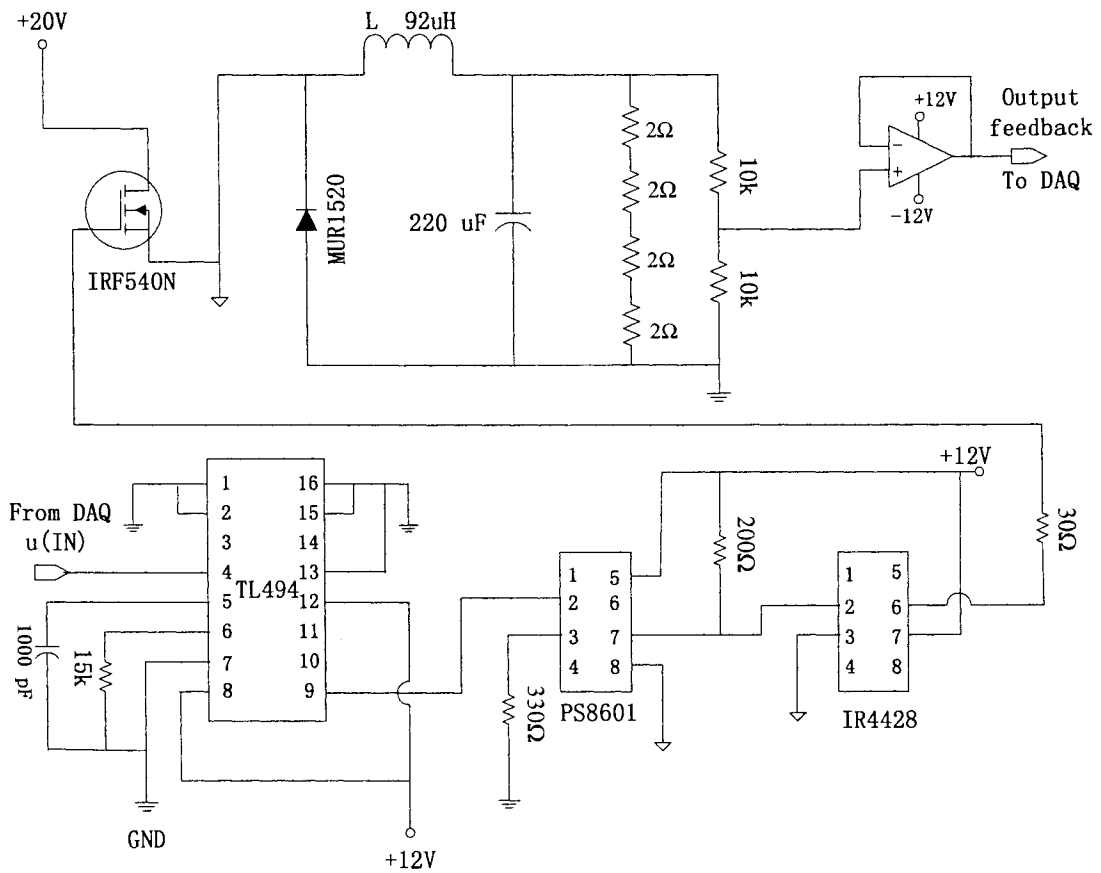


Fig.6-3: Buck converter circuit card

6.3 Experimental Results

The five control laws described in Chapter 4 have been implemented on the buck converter experimental system. Their behaviors are compared with the following basic criteria:

- Transient and steady state response to step output voltage references.
- Response to the load resistance changes
- Disturbances in the power supply.

In the design procedure of two adaptive controllers, the parameter estimators $\hat{\theta}_2$ and $\hat{\theta}_5$ appear in the denominators. It is worth taking a look at their values in the experiment.

The specifications of the buck converter circuit are given in Table.6-1. In the experiment, the value of the desired output voltage is set to $V_d = 8$ volts.

Parameter name	Symbol	Value
Power supply	E	20 volts
Inductance	L	92 μH
Capacitance	C	220 μF
Load resistance	R	8 Ω
Inductor resistance	R_L	74 $m\Omega$
Capacitor ESR	R_C	70 $m\Omega$
Diode resistance	R_D	30 $m\Omega$
Switching resistance	R_S	44 $m\Omega$
Switching frequency	f	70 KHz

Table.6-1: Specification of buck converter (experiment)

6.3.1 Current Estimated Using Reduced Order Observer

In this section, the inductor current is estimated with the designed reduced order observer.

The design parameters of the proposed controllers are shown in Table.6-2.

Control strategy	Design parameters
Backstepping	$c_0 = 0.75, c_1 = 150, c_2 = 400, L_{est} = 0.01$
Sliding mode	$K = 32000, L_{est} = 0.01$
Backstepping sliding mode	$c_0 = 0.75, c_1 = 150, k_1 = 400, k_2 = 5, L_{est} = 0.01$
Adaptive backstepping	$c_0 = 0.75, c_1 = 150, c_2 = 400$ $L_{est} = 0.01, \gamma_i = 10^{-2} (i=1, \dots, 5)$
Adaptive backstepping sliding mode	$c_0 = 0.75, c_1 = 150, k_1 = 400, k_2 = 5$ $\gamma_i = 10^{-2} (i=1, \dots, 5), L_{est} = 0.01$
Table.6-2: Specification of design parameters (estimated current)	

6.3.1.1 Response to Output Voltage Reference

The controller responses to the output voltage reference change from 8 volts to 10 volts are shown in Fig.6-4, Fig.6-5, Fig.6-6, Fig.6-7 and Fig.6-8. It can be seen that the five nonlinear controllers have good performances to the output reference change. All the controllers show about 40 millivolt overshoots. The sliding mode controller exhibits little chattering around the desired value.

The behaviors of the parameter estimators $\hat{\theta}_2$ and $\hat{\theta}_5$ for the two adaptive controllers are shown in Fig.6-9, Fig.6-10, Fig.6-11, and Fig.6-12. Their values are adjusted by

calculating the update laws to make the controller work well. It is clear that they never be zero.

Note that there are some disagreements between the experimental results and simulation results in terms of the overshoots and the settling time. This is mainly due to the parameters' deviation between the actual experimental circuit and the simulation program.

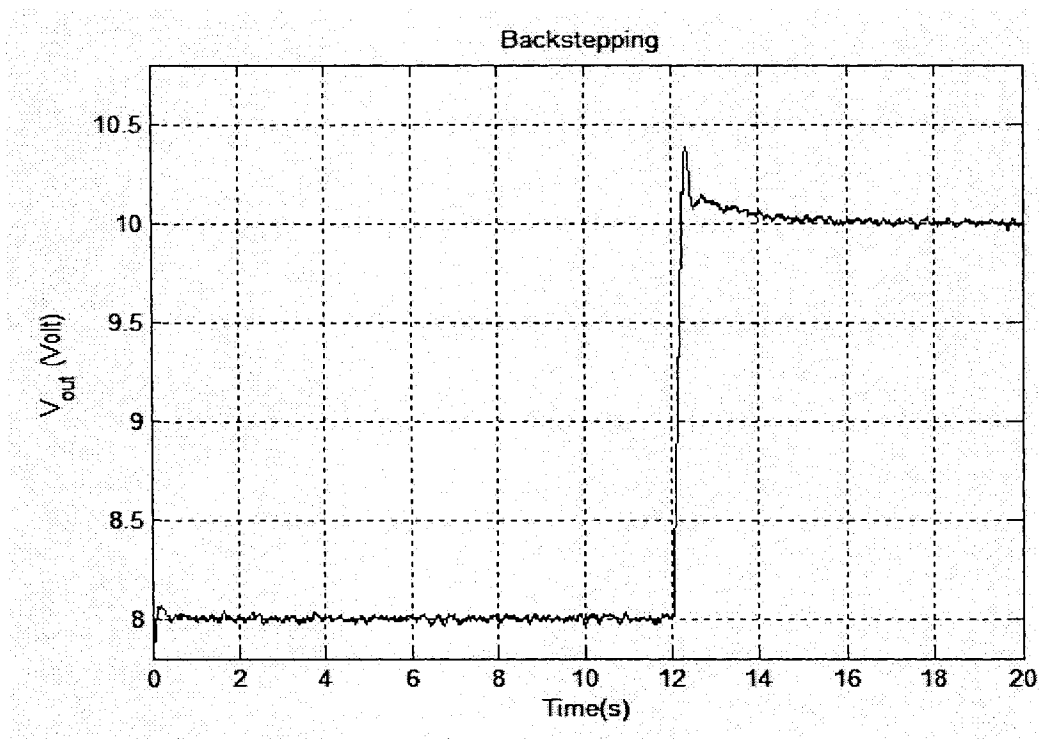


Fig. 6-4: Backstepping

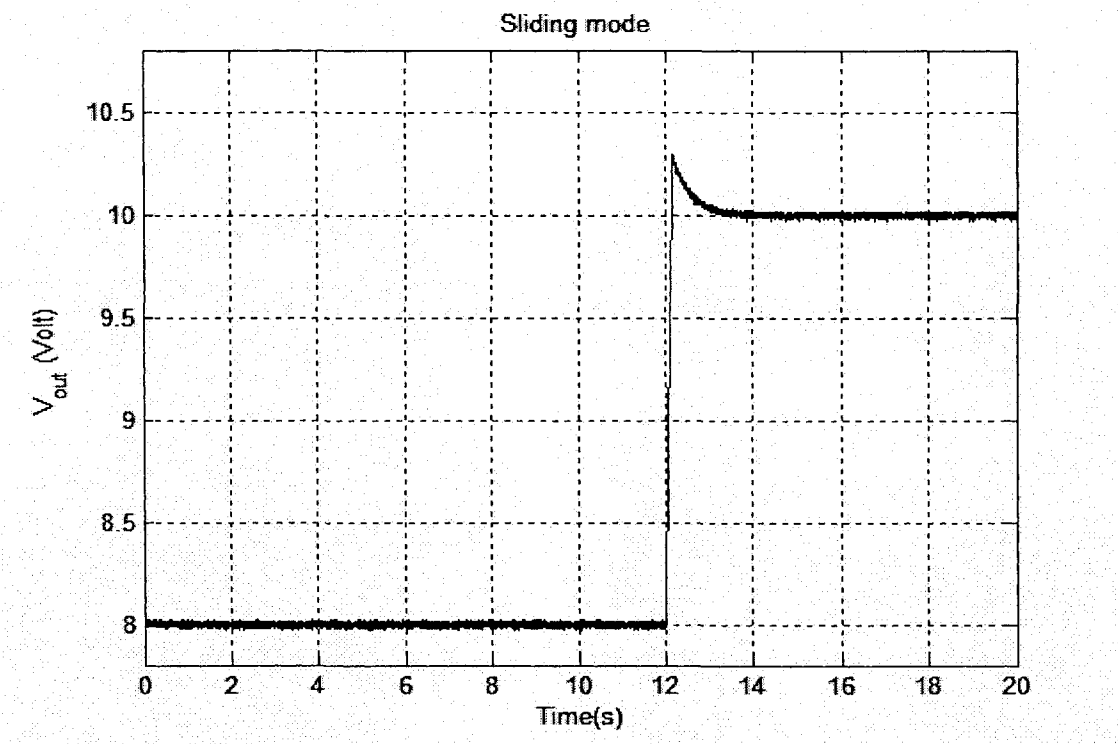


Fig. 6-5: Sliding mode

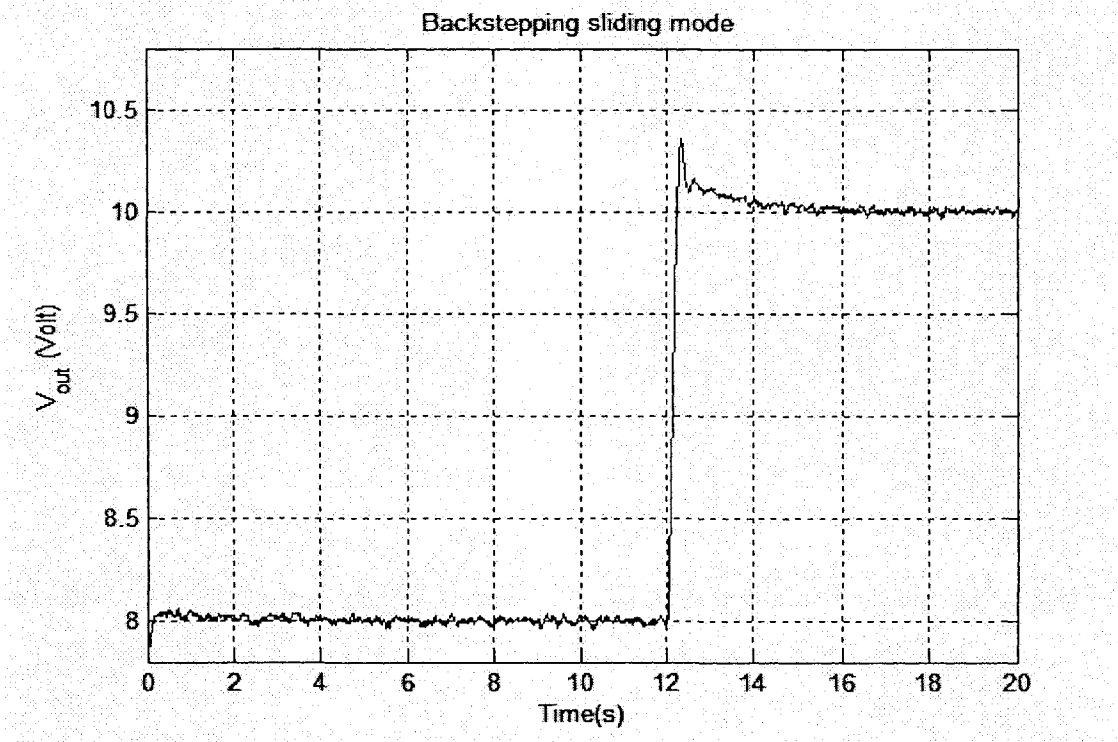


Fig. 6-6: Backstepping sliding mode

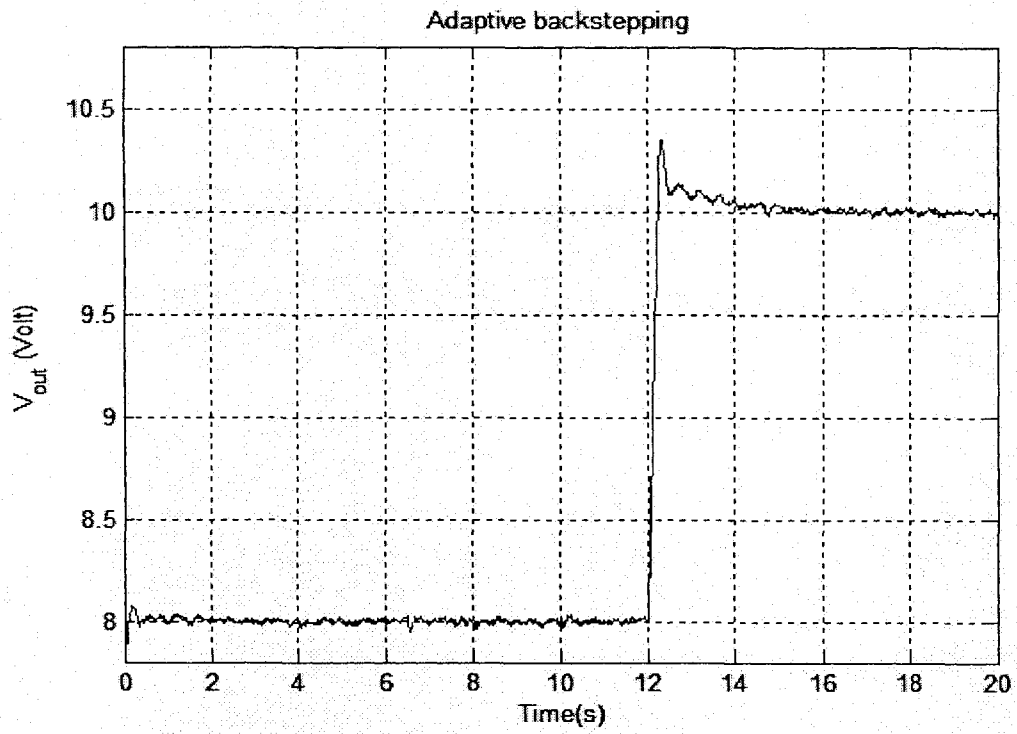


Fig. 6-7: Adaptive backstepping

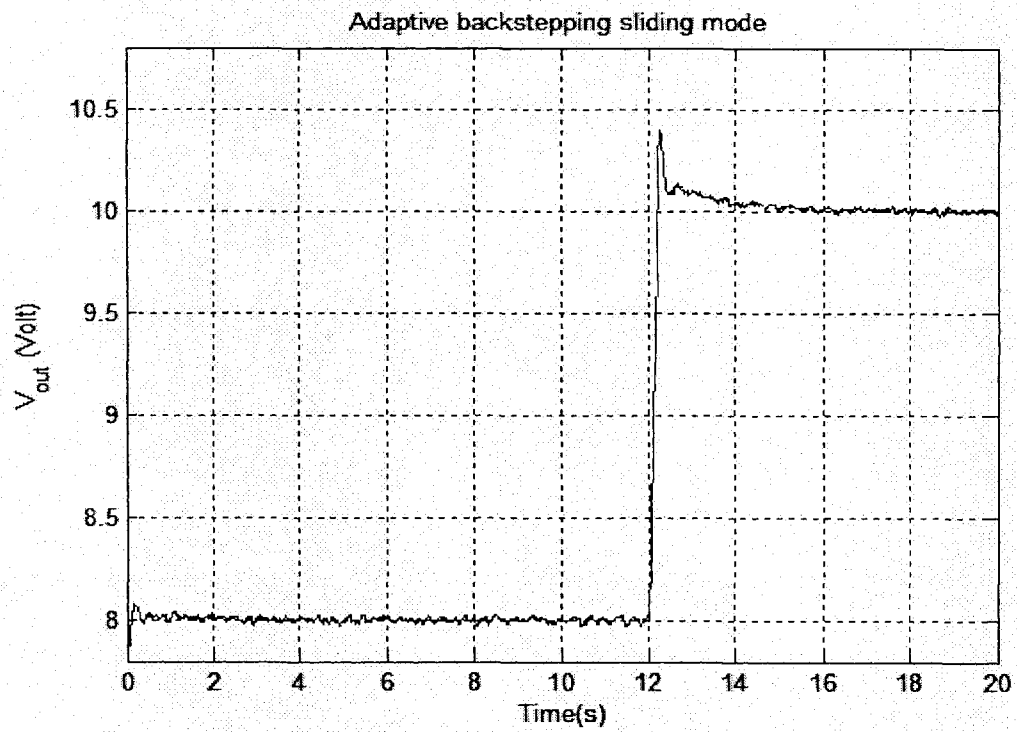


Fig. 6-8: Adaptive backstepping sliding mode

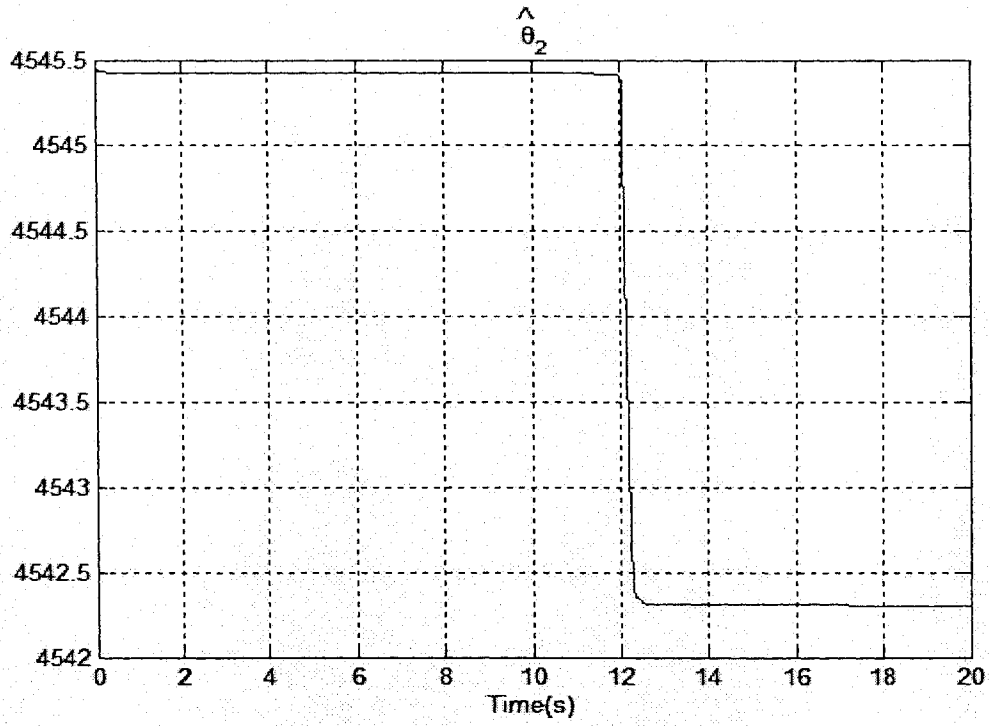


Fig. 6-9: $\hat{\theta}_2$ - Adaptive backstepping

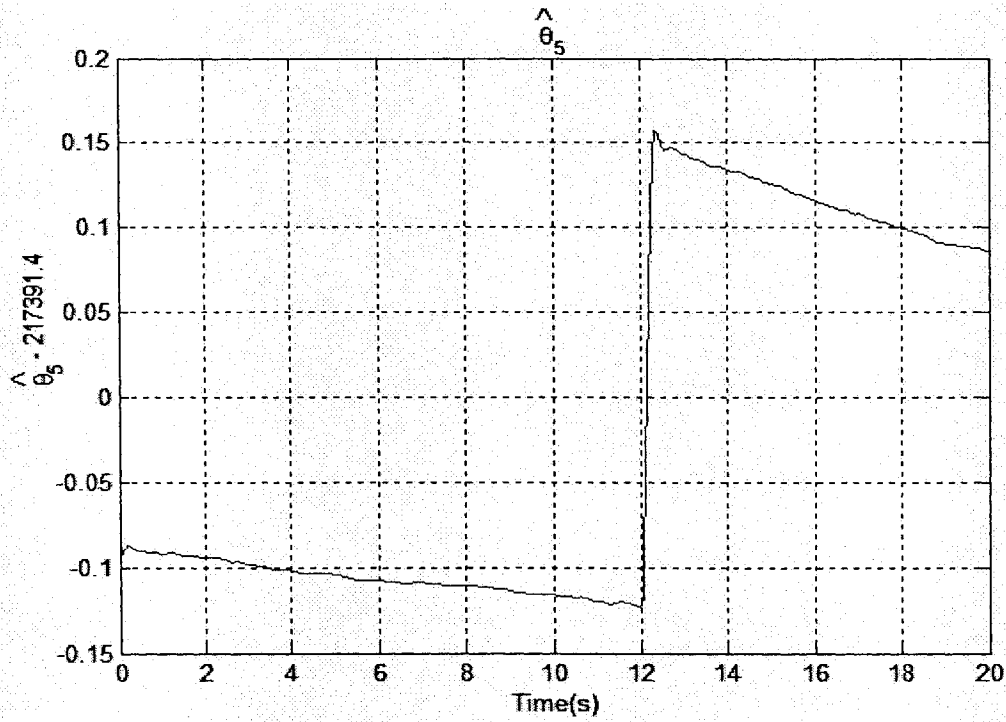


Fig. 6-10: $\hat{\theta}_5$ - Adaptive backstepping

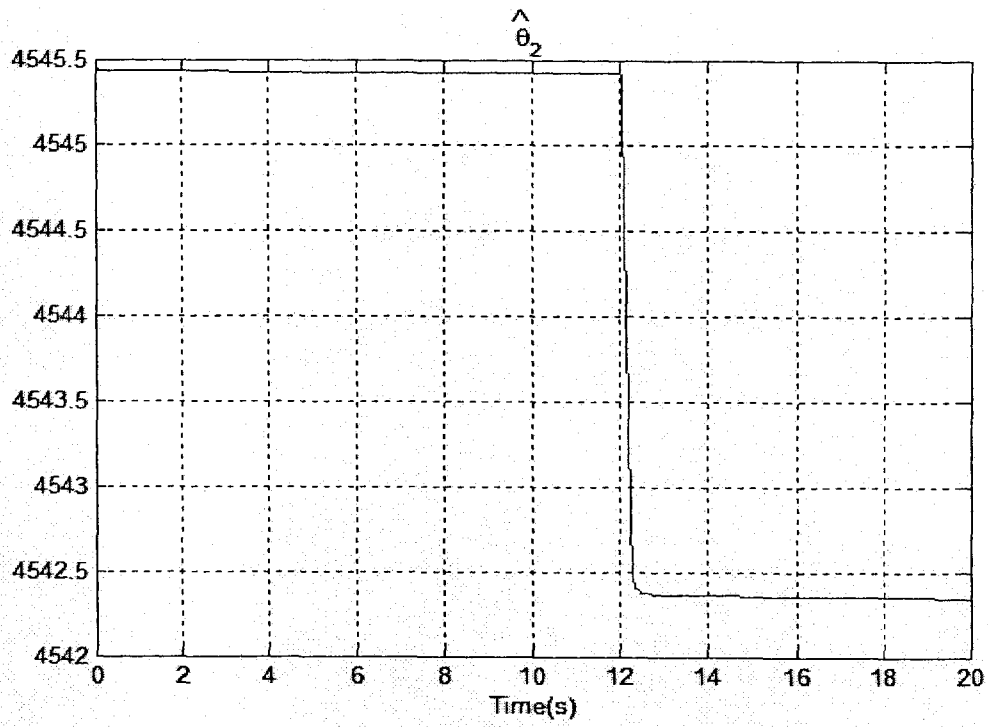


Fig.6-11: $\hat{\theta}_2$ -Adaptive backstepping sliding mode

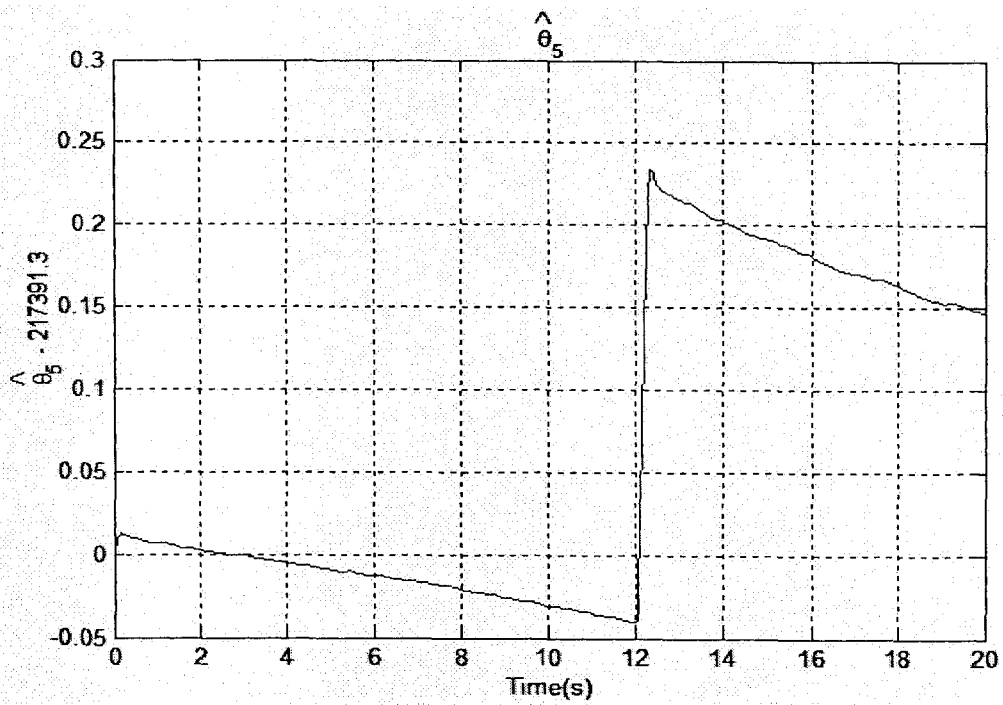


Fig.6-12: $\hat{\theta}_5$ -Adaptive backstepping sliding mode

6.3.1.2 Response to Load Change

In order to introduce a load change to the experimental system, the load resistance R is reduced from $R = 8\Omega$ to $R = 4\Omega$. The performance of the backstepping controller is shown in Fig.6-13. It can be seen that the output voltage dropped and recovered to the desired value during the load changes. The biggest steady state error is about $\pm 25mV$, and the transient response is about $90mV$.

In Fig.6-14, the sliding mode controller shows its robustness and faster response time to the load variations and exhibits $\pm 20mV$ chattering as well.

The behavior of the backstepping sliding mode controller is shown in Fig.6-15, it can be seen that there is no chattering. The steady state error is about $\pm 25mV$ and the transient response is $90mV$.

Fig.6-16 depicts the performance of the adaptive backstepping controller, from which about $\pm 25mV$ steady state error and $70mV$ transient response can be observed.

The behavior of the adaptive backstepping sliding mode controller is presented in Fig.6-17. It can be found that this controller shows no chattering problem, but it exhibits $\pm 20mV$ steady state error and $40mV$ transient response.

As shown in Fig.6-18, Fig.6-19, Fig.6-20 and Fig.6-21, the values of parameter estimators $\hat{\theta}_2$ and $\hat{\theta}_3$ for the adaptive controllers will never be zero.

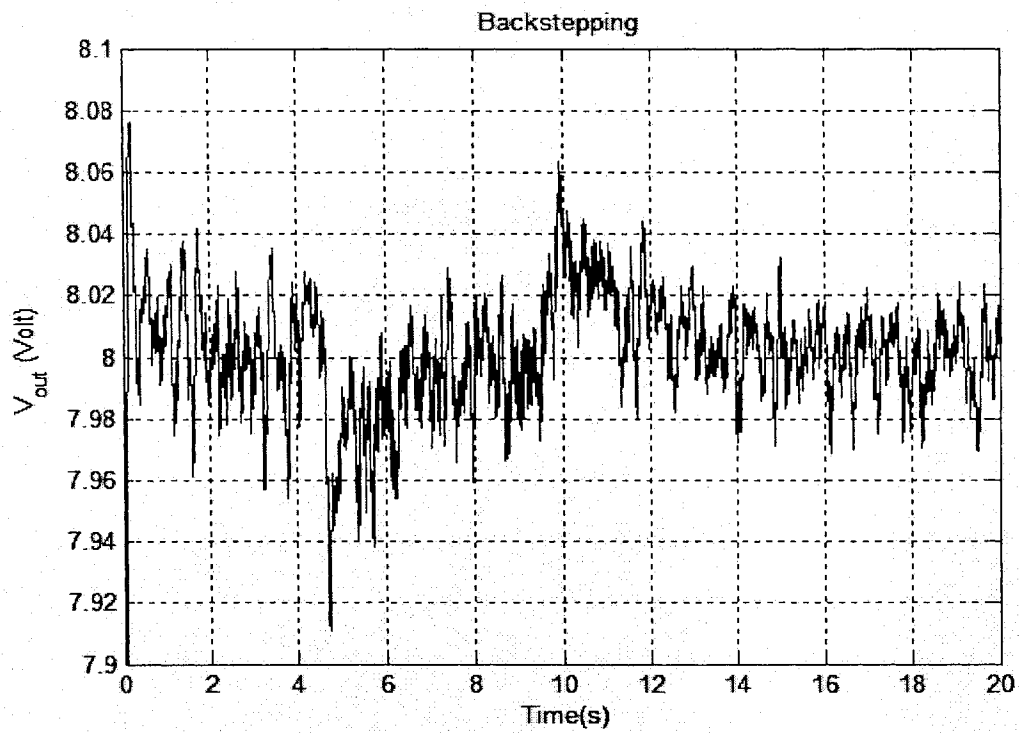


Fig.6-13: Backstepping

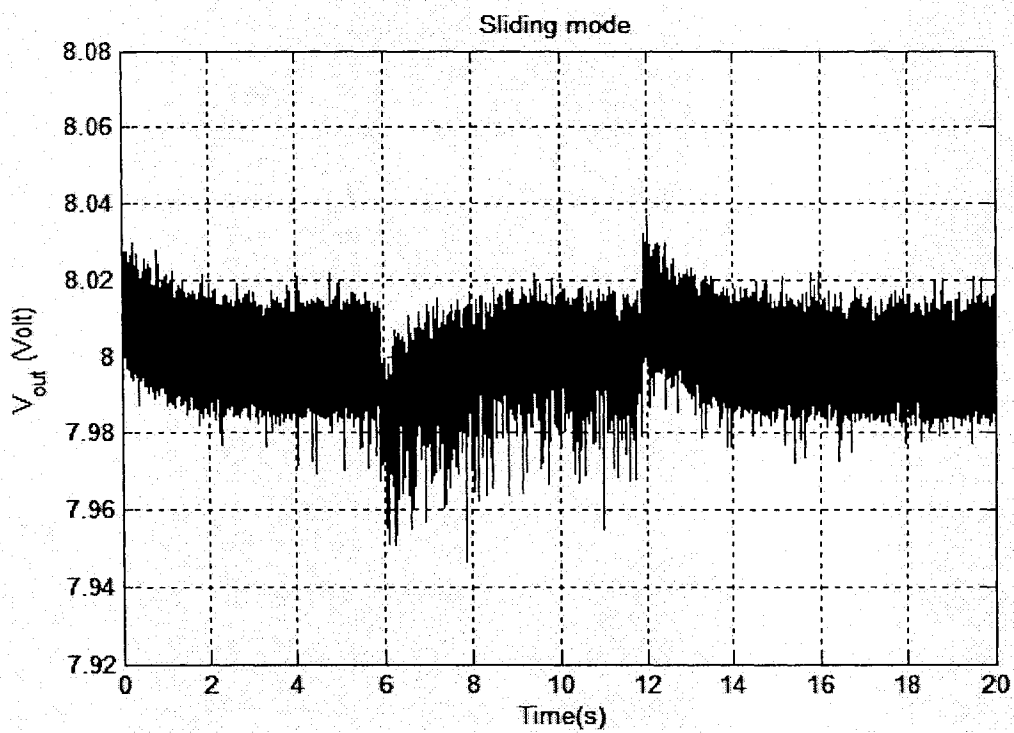


Fig.6-14: Sliding mode

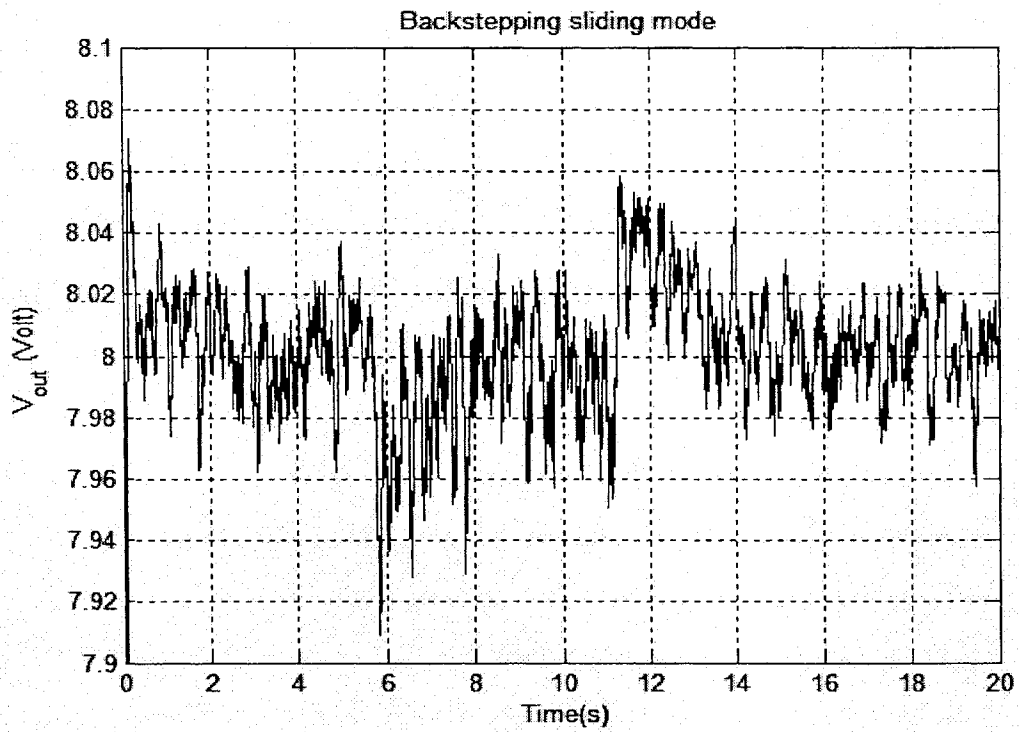


Fig.6-15: Backstepping sliding mode

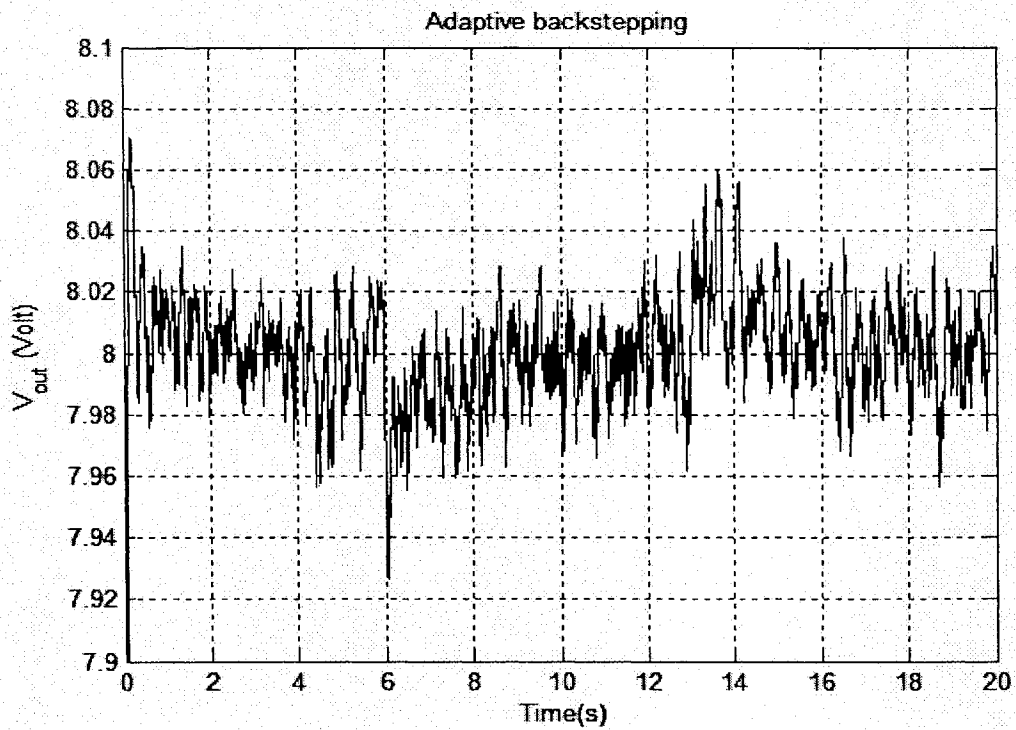


Fig.6-16: Adaptive backstepping

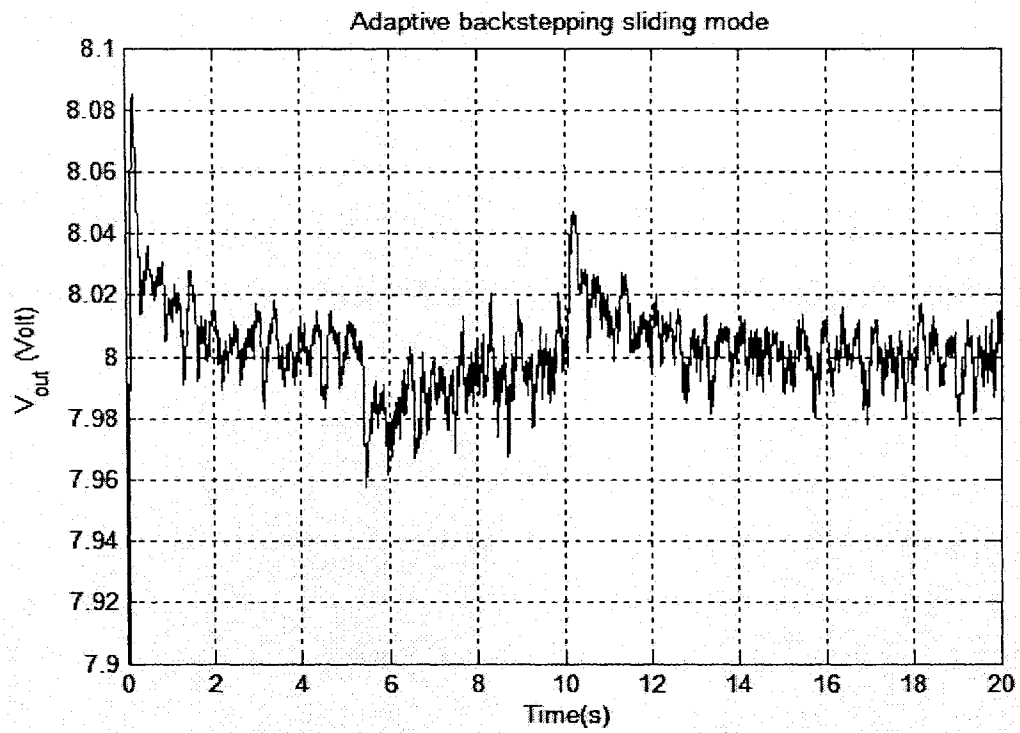


Fig.6-17: Adaptive backstepping sliding mode

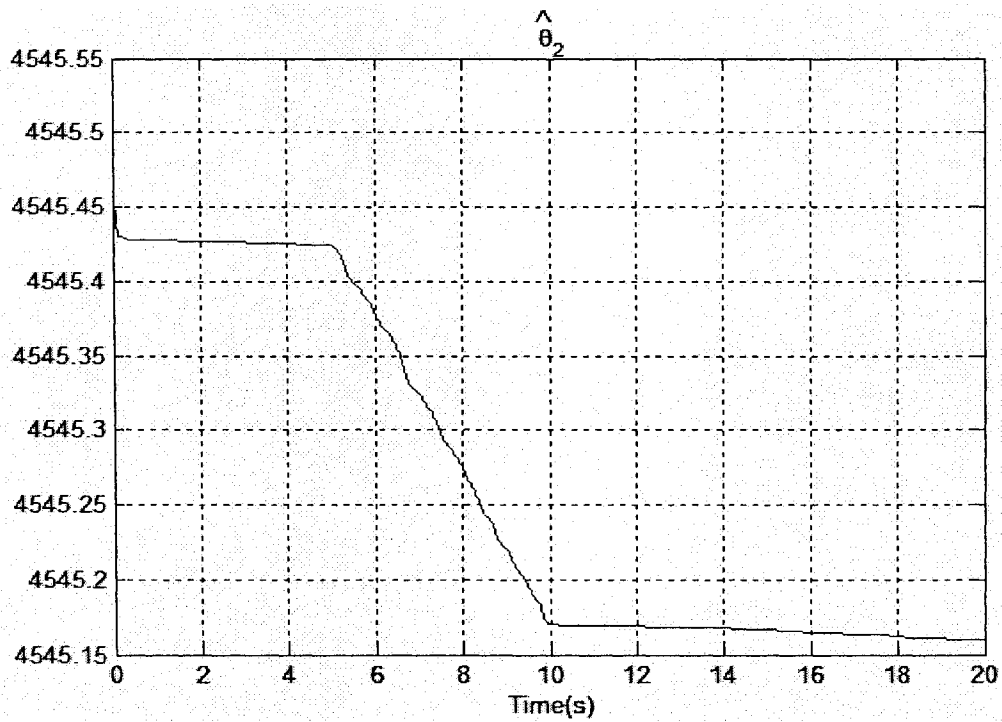


Fig.6-18: $\hat{\theta}_2$ -Adaptive backstepping

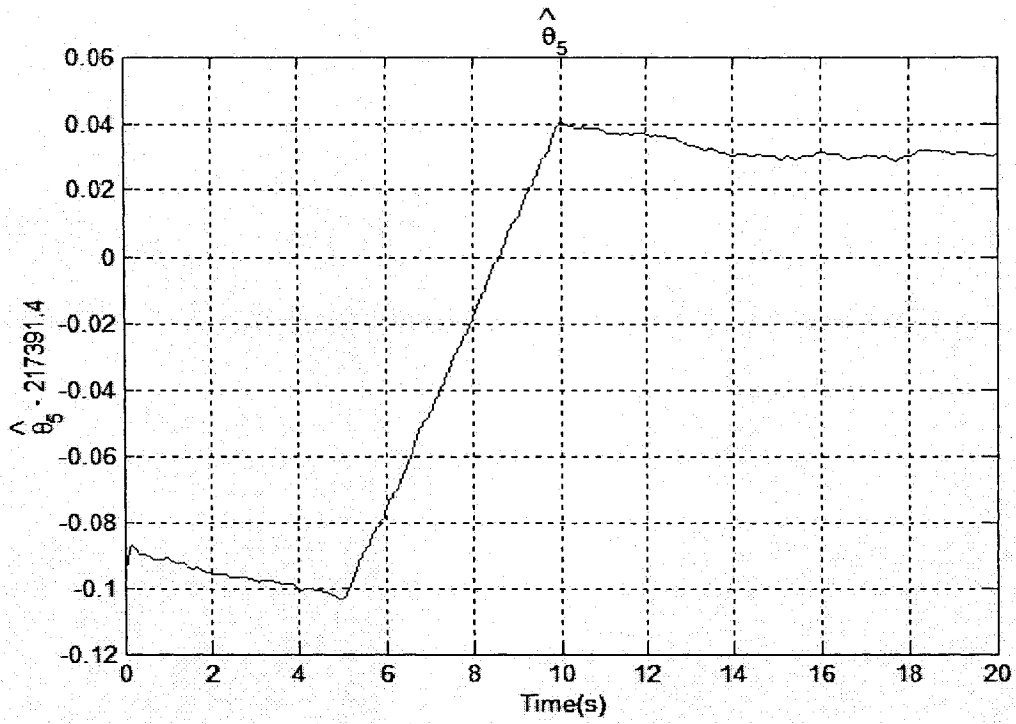


Fig.6-19: $\hat{\theta}_5$ - Adaptive backstepping

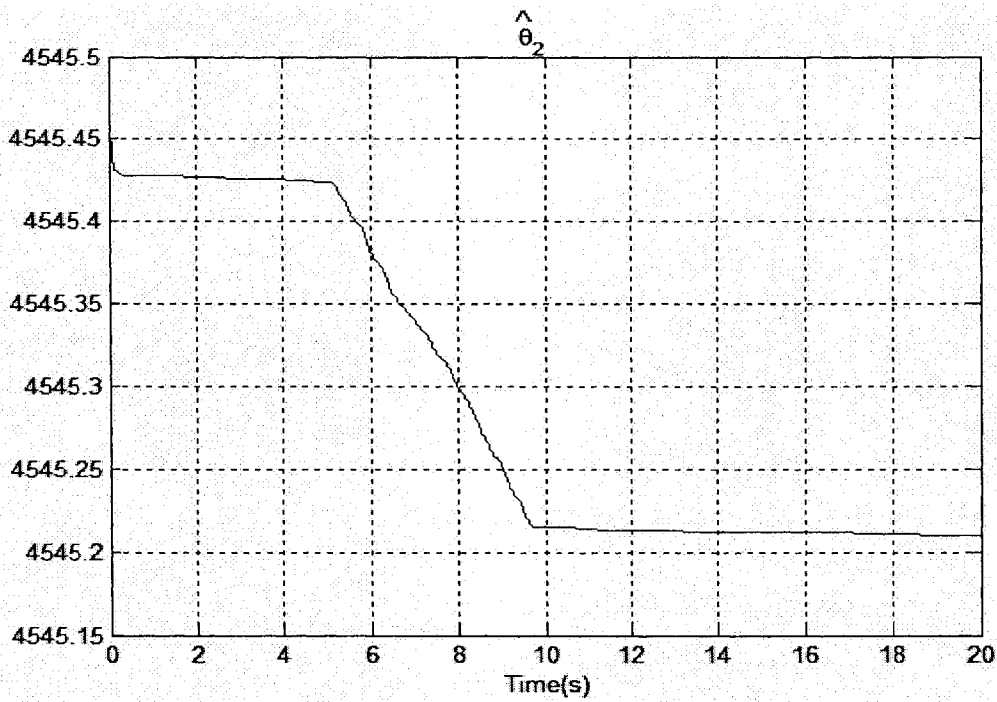


Fig.6-20: $\hat{\theta}_2$ - Adaptive backstepping sliding mode

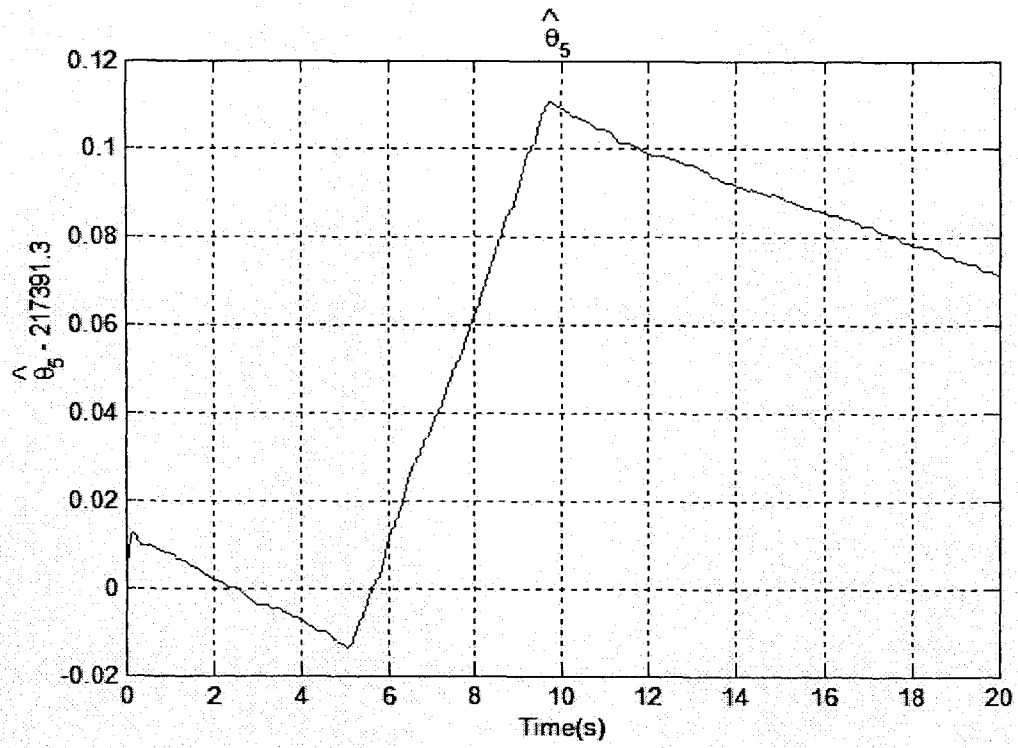


Fig.6-21: $\hat{\theta}_5$ -Adaptive backstepping sliding mode

6.3.1.3 Response to Source Voltage Change

For a practical buck converter system, the main disturbance is generated by the power source. It is important to study the nonlinear controllers' robustness to source disturbances. In this experimental system, the disturbance is introduced by changing the source voltage from 20 volts to 18 volts.

The performance of the backstepping controller, which is shown in Fig.6-22, reveals that the output voltage is less sensitive to the disturbance and it has about $\pm 25mV$ steady state error and $60mV$ transient response.

The performance of the sliding mode controller is shown in Fig.6-23, from which the controllers' robustness and faster response time to disturbances can be observed. Meanwhile, there also exists $\pm 20mV$ chattering.

As shown in Fig.6-24, the backstepping sliding mode controller doesn't have chattering. The steady state error is about $\pm 25mV$ and the transient response is $50mV$.

The performance of the adaptive backstepping controller is shown in Fig.6-25. This controller has $\pm 20mV$ steady state error and $50mV$ transient response.

Fig.6-26 shows the behavior of the adaptive backstepping sliding mode controller. It can be seen that the chattering problem is gone. The controller shows $\pm 20mV$ steady state error and $50mV$ transient response.

After checking the performances of the parameter estimators $\hat{\theta}_2$ and $\hat{\theta}_5$ for the adaptive controllers shown in Fig.6-27, Fig.6-28, Fig.6-29 and Fig.6-30, the values of the estimators are not zero.

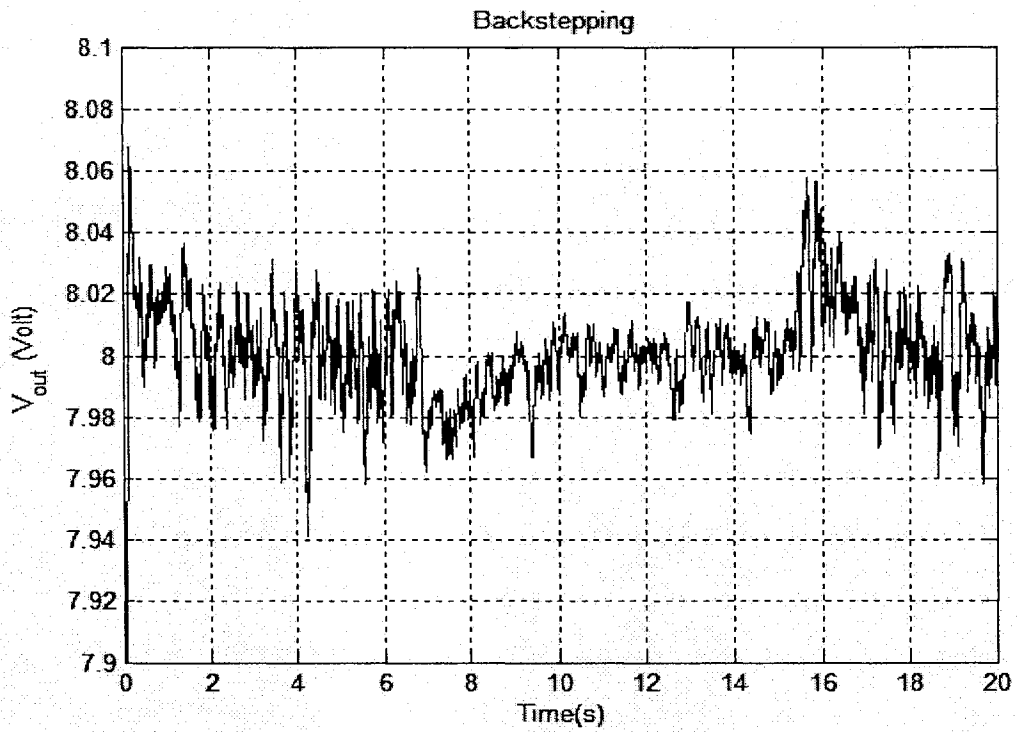


Fig.6-22: Backstepping

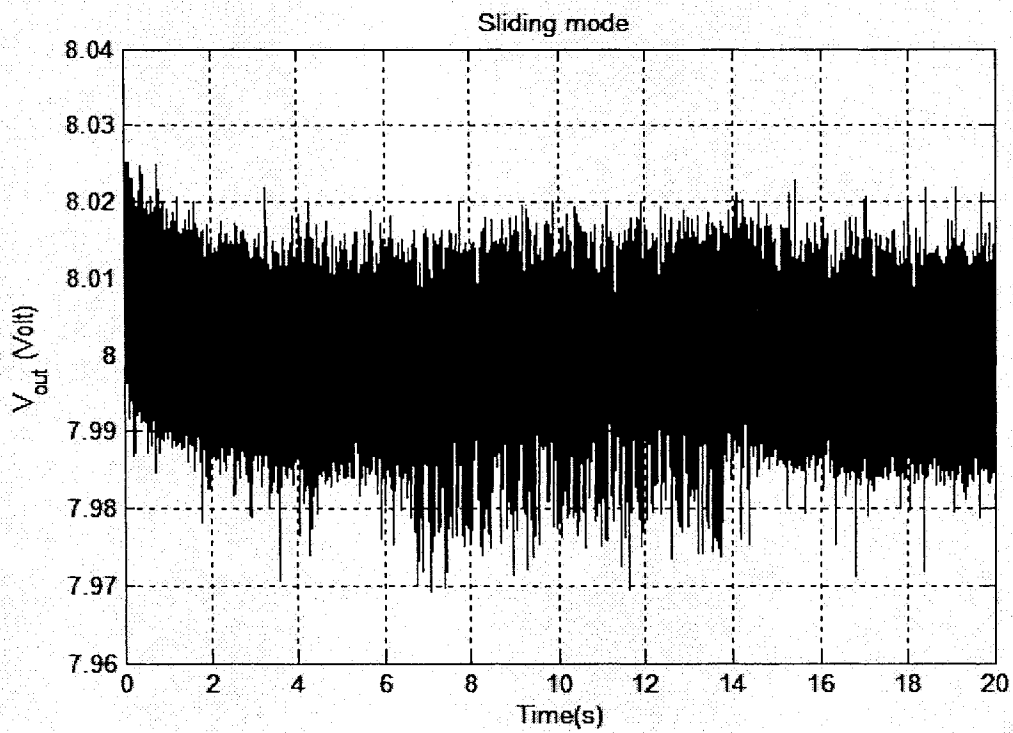


Fig.6-23: Sliding mode

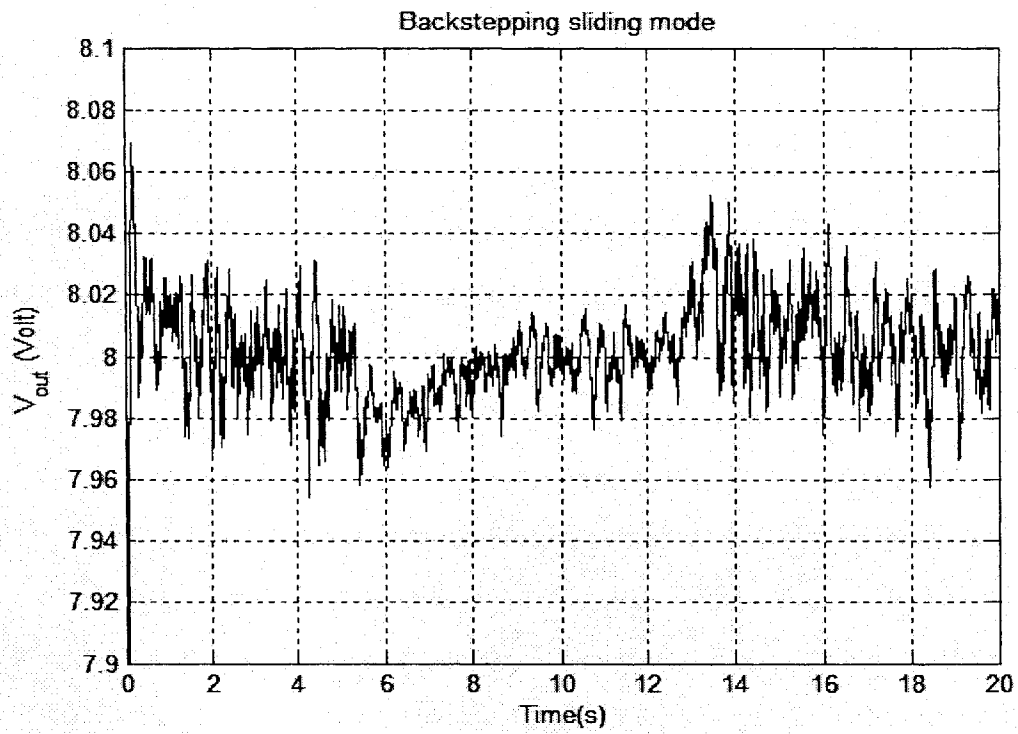


Fig.6-24: Backstepping sliding mode

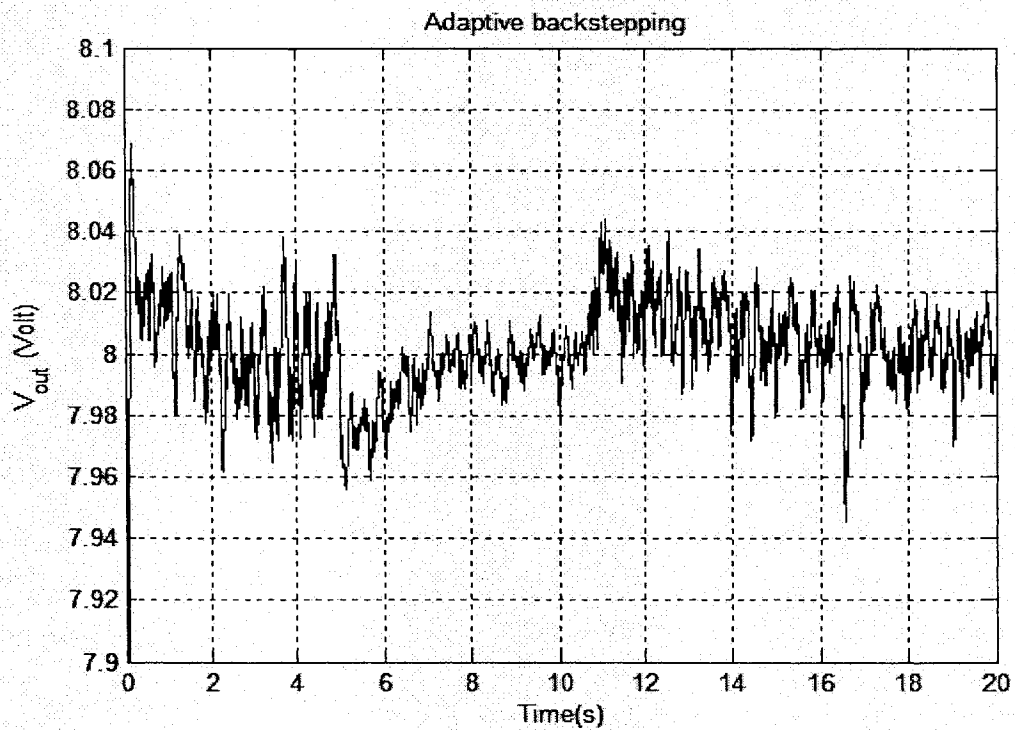


Fig.6-25: Adaptive backstepping

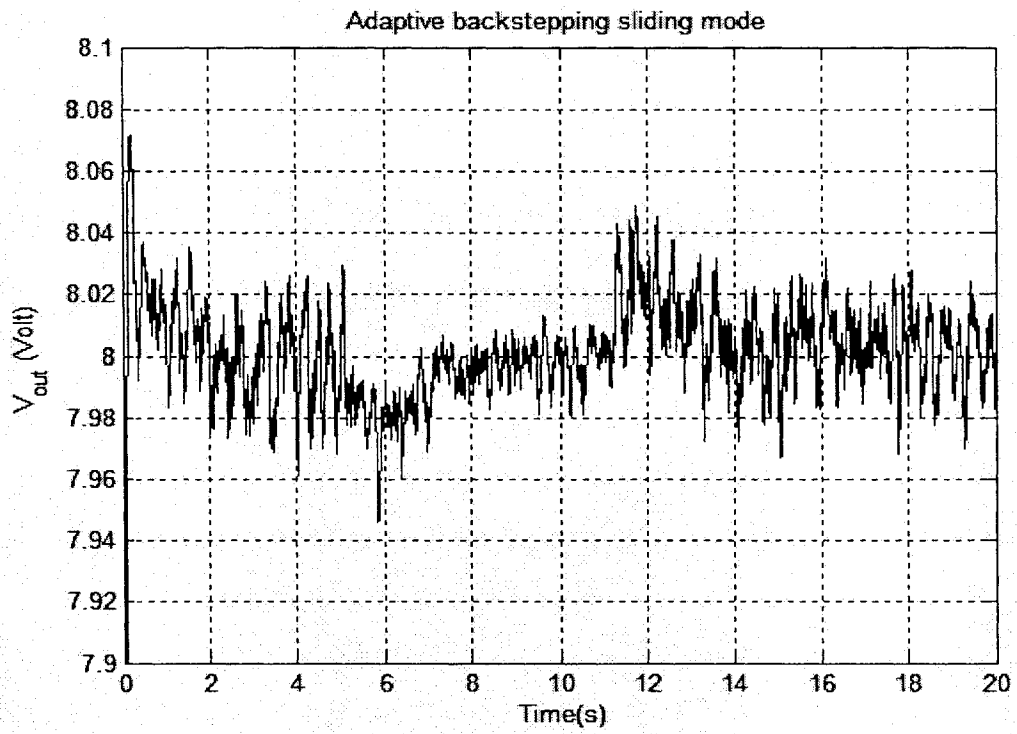


Fig.6-26: Adaptive backstepping sliding mode

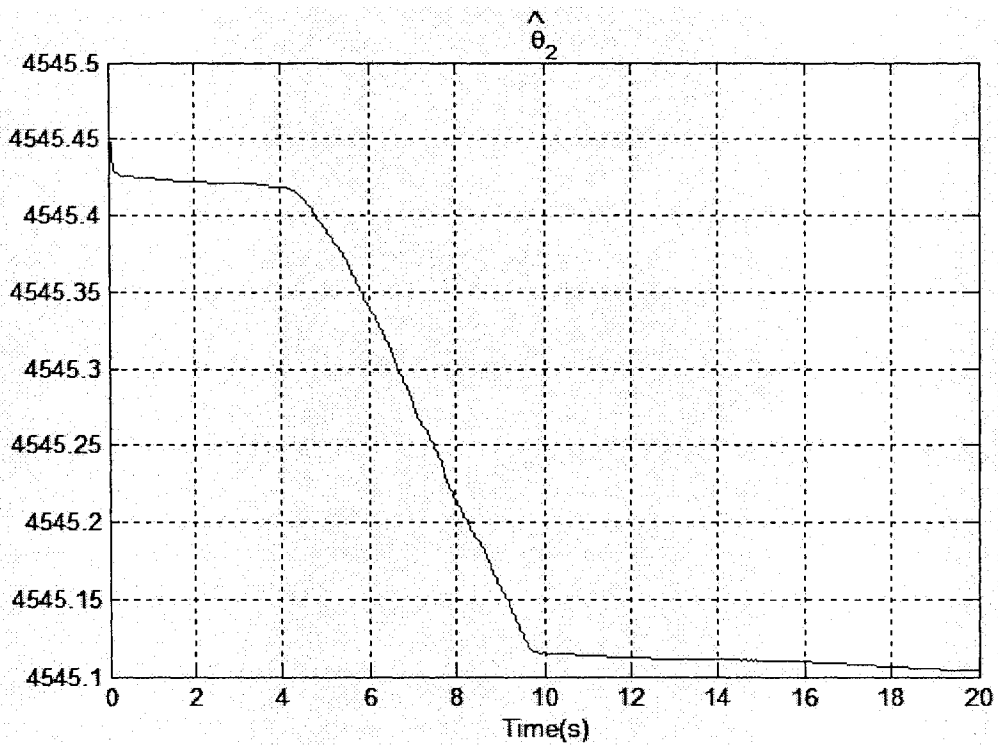


Fig.6-27: $\hat{\theta}_2$ -Adaptive Backstepping

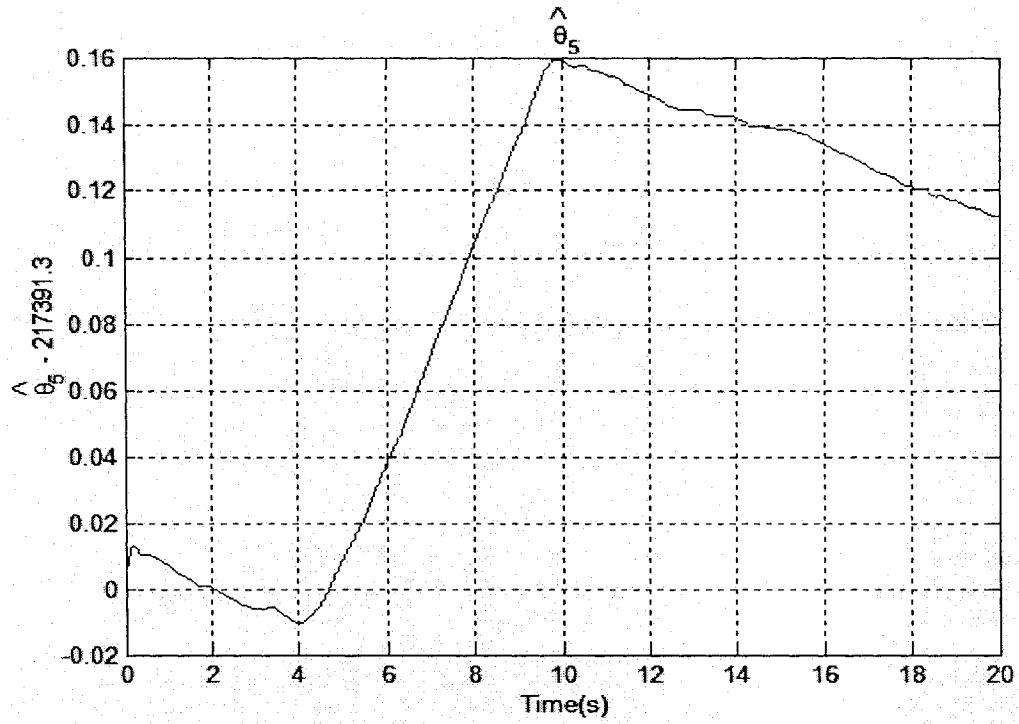


Fig.6-28: $\hat{\theta}_5$ - Adaptive backstepping

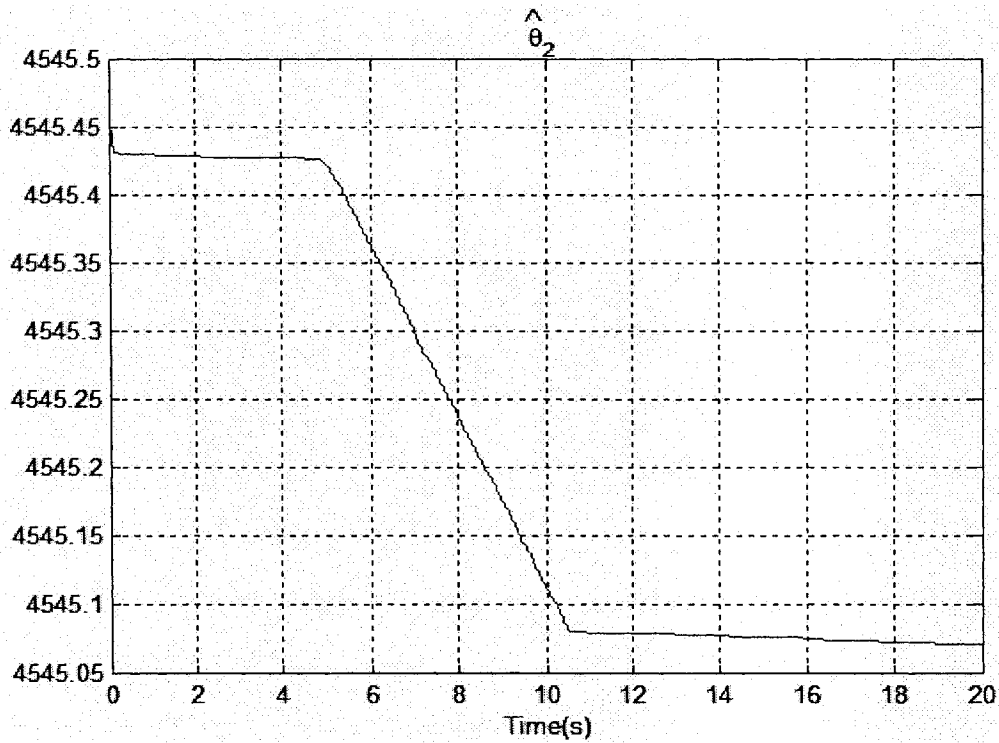


Fig.6-29: $\hat{\theta}_2$ - Adaptive backstepping sliding mode

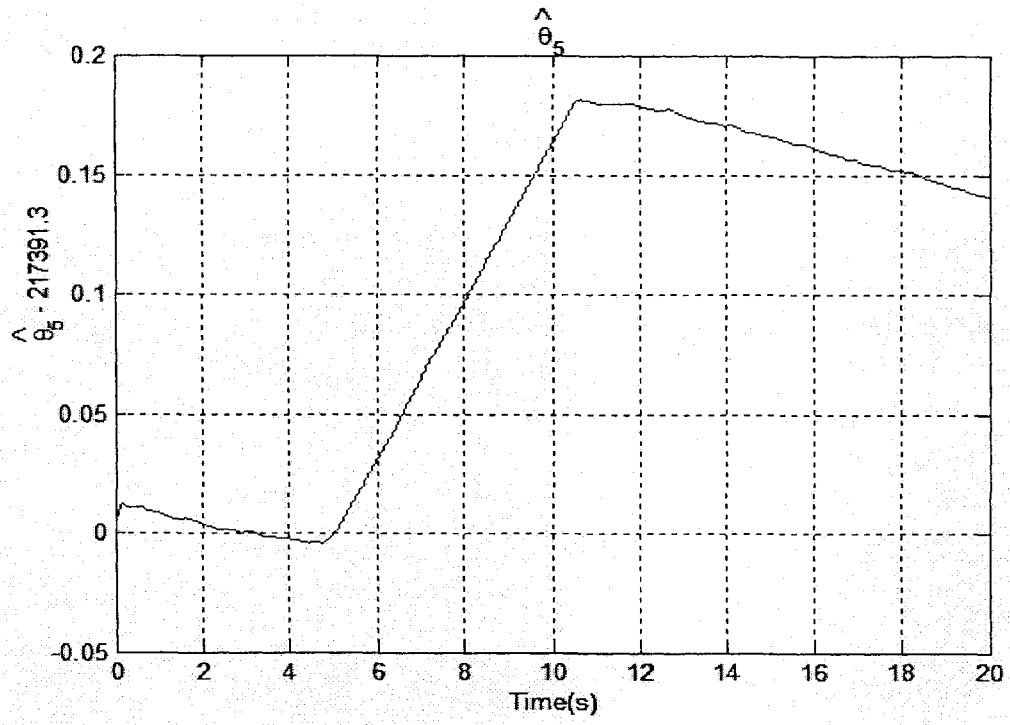


Fig.6-30: $\hat{\theta}_5$ -Adaptive backstepping sliding mode

6.3.2 Current Measured Using Current Transducer

In this section, the current transducer (LTS 6-NP) is used to measure the inductor current.

The design parameters of the proposed controllers are shown in Table.6-3.

Control strategy	Design parameters
Backstepping	$c_0 = 5, c_1 = 60000, c_2 = 56000$
Sliding mode	$K = 22000$
Backstepping sliding mode	$c_0 = 5, c_1 = 60000, k_1 = 56000, k_2 = 2000,$
Adaptive backstepping	$c_0 = 5, c_1 = 60000, c_2 = 56000$ $\gamma_i = 10^{-2} (i=1, \dots, 5)$
Adaptive backstepping sliding mode	$c_0 = 5, c_1 = 60000, k_1 = 56000, k_2 = 2000$ $\gamma_i = 10^{-2} (i=1, \dots, 5),$
Table.6-3: Specification of design parameters (current sensor)	

6.3.2.1 Response to Output Voltage Reference

The controller responses to the output voltage reference change from 8 volts to 10 volts are shown in Fig.6-31, Fig.6-32, Fig.6-33, Fig.6-34 and Fig.6-35. It can be seen that the five nonlinear controllers have good performances to the output reference change. The backstepping controller, backstepping sliding mode controller, adaptive backstepping controller and adaptive backstepping sliding mode controller show about 50 millivolt overshoots. The sliding mode controller has 30 millivolt overshoots.

The behaviors of the parameter estimators $\hat{\theta}_2$ and $\hat{\theta}_5$ for the two adaptive controllers are shown in Fig.6-36, Fig.6-37, Fig.6-38, and Fig.6-39. Their values are not zero.

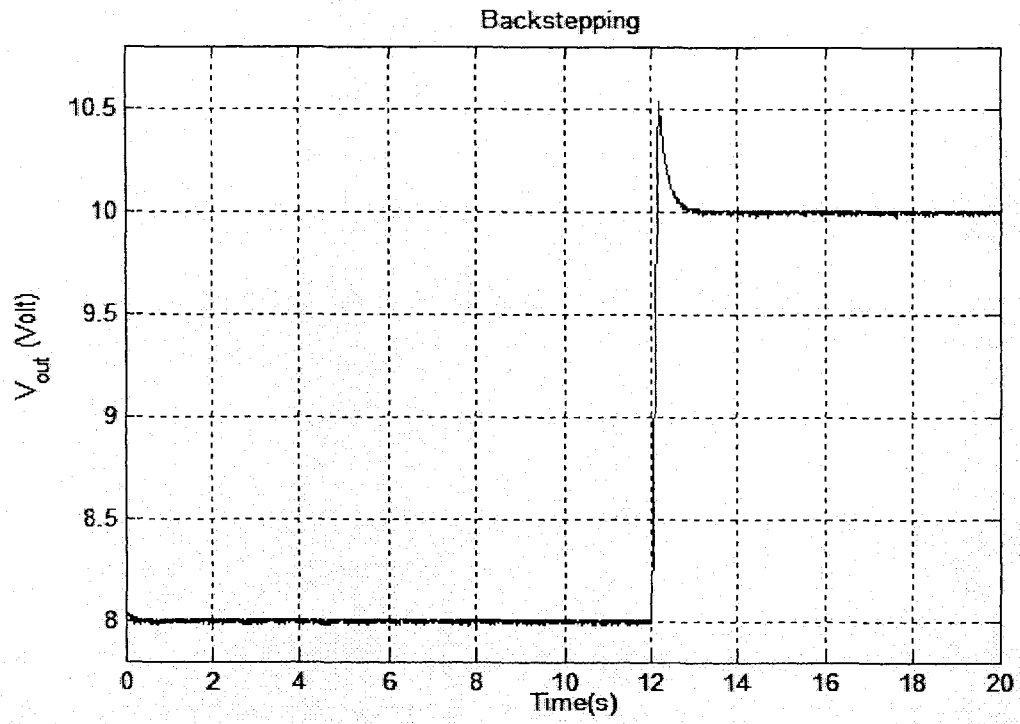


Fig. 6-31: Backstepping

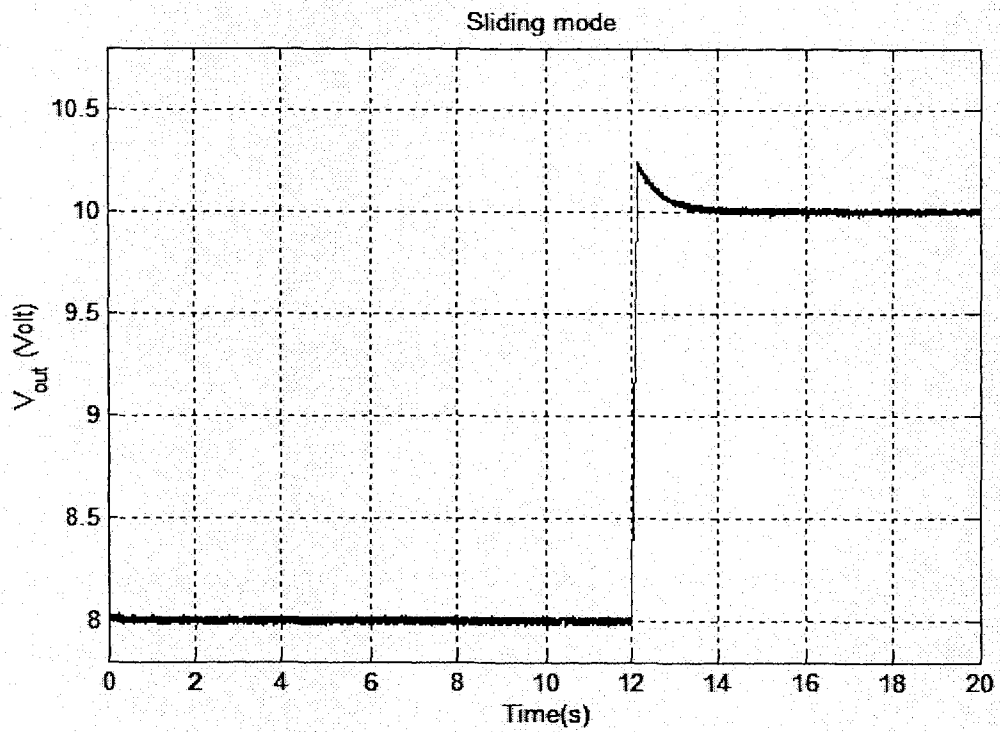


Fig. 6-32: Sliding mode

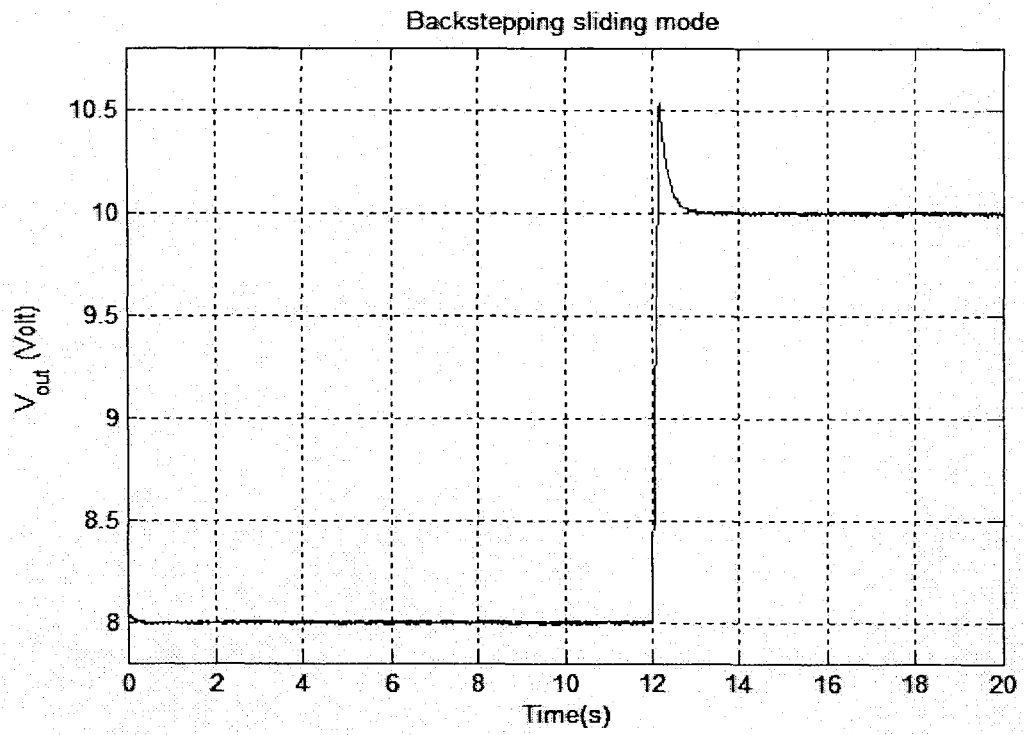


Fig. 6-33: Backstepping sliding mode

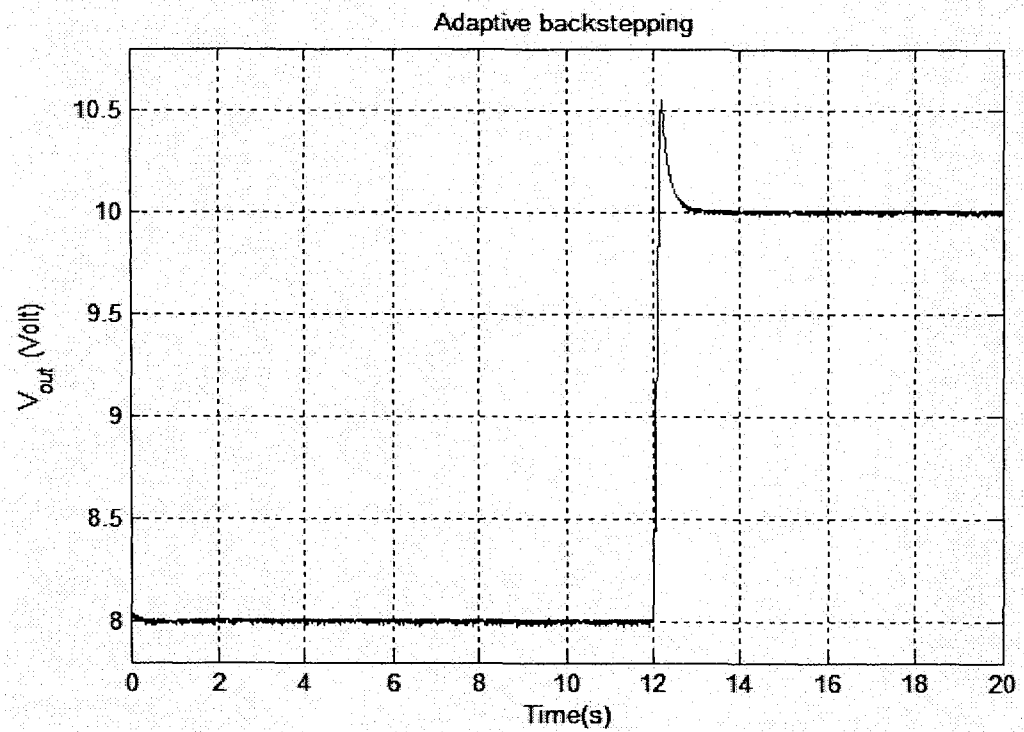


Fig. 6-34: Adaptive backstepping

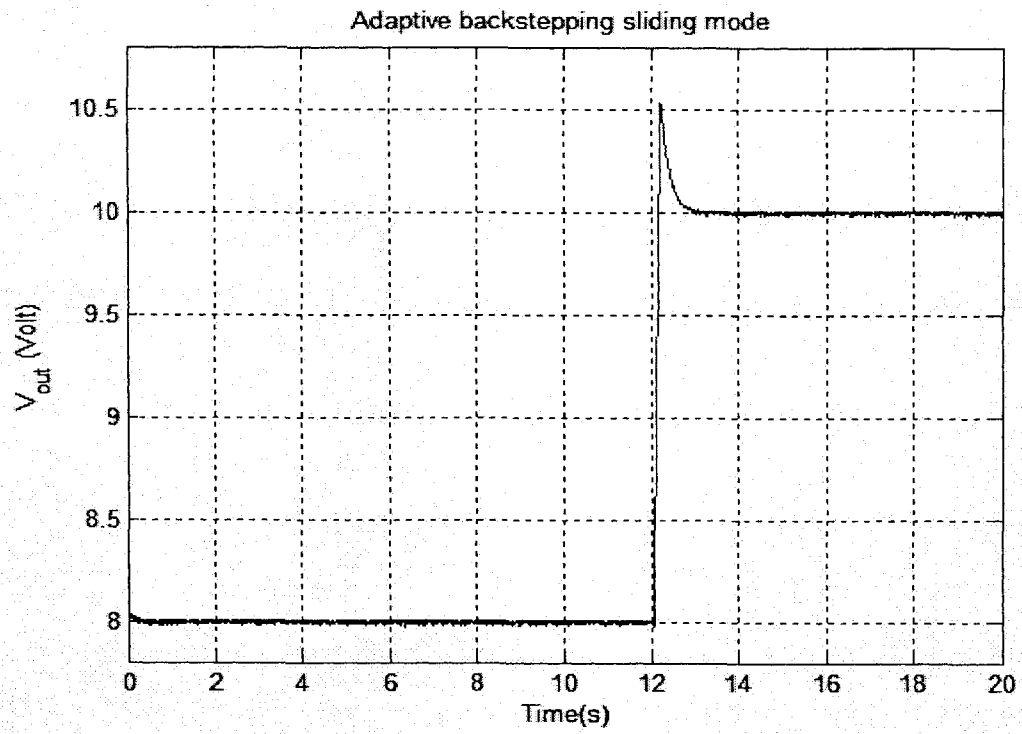


Fig. 6-35: Adaptive backstepping sliding mode

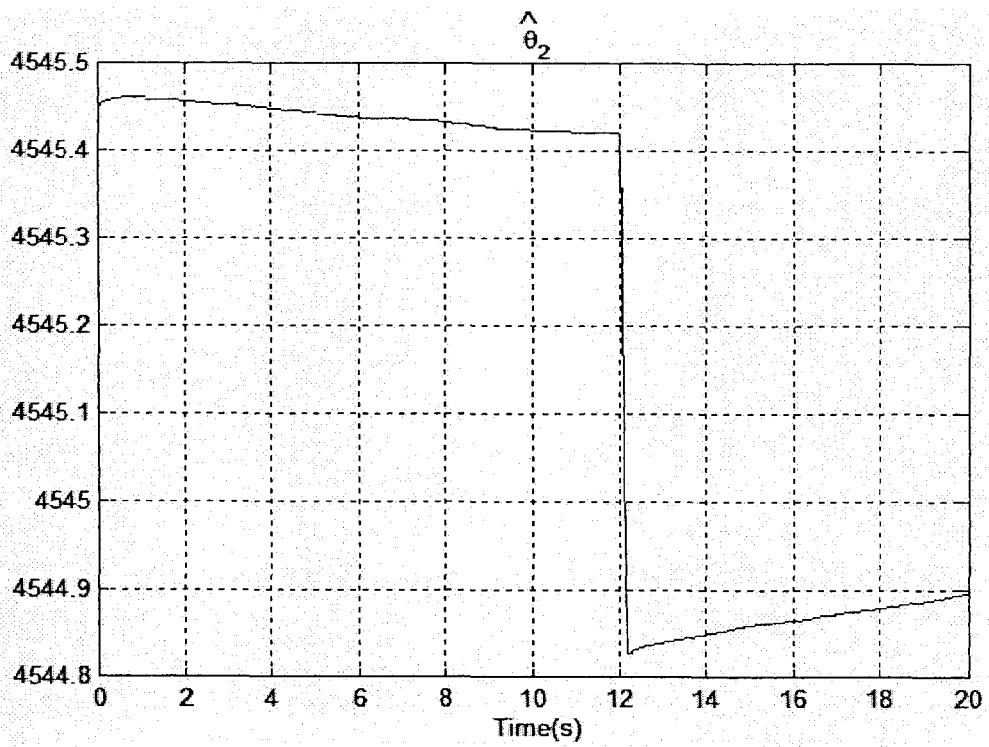


Fig. 6-36: $\hat{\theta}_2$ -Adaptive backstepping

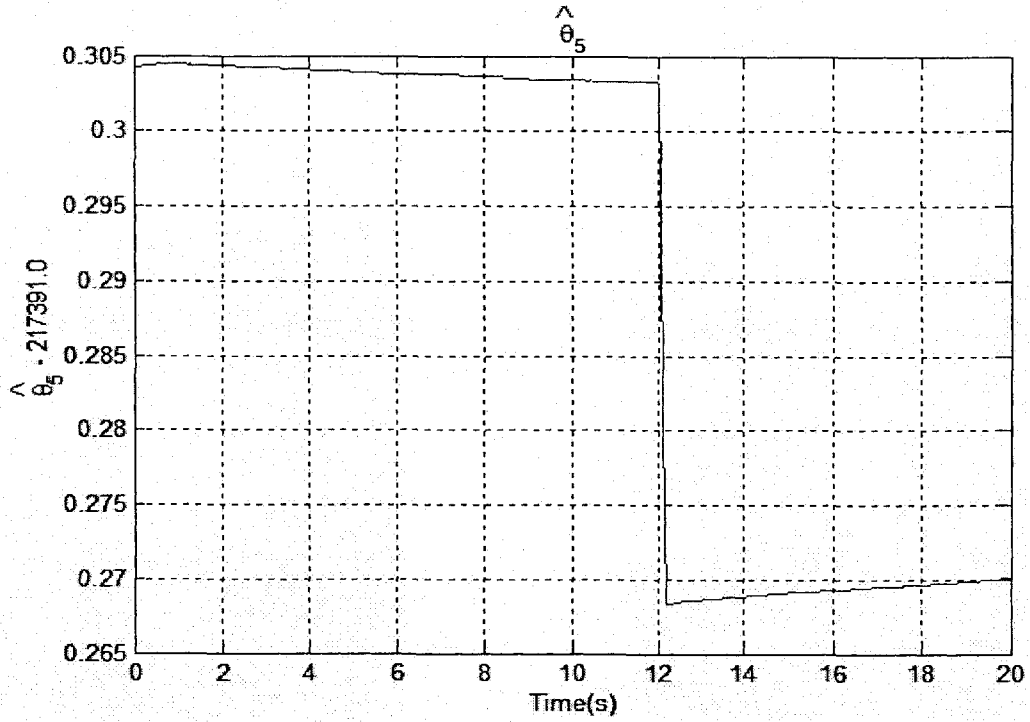


Fig. 6-37: $\hat{\theta}_5$ - Adaptive backstepping

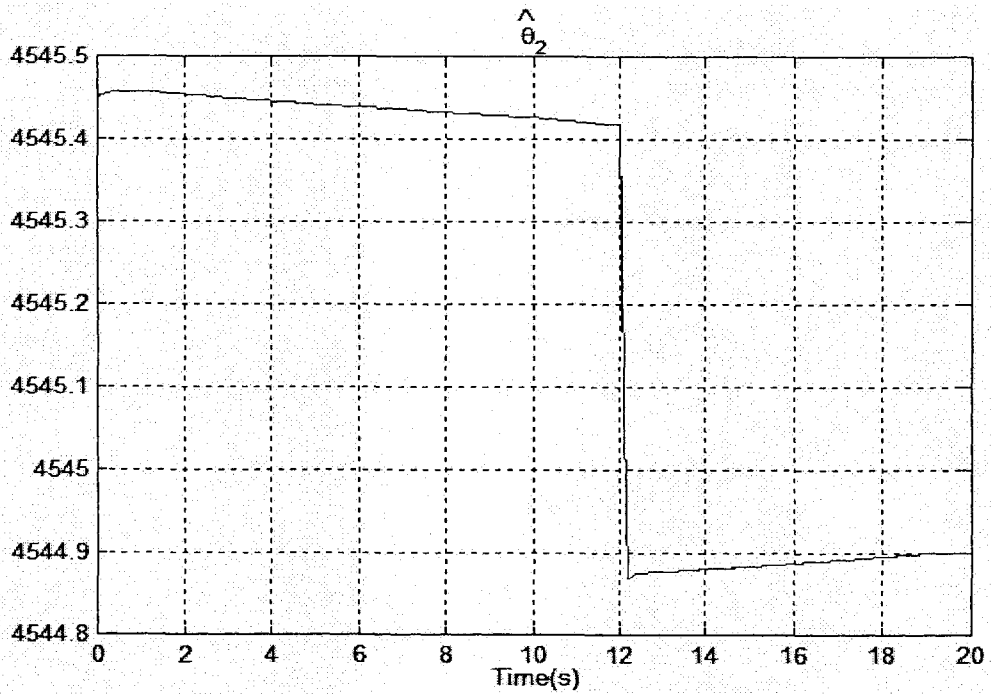


Fig. 6-38: $\hat{\theta}_2$ - Adaptive backstepping sliding mode

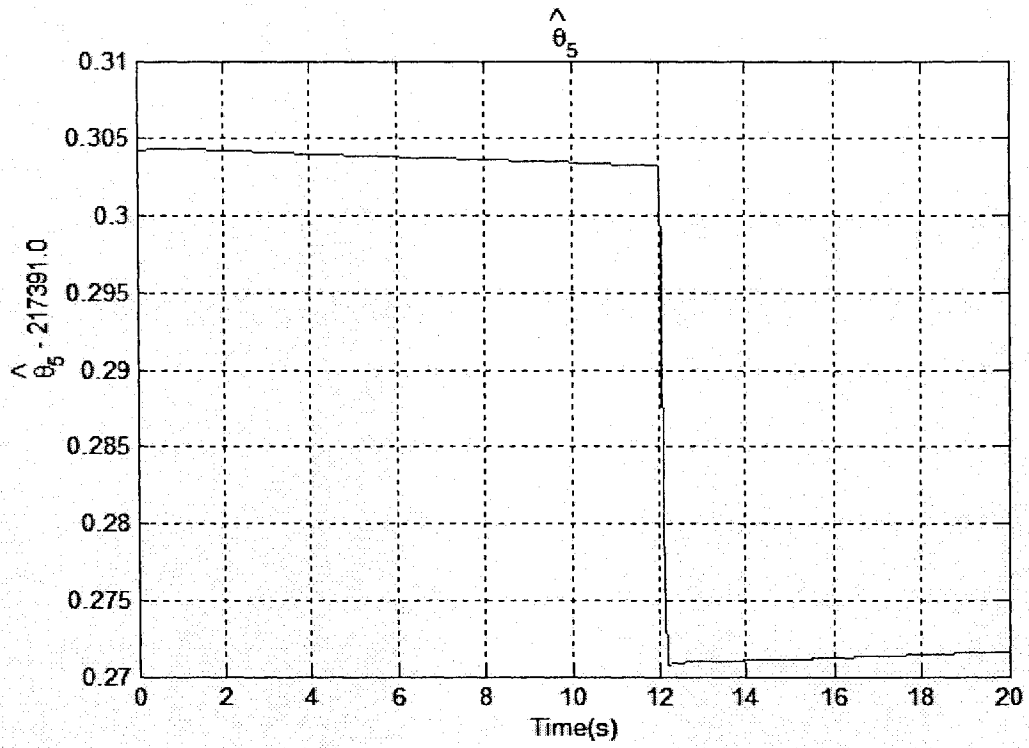


Fig.6-39: $\hat{\theta}_5$ -Adaptive backstepping sliding mode

6.3.2.2 Response to Load Change

The performance of the backstepping controller is shown in Fig.6-40. It can be seen that the output voltage dropped and recovered to the desired value during the load changes. The steady state error is $\pm 15mV$, and the transient response is about $50mV$.

In Fig.6-41, the sliding mode controller shows its robustness and faster response time to the load variations and exhibits $\pm 25mV$ chattering as well.

The behavior of the backstepping sliding mode controller is shown in Fig.6-42, it can be seen that there is no chattering. The steady state error is about $\pm 15mV$ and the transient response is $50mV$.

Fig.6-43 depicts the performance of the adaptive backstepping controller, from which about $\pm 15mV$ steady state error and $50mV$ transient response can be observed.

The behavior of the adaptive backstepping sliding mode controller is presented in Fig.6-44. It can be found that this controller shows no chattering problem, but it exhibits $\pm 10mV$ steady state error and $40mV$ transient response.

As shown in Fig.6-45, Fig.6-46, Fig.6-47 and Fig.6-48, the values of parameter estimators $\hat{\theta}_2$ and $\hat{\theta}_5$ for the adaptive controllers will never be zero.

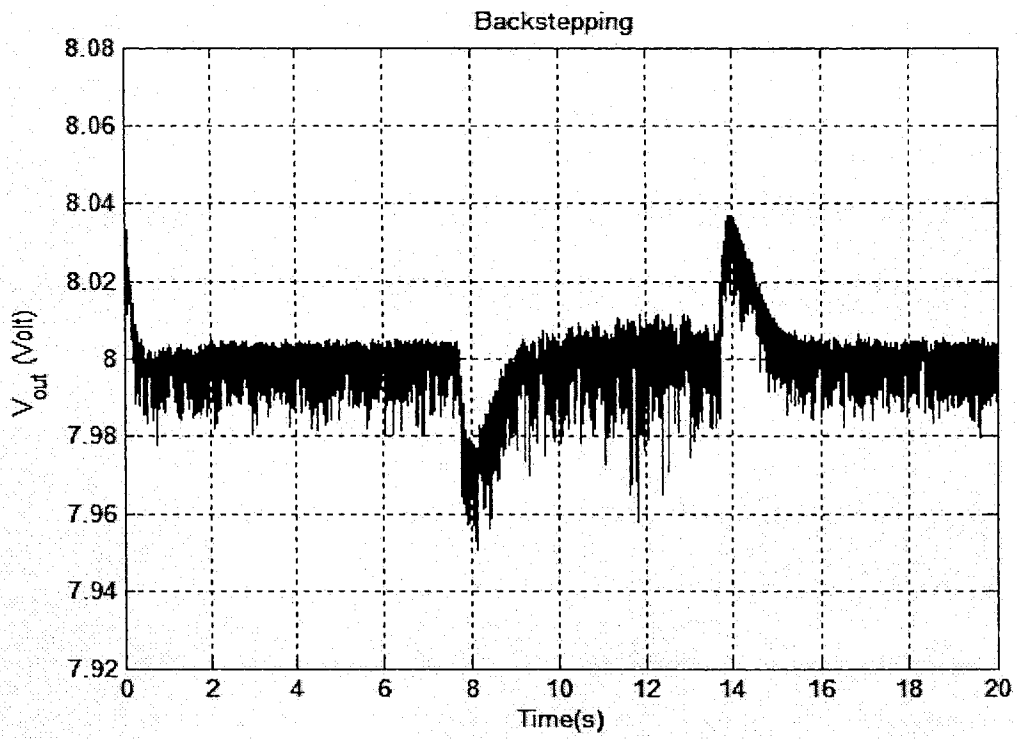


Fig.6-40: Backstepping

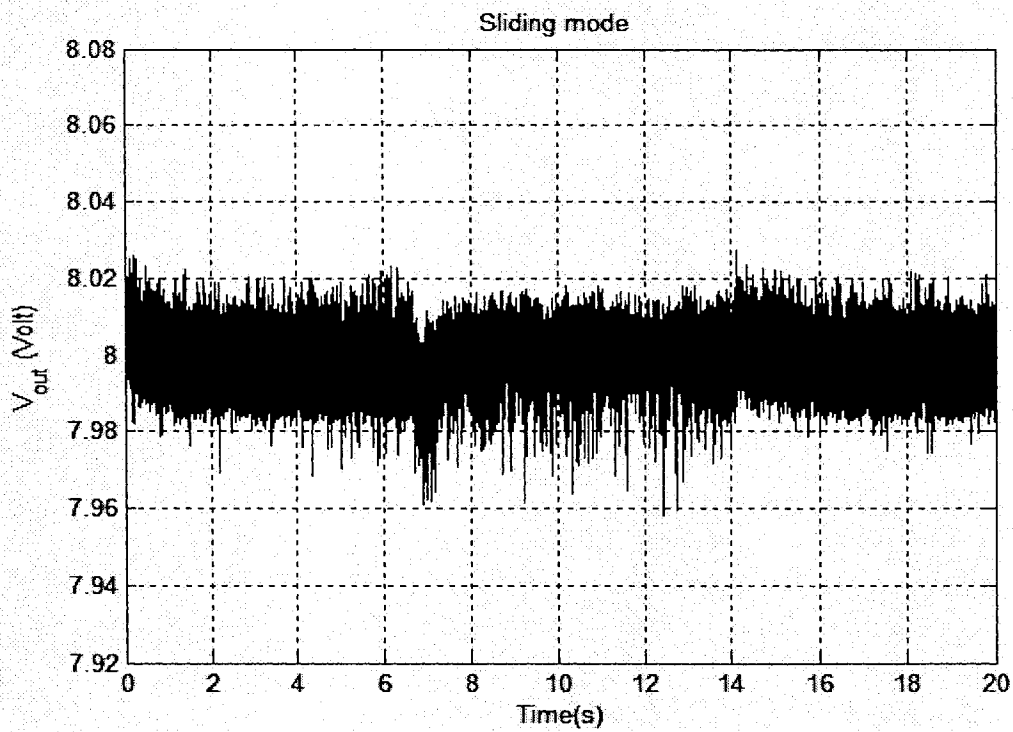


Fig.6-41: Sliding mode

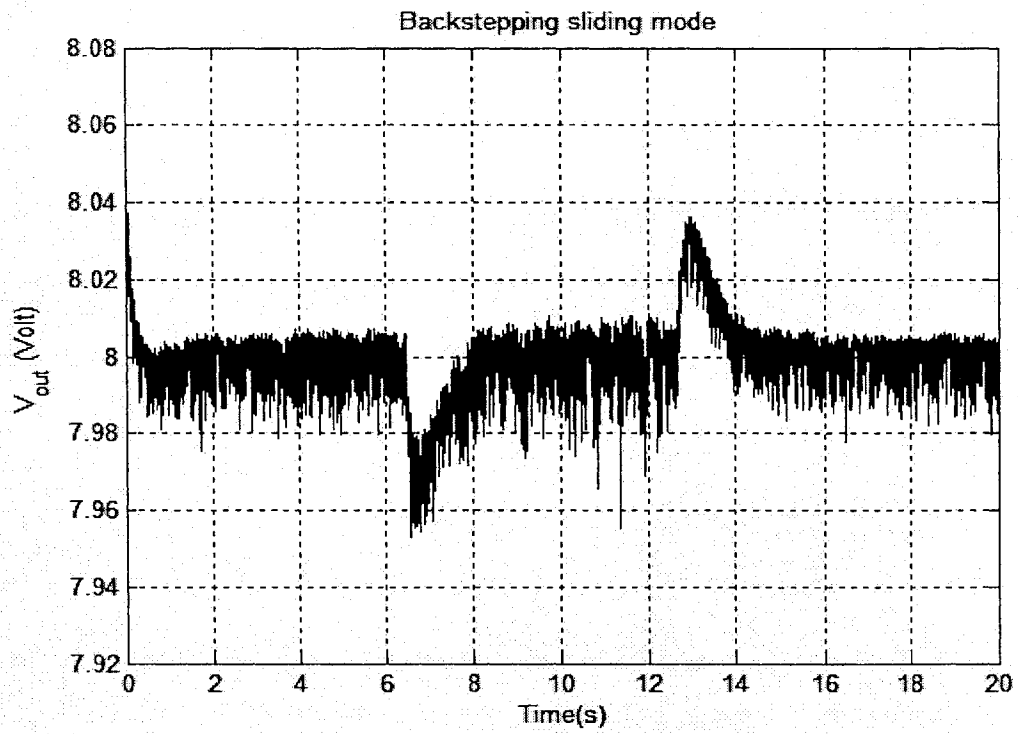


Fig.6-42: Backstepping sliding mode

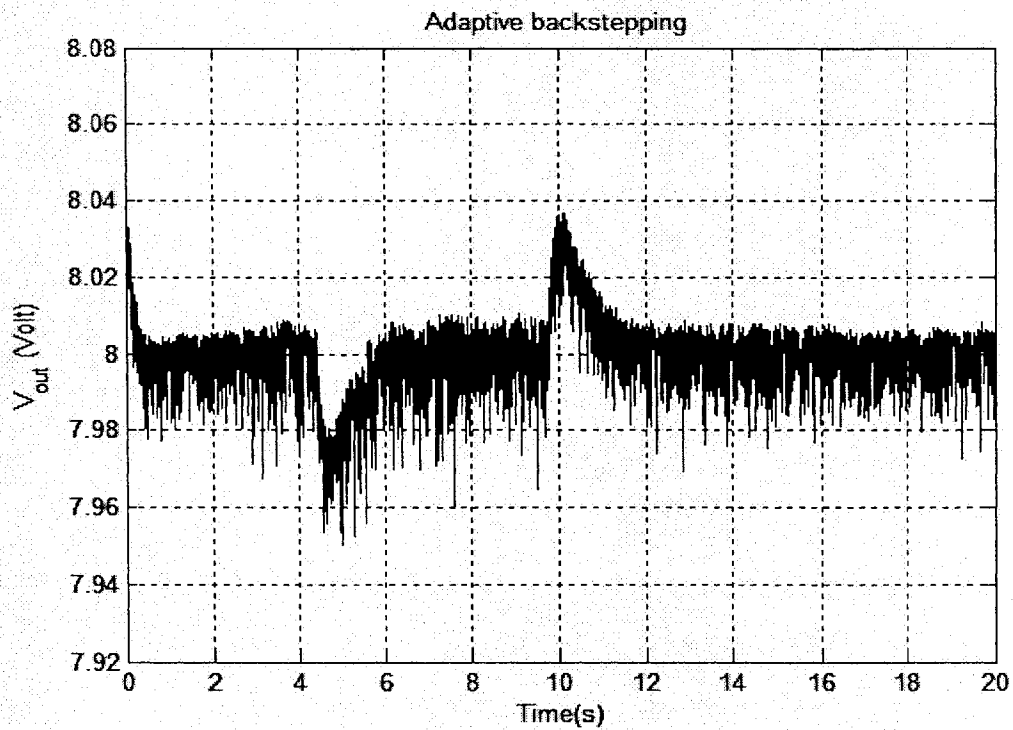


Fig.6-43: Adaptive backstepping

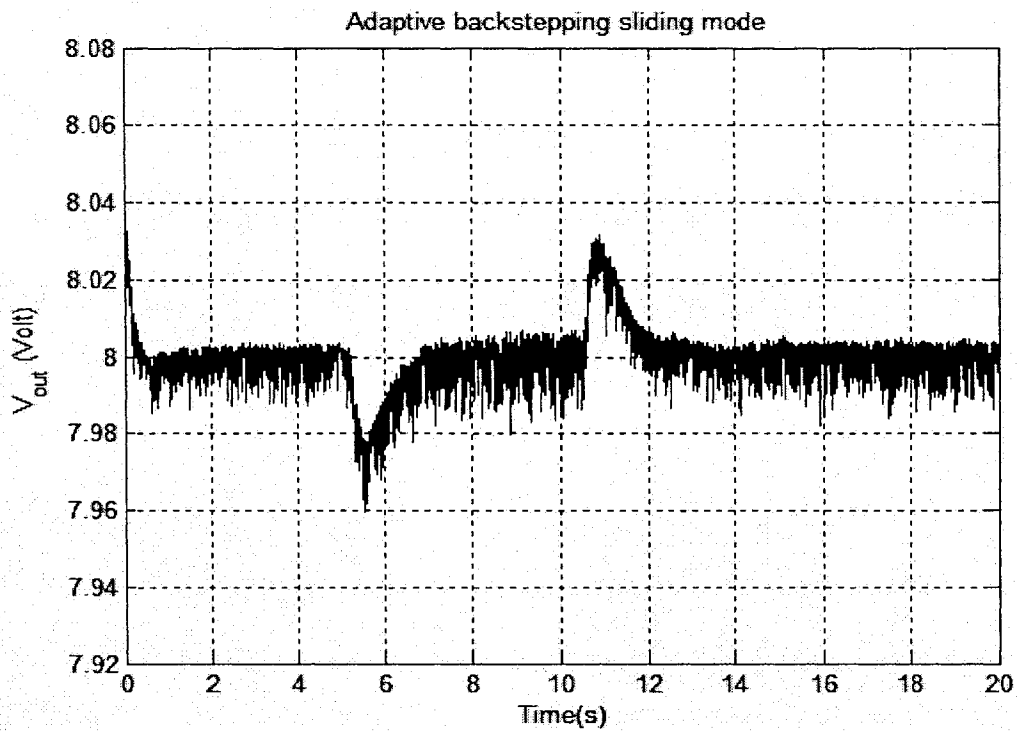


Fig.6-44: Adaptive backstepping sliding mode

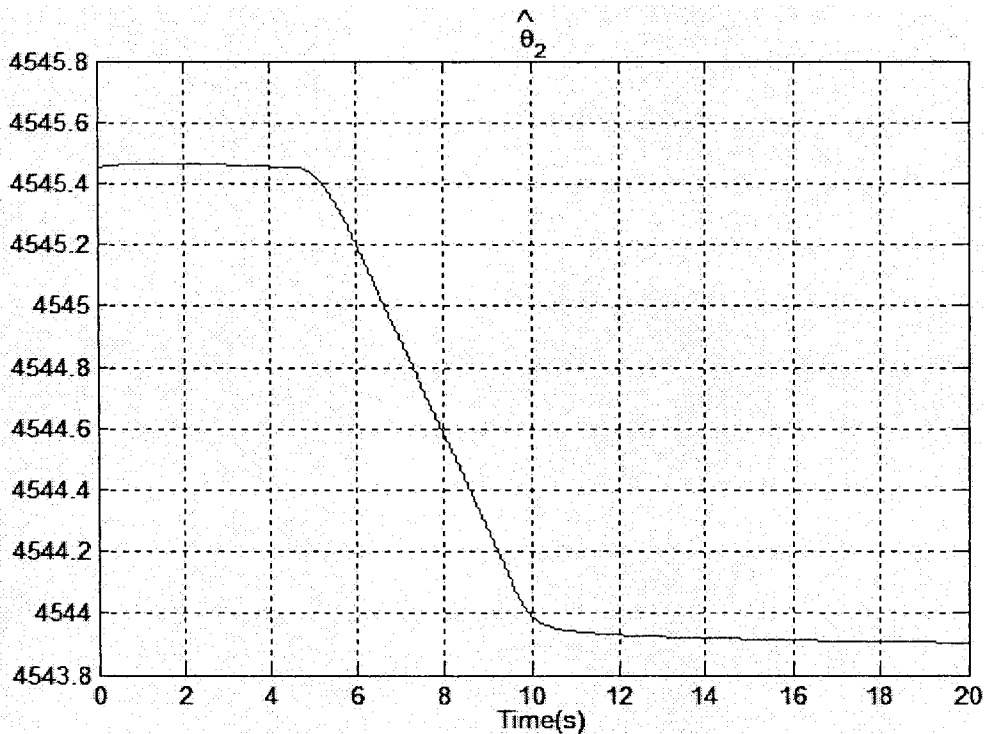


Fig.6-45: $\hat{\theta}_2$ - Adaptive backstepping

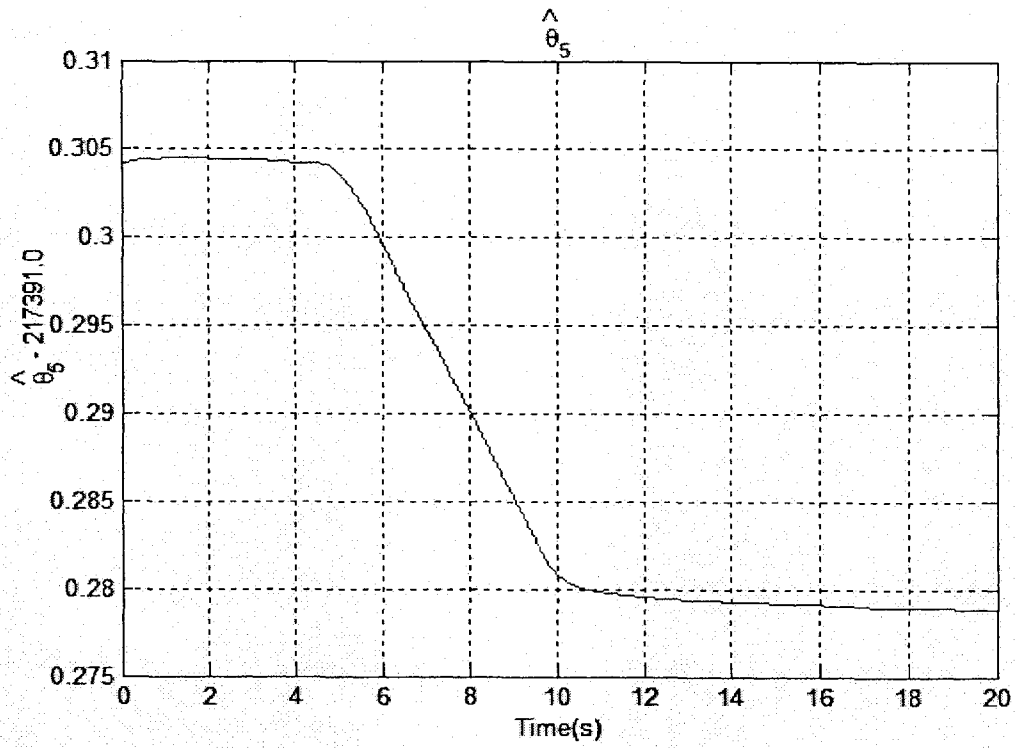


Fig.6-46: $\hat{\theta}_5$ - Adaptive backstepping

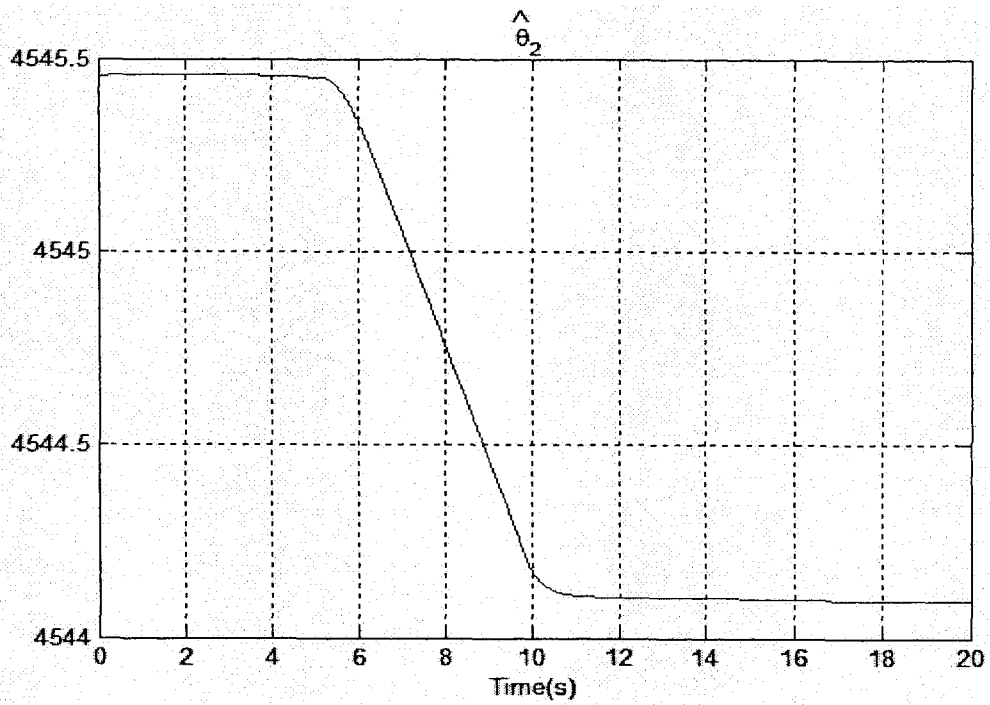


Fig.6-47: $\hat{\theta}_2$ - Adaptive backstepping sliding mode

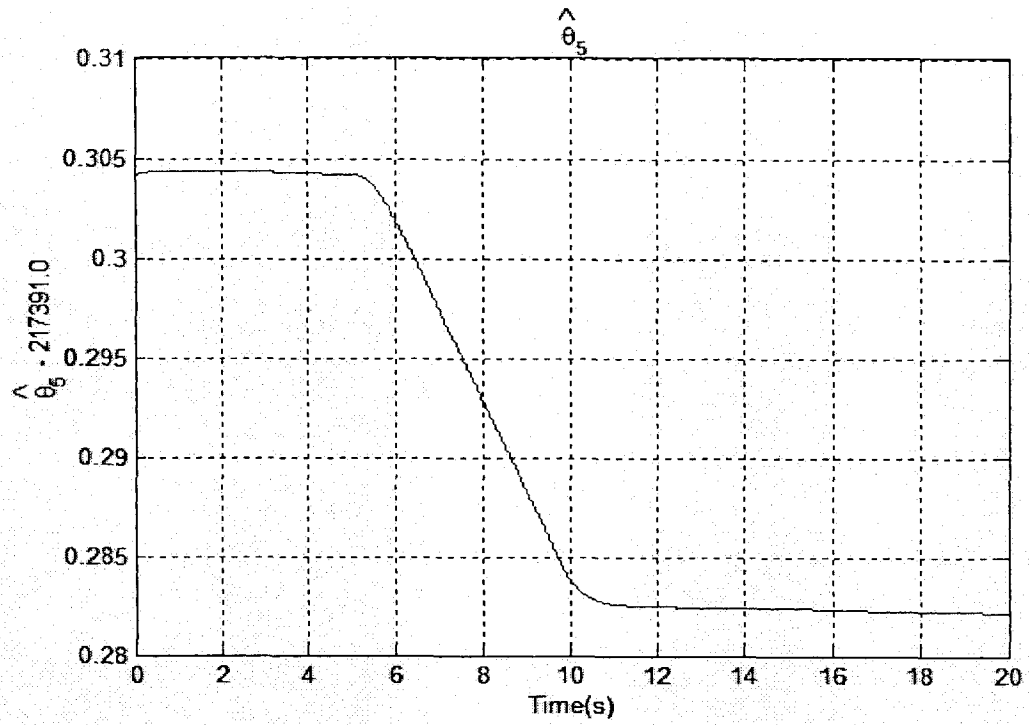


Fig.6-48: $\hat{\theta}_5$ -Adaptive backstepping sliding mode

6.3.2.3 Response to Source Voltage Change

The performance of the backstepping controller, which is shown in Fig.6-49, reveals that the output voltage is less sensitive to the disturbance and the steady state error is from $-25mV$ to $+10mV$.

The performance of the sliding mode controller is shown in Fig.6-50, from which the controllers' robustness and faster response time to disturbances can be observed. Meanwhile, there also exists $-30mV$ to $+20mV$ chattering.

As shown in Fig.6-51, the backstepping sliding mode controller doesn't have chattering. The steady state error is from $-22mV$ to $+10mV$.

The performance of the adaptive backstepping controller is shown in Fig.6-52. This controller has $-22mV$ to $+10mV$ steady state error.

Fig.6-53 shows the behavior of the adaptive backstepping sliding mode controller. It can be seen that the chattering problem is gone. The controller shows $-20mV$ to $+5mV$ steady state error.

After checking the performances of the parameter estimators $\hat{\theta}_2$ and $\hat{\theta}_5$ for the adaptive controllers shown in Fig.6-54, Fig.6-55, Fig.6-56 and Fig.6-57, the values of the estimators are not zero.

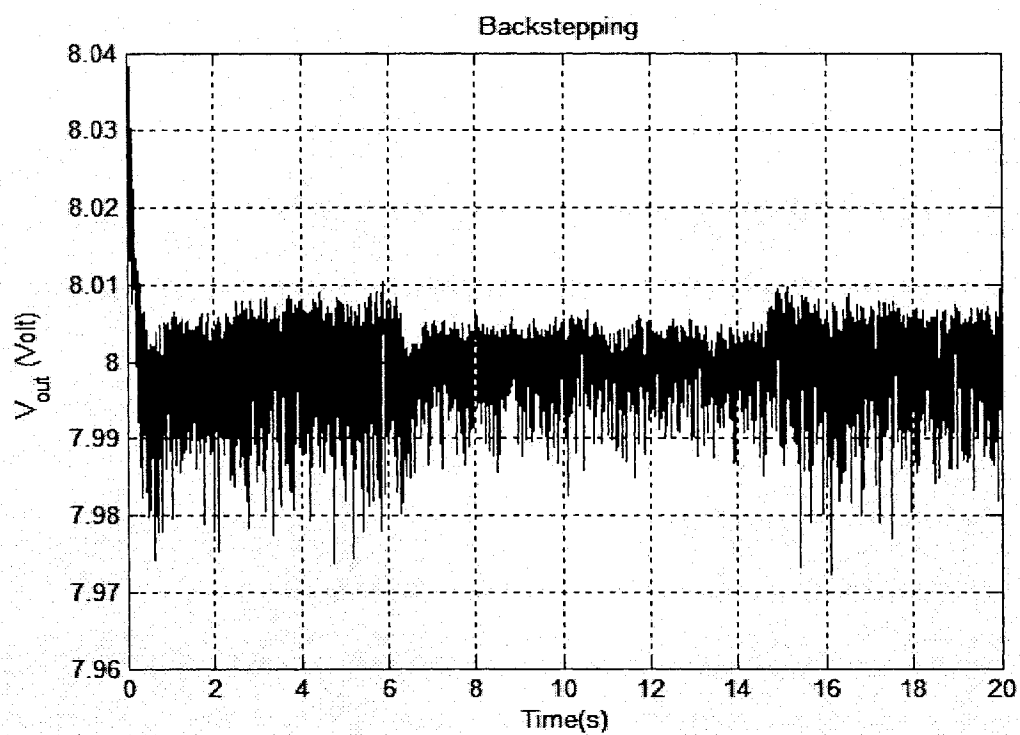


Fig.6-49: Backstepping

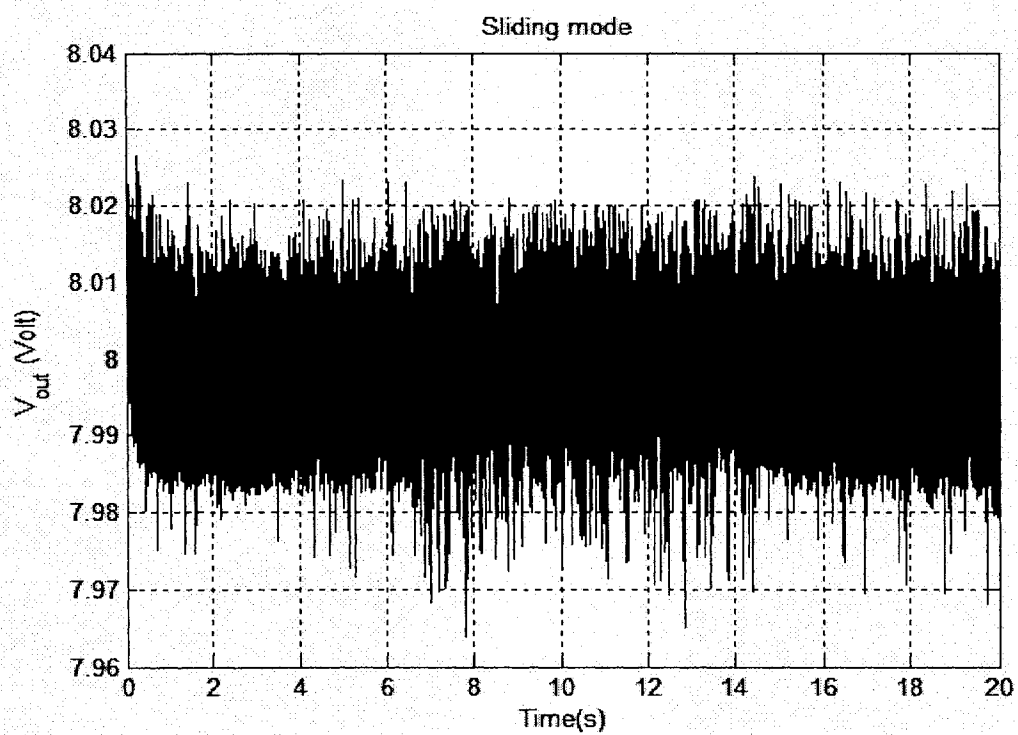


Fig.6-50: Sliding mode

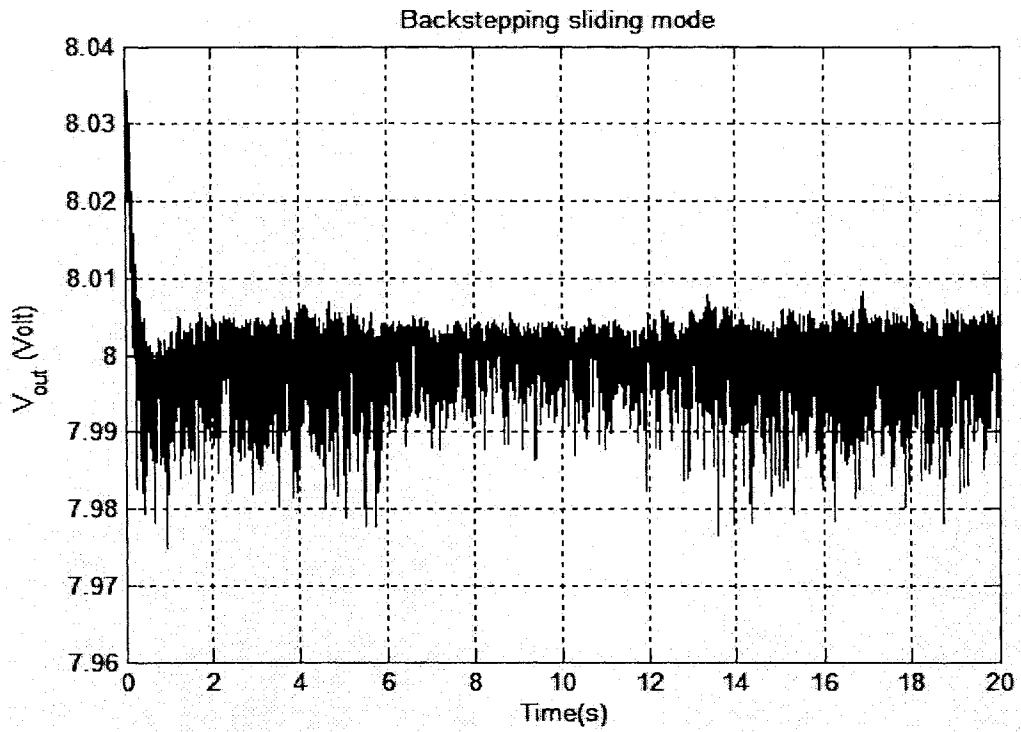


Fig.6-51: Backstepping sliding mode

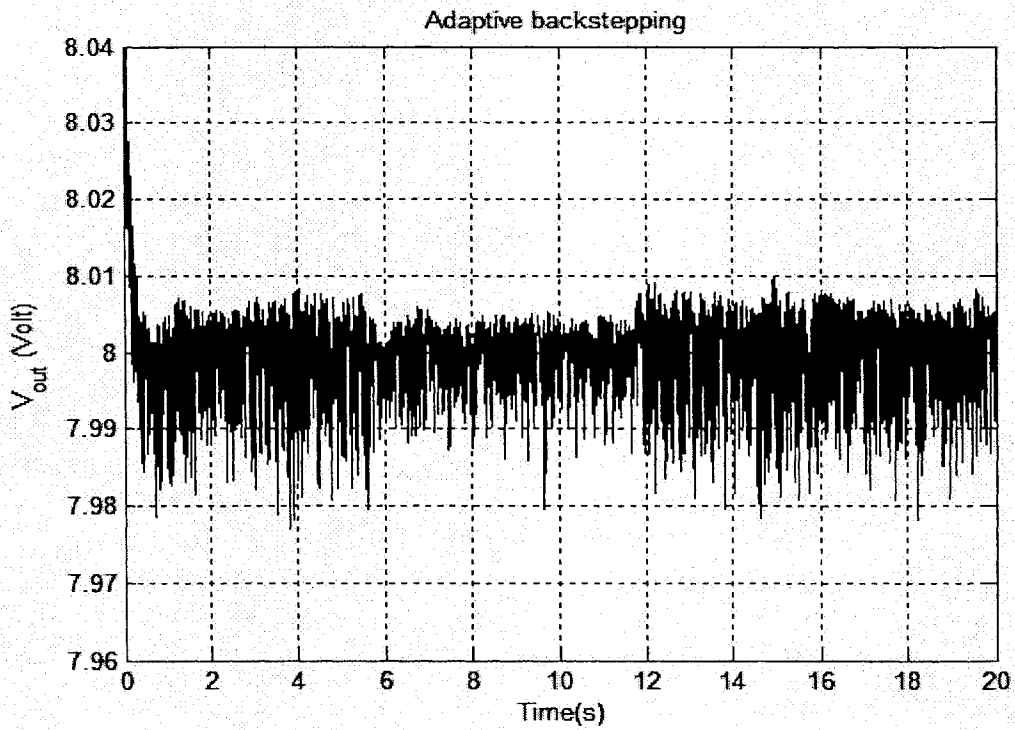


Fig.6-52: Adaptive backstepping

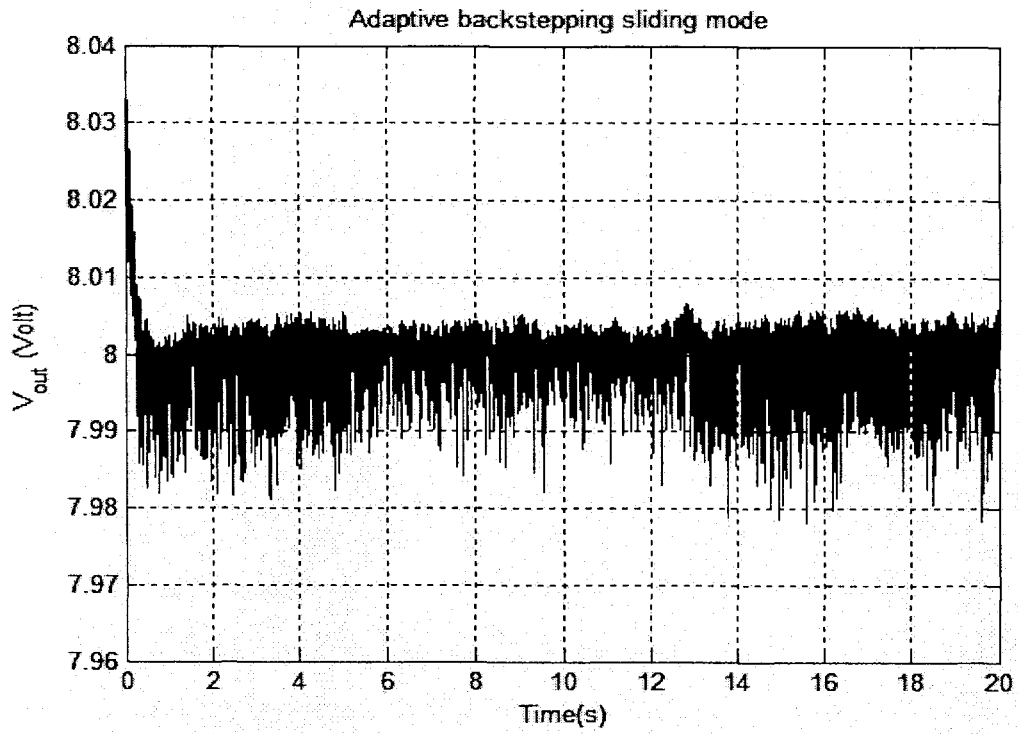


Fig.6-53: Adaptive backstepping sliding mode

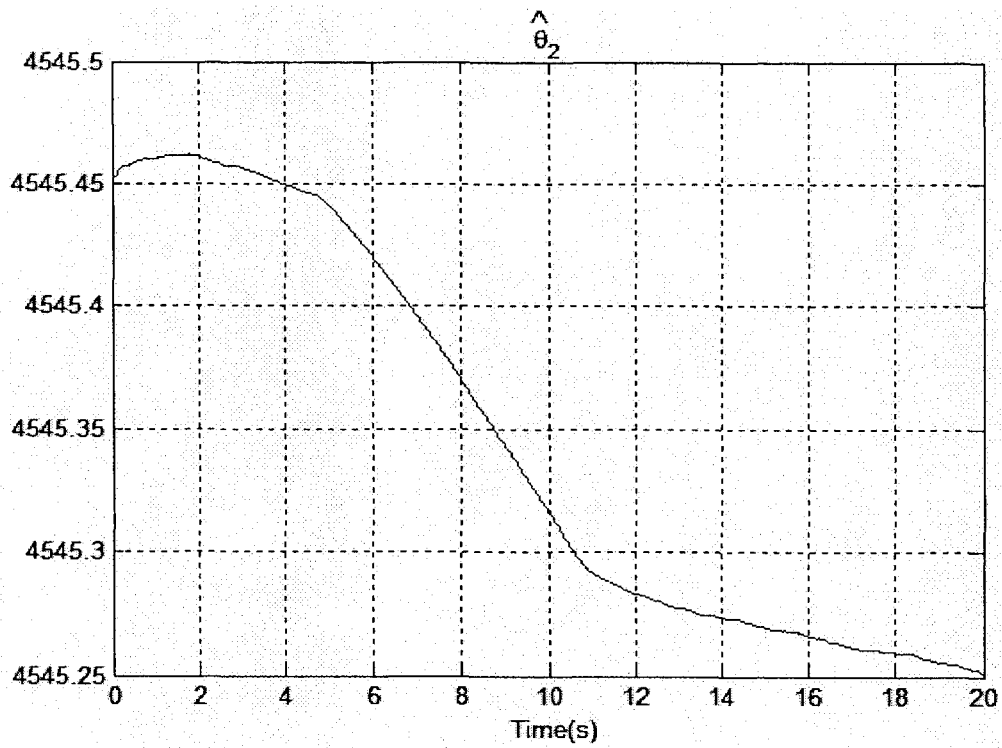


Fig.6-54: $\hat{\theta}_2$ -Adaptive Backstepping

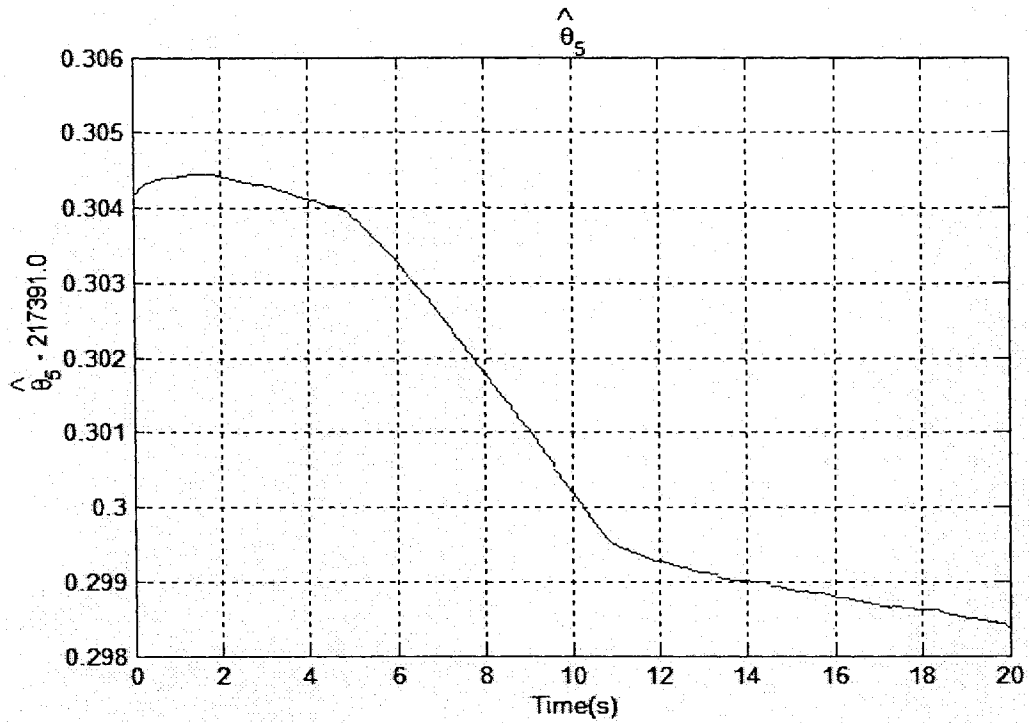


Fig.6-55: $\hat{\theta}_5$ - Adaptive backstepping

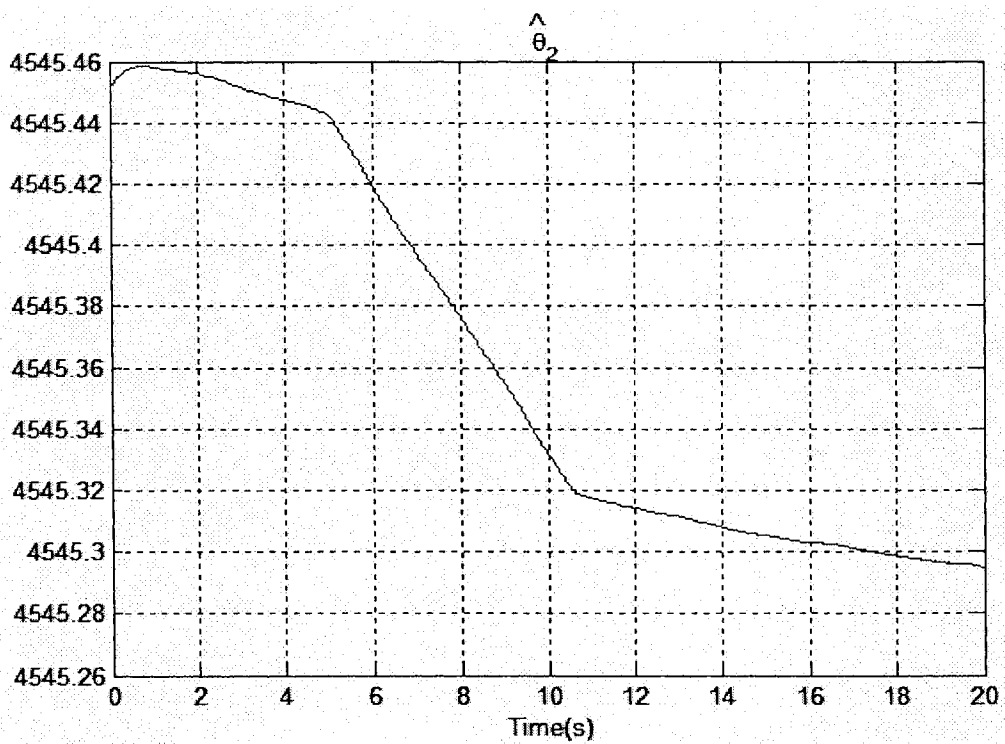


Fig.6-56: $\hat{\theta}_2$ - Adaptive backstepping sliding mode

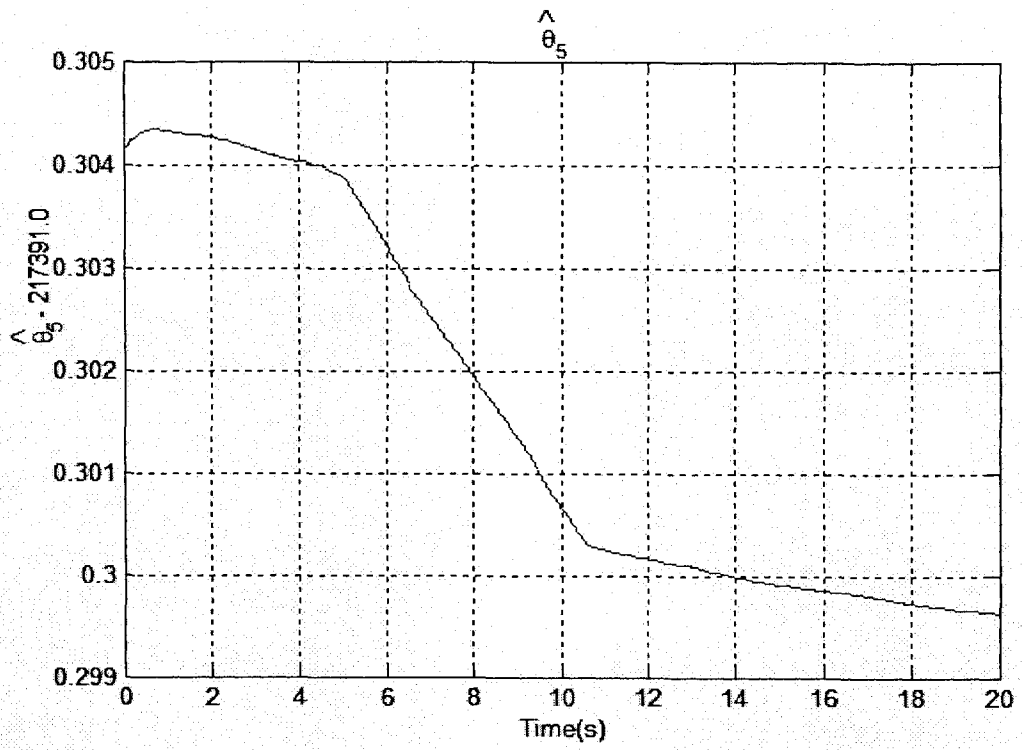


Fig.6-57: $\hat{\theta}_5^*$ - Adaptive backstepping sliding mode

6.3.3 PI Control Results

A PI controller is implemented on the buck converter with the gains $K_p = 25$, $K_i = 80$ under the three conditions. It can be seen that the PI controller has $40mV$ overshoots when the setpoint changed from 8 volts to 10 volts. For the load change, the steady state error is from $-40mV$ to $-15mV$ and the transient response is about $25mV$. The PI controller has good performance to the source voltage change.

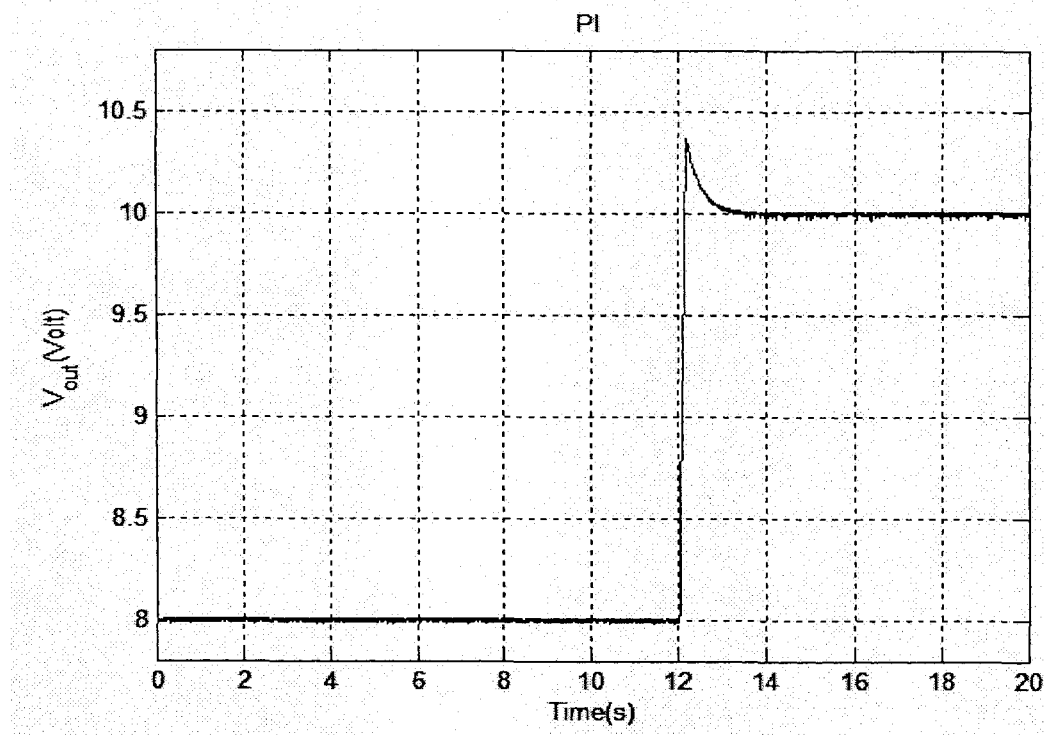


Fig.6-58: PI control – setpoint change

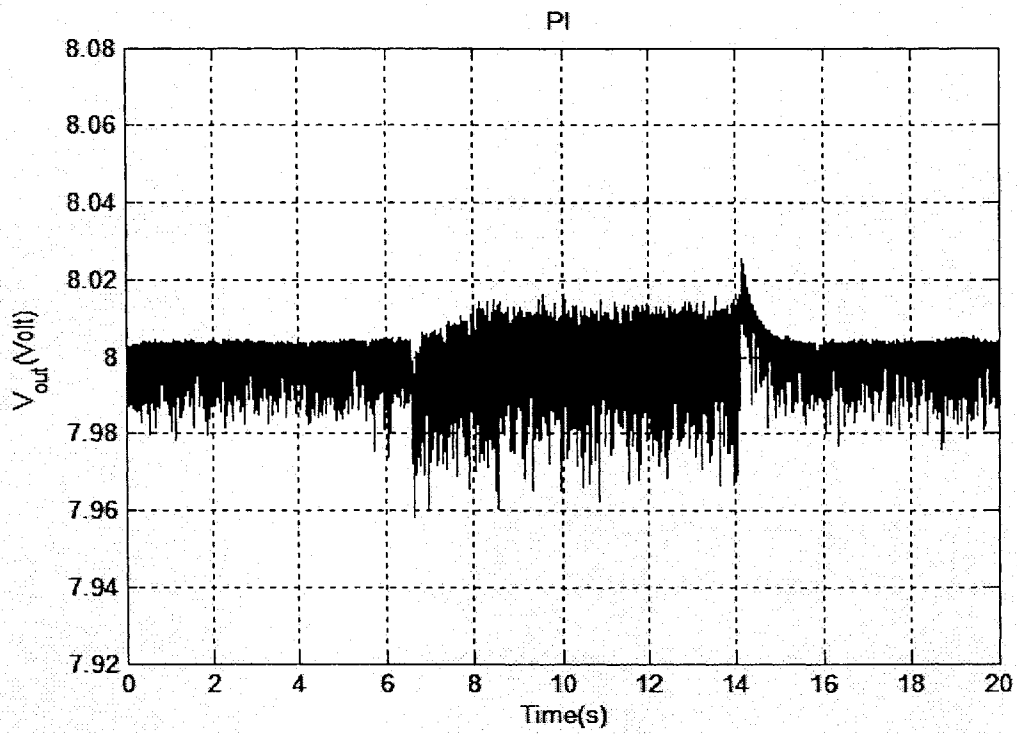


Fig.6-59: PI control

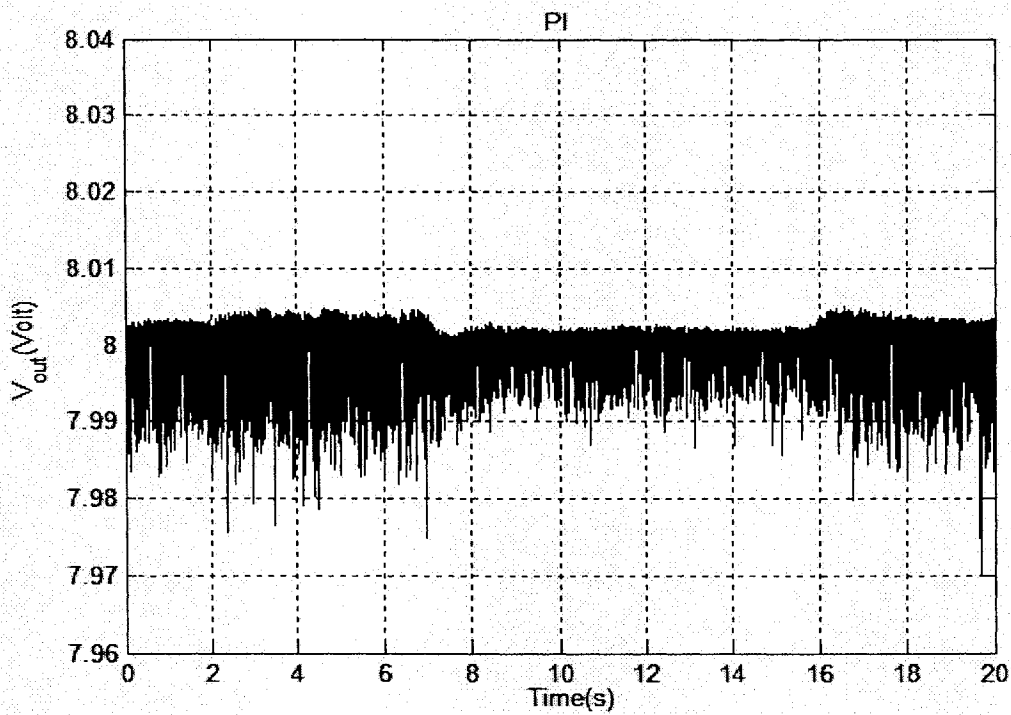


Fig.6-60: PI control

6.3.4 Experimental Results Comparison

All the designed nonlinear controllers are implemented on a buck converter under three conditions. Their performances are compared in terms of steady state error, transient response and settling time. Two sets of results, which are obtained using reduced order observer and current transducer, are shown in Table 6-4 and Table 6-5 respectively.

Control strategy		Setpoint change	Load change	Source voltage change
Backstepping	Steady state error	25.5 <i>mV</i>	32.5 <i>mV</i>	31.5 <i>mV</i>
	Transient response (peak value)	385 <i>mV</i>	63.7 <i>mV</i>	58 <i>mV</i>
	Settling time	3.8 <i>s</i>	2.1 <i>s</i>	1.5 <i>s</i>
Sliding mode	Steady state error	16 <i>mV</i>	21.5 <i>mV</i>	21.2 <i>mV</i>
	Transient response	295 <i>mV</i>	36.7 <i>mV</i>	19.8 <i>mV</i>
	Settling time	3.5 <i>s</i>	0.6 <i>s</i>	0.1 <i>s</i>
Backstepping sliding mode	Steady state error	25 <i>mV</i>	32.5 <i>mV</i>	31 <i>mV</i>
	Transient response	355 <i>mV</i>	58.2 <i>mV</i>	52.5 <i>mV</i>
	Settling time	3.5 <i>s</i>	2.1 <i>s</i>	1.5 <i>s</i>
Adaptive backstepping	Steady state error	24 <i>mV</i>	28.2 <i>mV</i>	31.5 <i>mV</i>
	Transient response	347 <i>mV</i>	58.5 <i>mV</i>	43.8 <i>mV</i>
	Settling time	3.5 <i>s</i>	1.6 <i>s</i>	1.2 <i>s</i>
Adaptive backstepping sliding mode	Steady state error	24 <i>mV</i>	17.3 <i>mV</i>	31.8 <i>mV</i>
	Transient response	348 <i>mV</i>	46.8 <i>mV</i>	42.6 <i>mV</i>
	Settling time	3.5 <i>s</i>	1.6 <i>s</i>	1.2 <i>s</i>
Table.6-4: Experimental results comparison (estimated current)				

Control strategy		Setpoint change	Load change	Source voltage change
Backstepping	Steady state error	18 <i>mV</i>	20 <i>mV</i>	25 <i>mV</i>
	Transient response (peak value)	532 <i>mV</i>	37.2 <i>mV</i>	16 <i>mV</i>
	Settling time	1.1 <i>s</i>	2.1 <i>s</i>	0.3 <i>s</i>
Sliding mode	Steady state error	14 <i>mV</i>	27.2 <i>mV</i>	23.7 <i>mV</i>
	Transient response	243 <i>mV</i>	17 <i>mV</i>	23.7 <i>mV</i>
	Settling time	1.5 <i>s</i>	1.0 <i>s</i>	0.1 <i>s</i>
Backstepping sliding mode	Steady state error	16 <i>mV</i>	36.5 <i>mV</i>	24 <i>mV</i>
	Transient response	528 <i>mV</i>	58.2 <i>mV</i>	14 <i>mV</i>
	Settling time	1.1 <i>s</i>	1.5 <i>s</i>	0.1 <i>s</i>
Adaptive backstepping	Steady state error	16 <i>mV</i>	35 <i>mV</i>	23 <i>mV</i>
	Transient response	536 <i>mV</i>	36.4 <i>mV</i>	12 <i>mV</i>
	Settling time	1.1 <i>s</i>	1.5 <i>s</i>	0.1 <i>s</i>
Adaptive backstepping sliding mode	Steady state error	15 <i>mV</i>	16 <i>mV</i>	22 <i>mV</i>
	Transient response	533 <i>mV</i>	31.5 <i>mV</i>	12 <i>mV</i>
	Settling time	1.1 <i>s</i>	1.4 <i>s</i>	0.1 <i>s</i>
PI controller	Steady state error	15 <i>mV</i>	30 <i>mV</i>	22 <i>mV</i>
	Transient response	366 <i>mV</i>	25.7 <i>mV</i>	13 <i>mV</i>
	Settling time	1.1 <i>s</i>	1.5 <i>s</i>	0.1 <i>s</i>
Table.6-5: Experimental results comparison (current transducer)				

Chapter 7

Conclusions and Future Work

7.1 Conclusions

This thesis has proposed five different nonlinear control techniques to minimize the steady state error for a DC-DC buck converter under source disturbances, setpoint changes and load variations. A state space averaging model has been derived from a non-ideal buck converter circuit. Based on this averaged model, several nonlinear controllers were designed. These include backstepping, sliding mode, backstepping sliding mode, adaptive backstepping, and adaptive backstepping sliding mode control. The two adaptive control methods have been developed to deal with the parameter uncertainties.

All these control techniques have been simulated on computer by using MATLAB. Moreover, a DC-DC buck converter experimental system was built in the laboratory to implement these control techniques. Comparing the simulation and experimental results on these control methods leads to the following conclusions:

- All the nonlinear controllers performed well in tracking the output voltage reference changes. They exhibited a less sensitivity to source voltage disturbances than to load resistance changes.
- Adaptive controllers have automatically tuned its control parameters for the DC-DC buck converter with unknown parameters.
- Sliding mode control does show its robustness to the source disturbances and load changes, however, it still has little chattering.

- PI controller has similar performance with these developed nonlinear controllers under setpoint variation and source deviation. For the load changes, the PI controller has better performance.
- These nonlinear controllers show better performance using current sensor than using the reduced order observer to estimate the current.
- The efficiency of the buck converter is over 90%.

7.2 Suggestions for Future Research

The DC-DC buck converter experimental system was constructed in laboratory with low cost commercial electronic components. However, the proposed controllers were implemented using a DAQ board mounted in a computer, which definitely made our control algorithms more expensive than any commercial solutions. An alternative solution to this problem is to use microprocessor control techniques to implement these control algorithms for the DC-DC buck converter.

Another interesting research area is the extension of the proposed control methods to boost converters and buck-boost converters.

BIBLIOGRAPHY

- [1] D.W. Hart. “*Introduction to Power Electronics*”. NJ, Prentice-Hall, 1997.
- [2] M.H. Rashid. “*Power Electronics: Circuits, Devices, and Applications*”. 2nd ED, NJ, Prentice-Hall, 1993.
- [3] J.J. Slotine and W. Li. “*Applied Nonlinear Control*”. Prentice Hall, 1991.
- [4] P.A. Ioannou and J. Sun. “*Robust Adaptive Control*”. Prentice Hall, 1995.
- [5] M. Krstic, I. Kanellakopoulos, and P. Kokotovic. “*Nonlinear and Adaptive Control Design*”. Wiley, New York, 1995.
- [6] D. Maksimovic and S. Cuk. “General Properties and Synthesis of PWM DC-to-DC Converters”. *IEEE Power Electronics Specialists Conference Record*, Vol.2, 1989, pp. 515-525.
- [7] A.J. Forsyth and S.V. Mollow. “Modelling and Control of DC-DC Converters”. *IEE Power Engineering Journal*, Vol.12, Oct. 1998, pp. 229–236.
- [8] L.R. Pujara, M.K. Kazimierczuk, and N.I. Shaheen, “Robust stability of PWM Buck DC-DC Converter”. *Proceedings of IEEE Conference on Control Applications*, 1996, pp. 632-637.
- [9] H. El Fadil, F. Giri, M. Haloua, and H. Ouadi. “Nonlinear and Adaptive Control of Buck Converters”. *Proceedings of the IEEE Conference on Decision and Control*, Vol.5, 2003, pp. 4475-4480.
- [10] Y.P. Zhang, B. Fidan, and P.A. Ioannou. “Backstepping Control of Linear Time Varying Systems with Known and Unknown Parameters”. *IEEE Transactions on Automatic Control*, Vol.48, Nov. 2003, pp. 1908-1925.
- [11] S.C. Lin and C.C. Tsai. “Adaptive Backstepping Control with Integral Action for PWM Buck DC-DC Converter”. *Proceedings of 2004 IEEE Asian-Pacific Conference on Circuits and Systems*, Dec. 2004. pp. 753-756.
- [12] S.C. Lin and C.C. Tsai. “Adaptive Voltage Regulation of PWM Buck DC-DC Converter Using Backstepping Sliding Mode Control”. *Proceedings of the 2004*

- IEEE International Conference on Control Applications*, Vol.2, 2004, pp.1382-1387.
- [13] M.A. Ghazy and A.M.A. Amin. "Self-Tuned Dither Control of Buck Converter". *IECON Proceedings (Industrial Electronics Conference)*, Vol.2, 2001, pp. 882-887.
- [14] H. Sira-Ramirez and M. Ilic. "A Geometric Approach to the Feedback Control of Switch Mode DC-to-DC Power Supplies". *IEEE Transactions on Circuits and Systems*, Vol.35, Oct. 1988, pp.1291-1298.
- [15] M.Rios-Bolivar and H. Sira-Ramirez. "An Extended Linearization Approach to Sliding Mode Control of DC-to-DC Power Supplies". *Proceedings of the IEEE Conference on Decision and Control*, Vol.3, 1991, pp.2148-2153.
- [16] M.Rios-Bolivar and H. Sira-Ramirez. "Sliding Mode Control of DC-to-DC Power Converters via Extended Linearization". *IEEE Transactions on Circuits and Systems I: Fundamental Theory and Applications*, Vol.41, Oct.1994, pp.652-661.
- [17] G. Spiazzi, P. Mattavelli, L. Rossetto, and L. Malesani. "Application of Sliding Mode Control to Switch-Mode Power Supplies". *Journal of Circuits, Systems and Computers (JCSC)*, Vol.5, Sep. 1995, pp.337-354.
- [18] E. Fossas and A. Ras. "Second Order Sliding Mode Control of a Buck Converter". *Proceedings of the 41st IEEE International Conference on Decision and Control*, Vol.1, 2001, pp.346-347.
- [19] P. Mattavelli, L. Rossetto, and G. Spiazzi. "Small-Signal Analysis of DC-DC Converters with Sliding Mode Control". *IEEE Transactions on Power Electronics*, Vol.12, Jan. 1997, pp. 96-102.
- [20] J. Mahdavi, A. Emadi, and H.A. Toliyat. "Application of State Space Averaging Method to Sliding Mode Control of PWM DC/DC Converters". *Conference Record - IAS Annual Meeting (IEEE Industry Applications Society)*, Vol.2, 1997, pp. 820-827.
- [21] J. Alvarez-Ramirez, G. Espinosa-Perez, and D. Noriega-Pineda. "Current-mode

- Control of DC-DC Power Converters: A Backstepping Approach”. *Proceedings of 2001 IEEE International Conference on Control Applications*, 2001, pp. 190-195.
- [22] S.C. Tan, Y.M. Lai, M.K.H. Cheung, and C. K. Tse. “A Pulse Width Modulation Based Sliding Mode Controller for Buck Converters”. *2004 35th Annual IEEE Power Electronics Specialists Conference, (PESC'04), Aachen, Germany, Vol.5, 2004*, pp. 3647-3653.
- [23] S.C. Tan, Y.M. Lai, C.K. Tse and M.K.H. Cheung, “An Adaptive Sliding Mode Controller for Buck Converter in Continuous Conduction Mode”. *APEC 2004. Nineteenth Annual IEEE Applied Power Electronics Conference and Exposition, Vol.3, 2004*, pp. 1395-1400.
- [24] P.Gupta and A. Patra. “Hybrid Sliding Mode Control of DC-DC Power Converter Circuits”. *IEEE Region 10 Annual International Conference, Proceedings/TENCON, Vol.1, 2003*, pp. 259-263.
- [25] S.C. Tan, Y.M. Lai, M.K.H. Cheung, and C.K. Tse, “On the Practical Design of a Sliding Mode Voltage Controlled Buck Converters”. *IEEE Transactions on Power Electronics, Vol.20, March. 2005*, pp. 425-437.
- [26] G. Escobar, R. Ortega, H. Sira-Ramirez, J-P. Vilain, and I. Zein. “An Experimental Comparison of Several Nonlinear Controllers for Power Converters”. *IEEE Control Systems Magazine, Vol.19, Feb. 1999*, pp. 66-82.
- [27] S.C. Tan, Y.M. Lai, M.K.H. Cheung, and C.K. Tse. “A Systematic Design Procedure for Sliding Mode Controlled Buck Converters”. *IEEE Region 10 Annual International Conference, Proceedings/TENCON, Vol.4, 2004*, pp. 120-123.
- [28] S.C. Tan, Y.M. Lai, C.K. Tse, and M.K.H. Cheung. “Adaptive Feedforward and Feedback Control Schemes for Sliding Mode Controlled Power Converters”. *IEEE Transactions on Power Electronics, Vol.21, Jan. 2006*, pp. 182-192.

- [29] J. Sustersic, Z. Gao, JR. Zeller, and R. Button. "Design and Implementation of a Digital Controller For DC-to-DC Power Converters", *The 2000 SAE Power Systems Conference*. Oct. 2000.
- [30] B.J. Patella, A. Prodic, A. Zirger, and D.Maksimovic. "High-Frequency Digital Controller IC for DC/DC Converters". *IEEE Transactions on Power Electronics*, Vol. 18, Jan. 2003, pp. 438-446.
- [31] M. Ahmed, M. Kuisma, K. Tolsa, and P. Silventoinen. "Implementing Sliding Mode Control for Buck Converter". *PESC Record - IEEE Annual Power Electronics Specialists Conference*, Vol.2, 2003, pp. 634-637.
- [32] X.F. Zhong, G.J.Ye, N.H.Chen, and J.L. Jiang, "Study on Sliding-Mode Control in Three-Level Converters". *Conference Proceedings IPEMC 2004. The 4th International Power electronics and motion control conference*, Vol.3, 2004, pp. 1105- 1110.
- [33] J. Guldner and V. I. Utkin. "The Chattering Problem in Sliding Mode Systems". *Proc. MTNS Conference*, 2000.
- [34] M.R. Rafimanzelat and M.J. Yazdanpanah. "A Novel Low Chattering Sliding Mode Controller". *2004 5th Asian Control Conference*, Vol. 3, 2004, pp. 1958-1963.